

Copyright  
by  
Kenneth Steven Plante  
2013

**The Dissertation Committee for Kenneth Steven Plante Certifies that this is the  
approved version of the following dissertation:**

**Production and Testing of a Novel Live-Attenuated Chikungunya  
Vaccine**

**Committee:**

---

Scott C. Weaver, PhD, Mentor

---

Judith F. Aronson, MD

---

Ilya V. Frolov, PhD

---

Richard B. Pyles, PhD

---

Robert B. Tesh, MD

---

Dean, Graduate School

**Production and Testing of a Novel Live-Attenuated Chikungunya  
Vaccine**

**by**

**Kenneth Steven Plante, B.S.**

**Dissertation**

Presented to the Faculty of the Graduate School of  
The University of Texas Medical Branch  
in Partial Fulfillment  
of the Requirements  
for the Degree of

**Doctor of Philosophy**

**The University of Texas Medical Branch  
November 21, 2013**

## **Dedication**

None of this work would have been possible but for great people that I had the pleasure of being surrounded by in my life. I would like to thank mainly my beautiful wife, Jessica, who took my last name just fast enough to be the first Plante to successfully defend a dissertation. She was able to calm me, and push me to be more of a man, scientist, and person than I ever thought possible. To me she is the world. I would also like to thank my family. My father, Ken, instilled in me early in life that nothing comes easy, especially praise. He worked every day of my childhood, and yet he never missed a football game in 8 years. He worked hard, and I know this because I worked with him for a decade. He is a great man and every day of my life I try and make him proud of me. My sister, Lindsey, was also instrumental to me. As my older sister she always looked out for me as a protective mother. She also was there to listen to my problems and offer educated advice. She and I were always very close and that was extremely important to me. I would like to thank my Goju Ryu Sensei, Gary Card. This man in all my years of training never once raised his voice in anger, yet he could laugh with the best of them. He is completely the reason I made it through college. Without his tutelage and discipline I am sure I would have never kept my grades up, or pursued graduate school. I would love to thank my friends in Galveston. Jordan and his wife Chrissy were always around to make light of any bad mood, and Jordan introduced me to the impressive sport of rugby, which did wonders for me. I would like several people I worked with and became great friends with. Charlie McGee and Kostantin Tsetsarkin were great mentors and even better pool players. Rodion Gorchakov was very helpful answering hundreds of

questions. Nicholas Bergren, who was always there to bounce ideas off of and help me with sequencing. Basically everyone in Dr. Weaver's laboratory had a part in my formal training and I thank them. I would especially like to thank Shannan Rossi for becoming a close friend and advocate. We spent many long days in the animal room together doing our and others' work. She is a professional and driven individual whose career is just starting and she will become a great scientist. I would like to thank my mentor directly. Dr. Weaver allowed me enough freedom to seek training and develop experiments while at the same time talking to me and guiding me. Finally, I would like to thank my dog Leo, who was always there to make me remember life is pretty good when you take a second to look at it.

## **Acknowledgements**

The work presented here represents the focus of my studies while at UTMB. However, I was helped by many different people with this work. Rodion Gorchakov was instrumental in helping me develop cloning strategies and answering hundreds of questions. I would like to thank the people of Takeda industries for helping us develop these vaccine candidates for future clinical trials and for their collaborations with some initial experiments. Dr. Shannan Rossi, Dr. Eryu Wang, Nick Bergren, and Dr. Robert Seymour were all integral in different aspects of these experiments. I would also like to thank Jeanon Smith for help obtaining the A129 mice and Michael Patterson for his assistance with the IVIS imaging. Dr. Weaver and everyone in his laboratory were always helpful in both small and crucial ways. Above all I would like to thank my wife Jessica, whose endless patience made this dissertation readable.

# **Production and Testing of a Novel Live-Attenuated Chikungunya Vaccine**

Publication No. \_\_\_\_\_

Kenneth Steven Plante, PhD

The University of Texas Medical Branch, 2013

Supervisor: Scott C. Weaver

The following work was focused on production and testing of a novel live-attenuated chikungunya virus (CHIKV) vaccine. To this end, multiple strategies were adapted from the IRES-based vaccine strategy first employed with VEEV vaccine strain, TC-83. The first strategy, CHIKV/IRESv1, was highly stable during cell culture passages in Vero cells, and was unable to replicate in mosquitoes. The vaccine was then tested for safety and efficacy in multiple mouse models. These tests demonstrated that CHIKV/IRESv1 had a highly attenuated phenotype and was able to produce a strong immunogenic response. The vaccine was also capable of protecting against a lethal challenge by wild-type CHIKV in multiple animal models. The use of immunocompromised animals became the focus of our testing due to the sensitivity of the type I IFN  $\alpha/\beta$  receptor knockout mouse, A129, to CHIKV infection. In-depth studies were completed using this animal to measure the differences between wild-type CHIKV, CHIKV/IRESv1, and the prototypical 181/25 vaccine. These studies expanded on the safety and efficacy knowledge of the vaccines. The work also discerned the beneficial attributes of CHIKV/IRESv1 in comparison to the 181/25 vaccine, such as increased stability in vivo following serial brain passages and other safety concerns. Overall, the CHIKV/IRESv1 vaccine is safer than and similarly efficacious to the 181/25 vaccine, which progressed to phase II clinical trials.

## TABLE OF CONTENTS

List of Tables .....	ix
List of Figures .....	x
List of Abbreviations .....	14
<b>CHAPTER 1 BACKGROUND .....</b>	<b>16</b>
General Alphavirus Information .....	16
Initial Discovery of Chikungunya Virus .....	20
Chikungunya Fever .....	24
Internal Ribosome Entry Site and its Relevance for Arbovirus Vaccine Development .....	26
Chikungunya Animal Models .....	31
Chikungunya Vaccine Development. ....	35
Chikungunya Transmission. ....	40
Chikungunya Fever Outbreaks and Distribution. ....	42
<b>CHAPTER 2 METHODS .....</b>	<b>46</b>
Production of Infectious Clones.....	46
Virus Rescue .....	51
RNA Radiolabeling and Electrophoresis .....	54
Basic Cell Culture .....	55
Viral Titrations/PRNT <sub>80</sub> /CPE assay.....	56
Replication Kinetics.....	58
Passages .....	59
Animal Work .....	60
Ethics Statement .....	60



Animal Models Used .....	60
Virulence and Efficacy Testing .....	61
Tissue Collection .....	62
Brain passage .....	63
Transcardial Perfusion .....	64
In-vivo Imagining .....	65
Histopathology Tissue Preparation .....	65
Mosquito Manipulation.....	66
<b>CHAPTER 3 PRODUCTION AND INITIAL TESTING OF VACCINE CANDIDATES .....</b>	<b>67</b>
Rationale .....	67
Results .....	68
Production of CHIKV/IRESv1 .....	68
Production of CHIKV/IRESv2 .....	73
Recovery of CHIKV/IRESv1 and CHIKV/IRESv2 .....	76
<i>in vitro</i> Stability of CHIKV/IRESv1 and CHIKV/IRESv2 .....	77
Production of Genomic and sg-RNA by CHIKV/IRESv1 and CHIKV/IRESv2b.....	79
Mosquito Infectivity of CHIKV/IRESv1 .....	80

Summary/Conclusions .....	83
<b>CHAPTER 4 SAFETY STUDIES .....</b>	<b>87</b>
Rationale .....	87
Results.....	88
Summary/Conclusions .....	98
<b>CHAPTER 5 EFFICACY.....</b>	<b>101</b>
Rationale.....	101
Results.....	102
Summary/Conclusions .....	111
<b>CHAPTER 6 EXTENDED SAFETY AND EFFICACY, TROPISM, AND STABILITY</b>	
<b>    IN-VIVO.....</b>	<b>115</b>
Rationale .....	115
Results.....	116
Summary/Conclusions .....	143
<b>CHAPTER 7 OVERALL SUMMARY, FUTURE DIRECTIONS, AND STATE OF</b>	
<b>    CHIKUNGUNYA VACCINE CANDIDATES.....</b>	<b>151</b>
Overall Summary .....	151
Future Directions .....	155
State of Chikungunya Vaccines .....	157
<b>REFERENCES.....</b>	<b>162</b>
Vita	171

## List of Tables

Table 1: Cloning and sequencing primers .....	70
Table 2: Mutations acquired by CHIKV/IRESv2 during passage in Vero cells.....	79
Table 3: Titer of wt-CHIKV or CHIKV/IRESv1 following passage in C6/36 cells ..	81
Table 4: Viremia in neonatal CD-1 mice .....	91
Table 5: Neutralizing antibody production in C57Bl/6 mice one month post-infection.....	103
Table 6: Statistical Analysis of Tissue Titers in Perfused A129 Mice .....	121
Table 7: Statistical Analysis of Tissue Titers in A129 Mice Infected with Parent and Passaged CHIKV .....	139
Table 8: Consensus substitutions acquired by 181/25 subsequent to passage in mouse brains.....	142
Table 9: Substitutions acquired by plaque purified 181/25 subsequent to passage in mouse brains .....	143

## List of Figures

Figure 1: IRES-based TC-83 vaccine strategies .....	29
Figure 2: Transmission cycle of CHIKV .....	41
Figure 3: CHIKV phylogenetic tree.....	45
Figure 4: Fusion PCR.....	47
Figure 5: Standard PCR cycle parameters .....	48
Figure 6: Big Dye PCR cycle parameters .....	50
Figure 7: Overview of cloning strategy .....	52
Figure 8: CHIKV/IRESv1 cloning.....	69
Figure 9: Schematic of CHIKV/IRES vaccine candidates .....	71
Figure 10: Replication kinetics of CHIKV/IRESv1, 181/25, and wild-type CHIKV.....	77
Figure 11: Chromatogram of CHIKV/IRESv1 poly-A tracts .....	78
Figure 12: RNA production by wt-CHIKV, CHIKV/IRESv1, and CHIKV/IRESv2b .....	80
Figure 13: CPE assay assessing the infectivity of CHIKV/IRESv1 and wt-CHIKV in <i>Aedes albopictus</i> .....	82

Figure 14: RT-PCR assessing the infectivity of CHIKV/IRESv1 and wt-CHIKV in <i>Aedes albopictus</i> .....	83
Figure 15: Replication in neonatal CD-1 mice .....	90
Figure 16: Virulence in STAT1 KO mice.....	92
Figure 17: Temperature, weight change, and viremia in 10-week-old A129 mice....	93
Figure 18: Survival and weight change in 3-week-old A129 mice following vaccination .....	95
Figure 19: Survival and weight change in 10-week-old A129 mice following infection with 2 <sup>nd</sup> generation vaccines. ....	97
Figure 20: Survival in neonatal CD-1 mice .....	98
Figure 21: Survival of C57Bl/6 mice challenged with neuroadapted CHIKV .....	103
Figure 22: Footpad swelling post-vaccination and post-challenge.....	104
Figure 23: Survival and weight change in 181/25 or CHIKV/IRESv1 vaccinated, wt- CHIKV challenged A129 mice.....	106
Figure 24: Splenic pathology in A129 mice .....	107
Figure 25: Survival of wt-CHIKV challenge in CHIKV/IRESv2b-vaccinated A129 mice.....	108
Figure 26: Long-term antibody production in CD-1 mice.....	109
Figure 27: Longitudinal efficacy in A129 mice.....	110

Figure 28: Longitudinal production of neutralizing antibody in A129 mice.....	111
Figure 29: Footpad swelling in A129 mice.....	117
Figure 30: Tissue tropism of wt-CHIKV in A129 mice .....	118
Figure 31: Tissue tropism of 181/25 in A129 mice .....	119
Figure 32: Tissue tropism of CHIKV/IRESv1 in A129 mice.....	120
Figure 34: Histopathology of the liver in A129 mice .....	124
Figure 35: Histopathology of the leg in A129 mice .....	125
Figure 36: Histopathology of the footpad in A129 mice .....	126
Figure 37: Impact of FfLuc on Lethality of wt-CHIKV in A129 mice .....	127
Figure 38: Overview of IVIS results.....	129
Figure 39: Foot-blocked IVIS images.....	130
Figure 40: Tissue titers for wt-CHIKV- and wt-CHIKV FfLuc-challenged A129 mice.....	130
Figure 41: Histopathology of spleen in wt-CHIKV- and wt-CHIKV FfLuc-challenged A129 mice.....	131
Figure 42: Titers and plaque morphologies during brain passaging .....	133
Figure 43: Weight change and footpad swelling induced by passaged CHIKV/IRESv1 .....	134

Figure 44: Survival of A129 mice challenged with CHIKV/IRESv1 and 181/25 parent and passage viruses .....	135
Figure 45: Weight change and footpad swelling induced by passaged 181/25 .....	136
Figure 46: Tissue titers of passaged CHIKV/IRESv1 and 181/25 .....	137
Figure 47: Footpad histopathology of A129 mice infected with parent or passaged CHIKV/IRESv1 or 181/25.....	140
Figure 48: Spleen histopathology of A129 mice infected with parent or passaged CHIKV/IRESv1 or 181/25.....	141
Figure 50: Location of important mutations in CHIKV E2 .....	149
Figure 51: Impact of 7139 infection on A129 mice.....	150

## List of Abbreviations

AA	amino acid
ABSL	animal biosafety level
ALT	alanine transaminase
ARC	animal resource center
AST	aspartate transaminase
bp	basepair
C	capsid
CHIKF	chikungunya fever
CHIKV	chikungunya virus
CPE	cytopathic effect
DENV	dengue virus
DMEM	Dulbecco's modified eagle media
ECSA	east/central/southern Africa
EEEV	eastern equine encephalitis virus
eIF	eukaryotic initiation factor
ELISA	enzyme-linked immunosorbent assay
EMCV	encephalomyocarditis virus
FBS	fetal bovine serum
FfLuc	firefly luciferase
fp	footpad
GLP	good laboratory practices
GMK	green monkey kidney
HCV	hepatitis C virus
IACUC	institutional animal care and use committee
IC	intracranially
ID	intradermally
IFA	immunofluorescence assay
IFN	interferon
IM	intramuscularly
IN	intranasally
IND	investigational new drug
IP	intraperitoneally
IRES	internal ribosome entry site
IT	intrathoracically
IV	intravenously
IVIS	<i>in vivo</i> imaging system
KO	knockout
Luc	luciferase



MAVS	mitochondrial antiviral signaling
MAYV	mayaro virus
mRNA	messenger RNA
NaOH	sodium hydroxide
NHP	non-human primate
nsP	non-structural protein
nt	nucleotide
ONNV	o'nyong nyong virus
ORF	open reading frame
PAPR	positive air pressure respirator
PBS	phosphate buffered saline
PRNT <sub>80</sub>	plaque reduction neutralization test at an 80% endpoint
PV	polio virus
RAS	Richard Allan Scientific
SC	subcutaneously
SFV	Semliki forest virus
sg-promoter	subgenomic promoter
sgRNA	subgenomic RNA
SINV	Sindbis virus
TRD	Trinidad donkey
UTR	untranslated region
VEEV	Venezuelan equine encephalitis virus
VLP	virus-like particle
WEEV	western equine encephalitis virus
wt	wild type

## CHAPTER 1 BACKGROUND

### General Alphavirus Information

The term *Togaviridae*, which means “cloaked virus” in Latin, describes a family of viruses containing two genera, *Rubivirus* and *Alphavirus*. The viruses in these genera are enveloped and contain small, single stranded, positive-sense RNA genomes. Rubella virus is the only member of the *Rubivirus* genus. The *Alphavirus* genus, however, contains multiple species, which are divided into two main groups: the Old World alphaviruses, which tend to be arthralgic, and the New World alphaviruses, which tend to be encephalitic. Examples of the New World alphaviruses are Venezuelan equine encephalitis virus (VEEV), eastern equine encephalitis virus (EEEV) and western equine encephalitis virus (WEEV). These viral agents cause febrile illnesses that often have a neurological component. The Old World alphaviruses, such as chikungunya virus (CHIKV), Sindbis virus (SINV), and o’nyong-nyong virus (ONNV), cause febrile illnesses with an arthralgic component. There are some viruses that do not follow this geographic rule, such as Mayaro virus (MAYV), which mimics Old World alphavirus signs and symptoms yet is found in South America [1].

Alphavirus virions are small, enveloped particles approximately 70 nm in diameter [2]. The viral genetic material is a single-stranded, positive-sense RNA genome of approximately 11.8 kb in length. The viral genome has a 5’ methylated cap and a 3’ poly-adenylated tail [1]. The genome also contains 5’ and 3’ untranslated regions (UTRs). Because the genome is a single strand of positive sense RNA, it is directly infectious and can act as a messenger RNA (mRNA). The RNA genome contains two separate promoters, which control translation for the two open reading frames (ORFs) encoded by the virus. The 5’ ORF encodes the four nonstructural proteins

(nsP1-nsP4) and is under the control of the 5' promoter. The subgenomic promoter (sg-promoter) is located in the nsP ORF just upstream of the small intragenic region, and it functions to transcribe a smaller, 2nd RNA called the subgenomic RNA (sgRNA) containing the structural protein genes: capsid (C), envelope (E) 3, E2, 6K, and E1. The alphaviruses share approximately  $\geq 60\%$  sequence identity of their nonstructural proteins (nsP) and  $\geq 40\%$  sequence identity of their structural proteins at the amino acid level.

Alphaviruses are capable of infecting many different types of cells. There is no universal cell receptor for these viruses, though some possible receptors have been identified. Most work has been done with SINV, and the CD209 integrin protein has been associated with attachment [3]. A 67kd laminin receptor protein has also been associated with SINV attachment to multiple cell lines [4]. Multiple studies have also shown that a glycosaminoglycan, heparan sulfate, is associated with SINV attachment to the cell surface [5,6]. It was also shown that SINV adapted to bind heparan sulfate more efficiently resulted in attenuation of the virus *in vivo* [6]. A receptor protein has not yet been elucidated for CHIKV.

After attachment to the host cell, alphaviruses enter through endocytosis. Cholesterol-rich lipid rafts are important sites for viral attachment in Old World alphaviruses, whereas they are not as necessary for New World alphaviruses [7-9]. However, recent work done by Kononchik *et al.* describes different mechanisms of alphaviral entry that focuses predominantly on plasma membrane fusion [10]. Virus and receptor proteins are then pulled into the cell through coated vesicles [11]. The vesicles become uncoated during the acidification of the endosome. This acidification is required for successful infection by SINV, Semliki forest virus (SFV), and other alphaviruses [12]. It is suspected that fusion is mediated by the acidified E1 protein. The E1/E2 heterotrimer breaks apart in low pH, allowing the E1 protein to form a homotrimer after its dissociation from E2 exposes new epitopes [13]. These homotrimeric E1 proteins then cause fusion through an exposed, hydrophobic peptide [14,15]. After fusion, the

nucleocapsid is ejected directly into the cytosol. Uncoating may be accomplished by C directly binding to the ribosome. Ribosome binding sites have been found between amino acids 94 and 106 of C protein. This region of the C also interacts directly with the viral RNA during the encapsidation process. It is hypothesized that C protein recruits ribosomes while simultaneously releasing the viral genomic RNA into the cytosol in close proximity to the recruited ribosome [16-18]. More recently, work has been done to test the theory of endocytosis in viral entry. Vancini *et al.* used temperatures not permissive to either vesicle formation or direct fusion during infections. Using SINV they found that particles were still able to empty their genomic contents into the cell through “stalk” like pores. It remains unclear whether this was a function of the nonpermissive nature of the experiments or a biologically relevant mechanism of alphavirus entry [19].

Cap-dependent translation of the first  $2/3$  of the genomic RNA, which includes the nsP-encoding ORF, proceeds until three concurrent stop codons are encountered at the end of the nsP ORF [1]. There is also a leaky stop codon located near the 3' end of the nsP3 gene. The gene products from this initial translation are the P123 and P1234 polyproteins, depending on whether the ribosome stops or scans through the nsP3 stop codon. Shortly after the production of these proteins, the P1234 polyprotein is cleaved into P123 and nsP4. The P123 and nsP4 complex forms the initial replicative machinery, which transcribes the viral RNA into a negative-stranded RNA template [20,21]. Eventually P123 is cleaved into its three component proteins. When the P123 complex is restricted from further processing through artificial mutations at the cleavage sites, the resultant virus is not able to replicate due to the disruption of positive strand RNA production [22]. The individual nsP1, nsP2, nsP3, and nsP4 proteins then reassemble to form a replicative complex that is very effective at transcribing the positive sense genomic RNA and sgRNA. Like the full genomic RNA, the sgRNA also has a 5' methylguanosine cap and a 3' poly-A tail. The structural proteins are translated from the

sgRNA in a cap-dependant mechanism approximately 2-3 hours post-infection [1]. Translation of the structural gene cassette produces a structural polyprotein from which the C protein self-cleaves in the cytoplasm. Further processing forms the P62 (E3/E2), 6k and E1 proteins, which are embedded in the endoplasmic reticulum [23].

After translation and cleavage, capsid (c) forms oligomers. Though the sgRNA is produced at much higher levels in the cell, C targets only the genomic RNA for encapsidation because of a packaging signal found at the 5' end of the viral RNA (which is therefore found in the full-length genomic RNA but not the sgRNA). More recently, nsP2 was also implicated in either direct or indirect packaging of VEEV genomic RNA [24]. The packaging signal in SINV is between nucleotide (nt) 945 and 1076 of nsP1, upstream of the sgRNA [25-27]. A deletion in this area did not stop particle formation, however the particles that formed generally encapsidated sgRNA [18].

Following assembly and encapsidation of genomic RNA, the nucleocapsid travels to the cell's plasma membrane, where it interacts with viral glycoproteins that have been integrated into the membrane. The membrane then encompasses the nucleocapsid as the particle begins to bud. As the virus begins to bud from the plasma membrane the lipid bilayer fuses around the nucleocapsid, releasing the virion [28,29].

During replication, alphaviruses employ a myriad of strategies to deal with the host immune response. One of these strategies is host transcription shutdown, which is done differently in New and Old World alphaviruses. In New World alphaviruses, transcription shutdown is accomplished by the C protein, which forms a tetramer with CRM1 and importin  $\alpha/\beta$  that is then able to block nuclear pores [30,31]. It has been shown that impeding cellular protein trafficking into the nucleus is an effective means for transcriptional shutoff [32-34]. The Old World alphaviruses, such as SINV and CHIKV, use nsP2 to accomplish a similar effect. The nsP2 protein is translocated into the nucleus [35-37]. Upon entry into the nucleus, nsP2 acts directly on RNA polymerase I and II, inhibiting their function. It was also shown that nsP2 in its free form is needed to

generate cytopathic effects (CPE) through transcriptional shutoff. If nsP2 remains part of the P123 polyprotein, it is unable to cause CPE [38]. These pathways lead to general host transcriptional shutoff within 6 hours of infection.

## **Initial Discovery of Chikungunya Virus**

The first recorded outbreak of disease caused by CHIKV was observed by Dr. Marion C. Robinson in 1952. While working in hospitals in Newala and Lulindi, Dr. Robinson observed 150 people with relatively high fevers of 102-105°C [39]. The hallmark of the disease was intense joint pain, which was so severe that patients were unable to sleep for the first few days after the onset of symptoms, and which lasted up to 4 months. Headache was also very common in afflicted individuals, as was a maculopapular rash on the abdomen. The incubation period was 3-12 days. Clinically, this newly described disease was very similar to dengue, but at the time dengue was not common in this area of eastern Africa [40]. The local population had no historical memory of any illness with these symptoms, and because of the joint pain they named the disease chikungunya, which means ‘that what bends up’ in Makonde.

Shortly after the initial observation of this chikungunya fever (CHIKF) outbreak, a team was sent in to begin classifying the etiologic agent. Epidemiological studies focused on an isolated plateau region in the Newala district of Tanganyika (currently named Tanzania). Three plateaus were in the immediate area: Rondo, Makonde, and Maiwa. The focus of the initial studies was on the central Makonde plateau, which was predominantly settled by the Makonde tribe. Several other tribes lived on the edges of the Makonde plateau and in the surrounding lowlands, but they experienced a much lower incidence of disease and thus were not the subject of intense study.

In addition to the aforementioned lack of dengue, the area also had a very low incidence of malaria. This absence of other major infectious diseases and the severity of the symptoms made it relatively easy for the team to track the 1952 outbreak. To understand how many people in this region had developed the disease, the team “interrogated” 62 chiefs in the surrounding areas. Also, while collecting mosquitoes, the team asked the residents of the huts if anyone in the dwelling had developed any of the signs or symptoms of this disease. The first cases seemingly appeared in the region in July of 1952. In September of 1952 people in adjacent areas of the plateau started presenting with the same signs and symptoms. The outbreak reached its peak in January 1953, with 49 of the 62 localities simultaneously reporting disease. The spread and peak of disease roughly correspond with the local rainy season, which runs from November to May and is responsible for most of the average annual rainfall of 94.9cm. Average temperatures in the region are highest at the beginning of the rainy season at 28.5°C and fall to 21.8°C at the end of the season [40]. It is believed that initiation ceremonies, in which many people travel to a centralized location, and the start of the annual rainy season may have led to the spread.

The population of the Makonde plateau at the time lived in small tribes consisting of roughly 50-150 people generally living in 9 huts per locality. In the different localities, morbidity in regards to the unidentified infection ranged from 5-83%. The incidence of transmission for children and adults was quite similar, with overall means of 53.5% and 47.6% respectively. This apparent lack of any preexisting immunity in the adult population seemed to confirm the local accounts that this was a new disease in the region. Dr. Lumsden looked at the incidence rates in huts that housed afflicted persons. He found that it was very common to have multiple infected individuals in the same hut. He generally found that inhabitants of these domiciles were either not affected at all, or that a large number of people in a given hut were symptomatic.

Because they lived high up on the Makonde plateau, the people of the hard-hit Makonde tribe, who had a fear of settling near rivers or in the surrounding lowlands, would have had to travel as far as 8 km to obtain water from the rivers. To avoid the need for this long and arduous trip, they would dig large “saucer-shape depressions” [40] which could, for a short time, catch and hold water during the rainy season. This water would be harvested and stored in large clay pots, which were kept inside of their huts. Some homes would have as many as 8 of the storage jars. Dr. Lumsden believed that since these jars remained at least partially full, they would make good larval habitats for mosquitoes [40]. This, combined with the relatively lower incidence of disease amongst the tribes living closer to the rivers, who had no need to store standing water in their dwellings, led Dr. Lumsden to believe that chikungunya disease might be caused by an arbovirus.

To investigate the possibility of an arbovirus as the causative agent of CHIKF, Dr. Lumsden began to catch and isolate various arthropods for further study. The most abundant insects in the areas where transmission was likely, such as huts with symptomatic people, were *Aedes aegypti* and *Culex fatigans* (currently known as *Culex quinquefasciatus*). These mosquitoes were present in 82% and 81% of the active disease sites, respectively. A precipitin test was performed on the engorged mosquitoes to determine which species they had fed upon. All of the *A. aegypti* collected in the plateau region with recent bloodmeals reacted positively to human antigens. Of the *C. fatigans* collected, 79% were positive for human antigens, 39% were positive for fowl antigens, and 18% had mixed bloodmeals. The frequent presence of mosquitoes in affected dwellings, along with the large number who were found to have fed on humans, was further circumstantial evidence that CHIKF was a mosquito-borne illness.

Following the initial description of disease and epidemiological investigation, Dr. Ross attempted to isolate and study the etiological agent of CHIKF. Dr. Ross had cohorts of mice shipped to his workstation in Newala. The mice were of the albino Swiss strain



from the Entebbe Institute colony. They were fed bread and milk, and upon arrival they were fed baby food which was unfit for human consumption. Work was slow due to cannibalism in the mouse colony and illnesses such as *Salmonella typhimurium* and Theillers mouse encephalomyelitis. The research team also obtained 2 juvenile rhesus monkeys for use in their studies [41].

Dr. Ross attempted to isolate the virus from various sources. Due to the similarity of this illness to dengue, the speed with which it spread, and Dr. Lumsden's observations, he focused on arthropods. Dr. Ross began by studying arthropods caught in what was believed to be the active transmission area, bed bugs caught in the hut of an infected individual, and freshly reared mosquitoes allowed to feed on febrile patients. Since the goal of this work was to isolate the agent, acute human sera were also collected. Dr. Lumsden provided the arthropods for testing.

To isolate the etiological agent of CHIKF, mice were injected either IC or IP with acute sera. Some of serum samples were lethal in mice, with IC injections more likely to lead to death than IP injections. Also, the time to death was shorter on average in animals that received the inoculation IC. The animals that were given acute sera had a 34.1% survival rate [41].

Forty mosquitoes were bred and allowed to feed on febrile patients. Of these, 28 survived and were tested further. Seventeen of the mosquitoes, or 61%, produced a lethal infection when homogenized and used to inoculate mice. Of the 17 infected mice, 5 were selected to generate brain homogenates, which were shown to be capable of infecting other mice. A brief attempt was made to have these deliberately infected mosquitoes feed on baby mice with no success. Wild-caught mosquitoes were pooled by genus and homogenized in saline. Overall, 18 pools were produced and used to infect mice, of which 16 groups (89%) experienced mortality. Bed bugs were also collected and homogenates were used to infect mice, some animals did become moribund, but brain homogenates from these mice were not able to infect other mice. Mosquito homogenates

were passed through a Seitz filter and were still found to be lethal in mice. The ability of filtered brain homogenates from infected mice to remain lethal pointed to this agent being a virus. The ability of filtered mosquito homogenates to cause lethal infection pointed to a mosquito-borne arbovirus.

In a preliminary attempt to characterize the taxonomy of the newly isolated CHIKV, a series of cross neutralization tests was performed. For these experiments, mouse hyperimmune sera were generated against CHIKV, 2 strains of dengue virus (DENV) type 2, and SINV. As expected, the anti-CHIKV serum was able to neutralize CHIKV. Interestingly, anti-DENV-2 Hawaii serum had low to moderate levels of cross-neutralization, but anti-SINV serum had no neutralization despite the fact that we now know CHIKV belongs to the same genus as SINV [41]. A couple of years later, 2 separate scientific groups completed serological and antigenic testing. These groups saw that the causative agent of CHIKF was probably an alphavirus closely related to SFV and MAYV [42].

### **Chikungunya Fever**

As stated earlier, Dr. Robinson was the first physician to observe and report CHIKF [39]. CHIKF is generally symptomatic. Only 3-25% of people who seroconvert are asymptomatic [43]. The clinical manifestation of CHIKF is very similar to that of dengue. The observations that were seen by Dr. Robinson remain relevant in the more recent outbreaks caused by CHIKV. The incubation varies between 1-12 days. Generally the virus is not lethal; however it is believed that roughly 1 in 1,000 infected people will develop complications and succumb to the illness [44]. Onset of the acute illness is generally very sudden and is characterized by intense arthralgia accompanied by a high fever reaching upwards of 105°F. Rash is another common sign (40.1%) and is generally found on the trunk and medial portions of the limbs. Neurological involvement

is less common, with signs and symptoms such as delirium, dizziness, and convulsions occurring in only 12% of patients [43,44]. The arthralgic symptoms are generally symmetrical and focus on multiple joints such as elbows, fingers, toes, and wrists. CHIKV is especially noteworthy for its ability to produce chronic arthralgia relative to SINV and ONNV [45].

One recent study was done after a CHIKV epidemic ravaged La Reunion island [46]. In this retrospective study, Sissoko *et al.* interviewed 3,539 people who were infected during the original outbreak on La Reunion between March 1st and June 30th 2005. Of those, only 147 people were able to fulfill all of the inclusion criteria for the study. Upon interview, 43% of the people claimed that they have completely recovered and 21% of the people claimed a single episode of recurrence of the arthralgic symptoms. The remaining 36% of the patients were still experiencing symptoms over the period of 15 months after the infection.

Diagnosis of CHIKF is done epidemiologically, clinically, and through laboratory techniques. Generally, a case becomes probable if the patient resides in or recently traveled to an epidemic site. However, due to the similarity of dengue fever and CHIKF and the fact that they are present in some of the same areas, a strong focus is put on to laboratory confirmation. Techniques for confirmation include viral isolation, viral RNA detection using RT-PCR, and antibody analysis. Generally, it is best to obtain samples within two days of the onset of illness. The RT-PCR can prove useful for diagnosis up to one week after the onset of symptoms [47-49]. Using an indirect immunofluorescence assay (IFA) or IgM enzyme-linked immunosorbent assay (ELISA), antibodies can be seen 2-7 days after onset and IgG can be found as early as two days after onset [50,51].

## **Internal Ribosome Entry Site and its Relevance for Arbovirus Vaccine Development**

In eukaryotic cells, production of proteins is generally accomplished by translation of mRNA in a cap-dependent manner. The 5' methylated cap is used to recruit a series of eukaryotic initiation factors (eIF) that forms a complex which is used to recruit ribosomes. The ribosomes then scan in a 5' to 3' direction until a start codon is found [52]. Most viruses, including alphaviruses, also use this cap-dependent method to produce viral proteins. Some viruses, however, use a different mechanism to initiate translation of viral proteins. Poliovirus (PV) and encephalomyocarditis (EMCV) do not require a 5' cap to initiate translation [53,54]. An internal sequence in the RNA genomes of these viruses is necessary for translation and was named the internal ribosome entry site (IRES). To demonstrate the internal initiation of translation, an IRES was inserted into a circular RNA. Chen *et al.* then removed all stop codons from the RNA. They found that ribosomes were able to bind and produce polyproteins that only could have been made by ribosomes translating the RNA multiple times. The researchers also demonstrated that if the IRES sequence was mutated, translation did not occur [55]. IRES sequences and conformation vary dramatically, and currently there is no bioinformatic approach to identify them. Therefore, IRES elements are classified through functional assays, which measure an RNA sequence's ability to initiate translation internally [56,57].

Multiple viruses utilize IRES elements, and these IRESs can be classified into 4 distinct types. The classification is based on the RNA secondary structure that the IRES element contains and how this secondary structure recruits ribosomes and eIFs. A representative of the type 1 IRES is found in PV. The EMCV IRES element is the prototypical type 2 IRES. Type 1 and type 2 IRES elements recruit multiple eIFs,

forming a complex which allows the ribosomes to sit upstream from (type 1) or directly on (type 2) the start codon [58,59]. A type 3 IRES-containing virus is hepatitis C virus (HCV), and its elements only require eIF3 and eIF2a to recruit the small ribosomal subunit directly on the initial start codon [60,61]. The final type of IRES element actually requires no initiation factors. The type 4 IRES element used by hepatitis A virus initiates translation on a non-AUG codon. This IRES directly recruits the 40s subunit and initiates translation almost immediately [62].

The EMCV IRES is commonly used in eukaryotic expression systems to produce proteins. However, during an experiment by Finkelstein *et al.* an interesting attribute of the EMCV IRES was discovered [63]. They were using the IRES element in the SF9 *Spodoptera frugiperda* cell line, which is from the Fall Armyworm Moth. It was found that the EMCV IRES was unable to initiate translation of luciferase (Luc) in these insect cells. When the 450 nucleotide IRES element was removed, the reporter was expressed at normal levels due to cap-dependent translation. The researchers then wanted to make sure the RNA remained intact after electroporation. To this end they completed a northern blot and found that the IRES-containing RNA was intact. The researchers concluded that the EMCV IRES elements “do not efficiently support internal initiation” in insect cells [63].

The EMCV IRES’s unique ability to translate efficiently in mammalian cells but not in insect cells drew attention to its potential use for vaccine development. This is important due to the nature of dual-host nature of the alphavirus lifecycle; by removing the ability of the virus to infect arthropods, the virus loses its ability to spread. A vaccine for VEE, called TC-83, was developed in 1961, but remains unlicensed; it is only available for laboratory workers and military personnel under an Investigational New Drug (IND) protocol. The vaccine was produced by serially passaging a strain of VEEV, Trinidad donkey (TRD), in a guinea pig heart cell line [64]. The vaccine remains partially virulent, causing symptoms resembling a wild-type (wt) VEEV infection in

approximately 40% of vaccinees [65]. Another drawback of this vaccine is its ability to infect mosquitoes, opening the door to unintended spread of the vaccine by mosquitoes to naive individuals, followed by reversion and the potential to generate an equine-amplified epidemic. The TC-83 vaccine is able to infect mosquito cells *in vitro* and mosquitoes are able to become infected *in vivo* by feeding on vaccinated animals. The problem was realized when the vaccine strain was isolated from wild mosquitoes in Louisiana in 1971 [66].

Volkova *et al.* set out to develop a strategy to render an alphavirus incapable of infecting mosquitoes, utilizing the TC-83 vaccine strain for the initial proof of concept [67]. Multiple strategies were developed to insert the EMCV IRES element into the TC-83 genome (Figure 1). The IRES element plus 4 codons of EMCV sequence were inserted at the 5' end of the structural ORF. One version (VEEV/IRES) left the sg-promoter intact, and a second version (VEEV/mutSG/IRES) inactivated the sg-promoter through synonymous point mutations. The point mutations needed to be synonymous to preserve the wt amino acid sequence encoded by the nsP4 gene. In both cases, the translation of the structural genes would have to be initiated via ribosome binding mediated by the IRES. The difference between the two constructs is that VEEV/IRES produces a sgRNA to act as template as well as the genomic RNA, while VEEV/mutSG/IRES relies entirely on internal initiation for the production of structural gene products [67].

Initial experiments focused on the ability of the IRES-containing VEEV strains to replicate in vertebrate cells. VEEV/IRES replicated to high titers in baby hamster kidney (BHK) cells, however VEEV/mutSG/IRES virus only replicated to  $10^7$  pfu/ml post-electroporation. Five separate plaques were selected from the 24 hour post-electroporation plaque assay. There were mutations found in each VEEV/mutSG/IRES at amino acid (AA) positions 370 or 371 of the nsP2 protein which, when reintroduced into the parent virus, allowed for higher titer production in cell culture. The capabilities of the

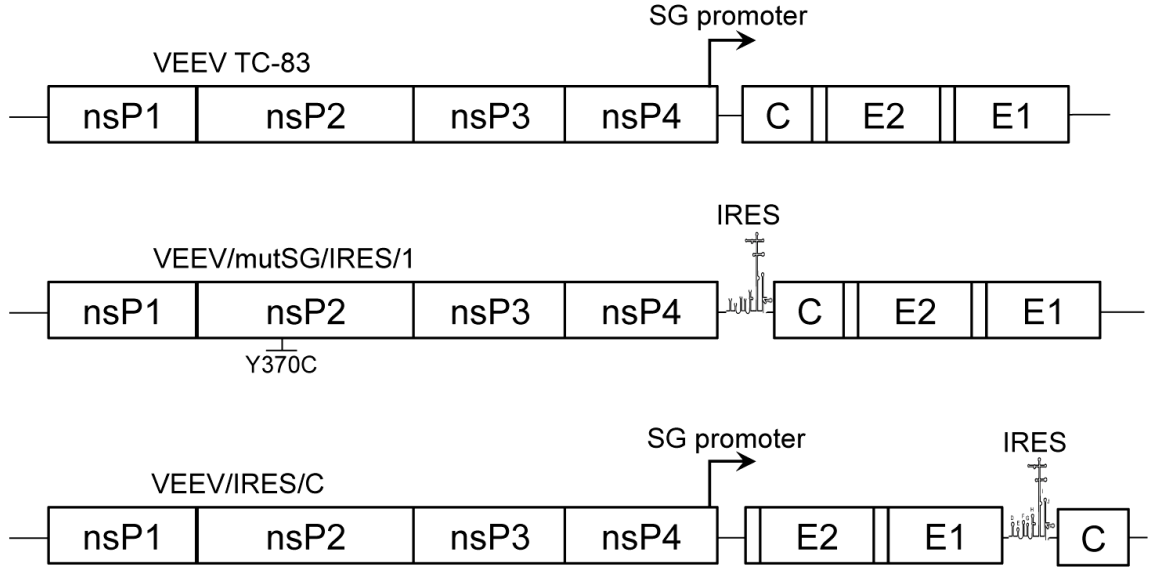


Figure 1: IRES-based TC-83 vaccine strategies

Diagram of IRES versions 1 and 2 compared to wild-type TC-83. Reproduced with permission from Guerbois *et al.*[68]

constructs to produce genomic and sgRNA species were then determined. As expected, the wt-VEEV was able to produce a full length and sgRNA. VEEV/IRES, with its intact sg-promoter, was also able to produce the 2 separate RNAs, whereas VEEV/mutSG/IRES was only able to produce the genomic RNA.

Following initial characterization in mammalian cells, the viruses' ability to replicate in C7/10 *Aedes albopictus* cells was examined. It was found during the initial passage that VEEV/IRES was able to replicate to  $10^{10}$  pfu/ml. This high titer was achieved in the subsequent passage as well. VEEV/mutSG/IRES, however, only replicated to 150 pfu/ml after the first passage and was undetectable after the 2nd passage. This indicates that the VEEV/IRES vaccine is able to replicate in mosquito cells, but VEEV/mutSG/IRES is not. To confirm this, the viruses were directly electroporated into the C7/10 cells and a growth curve was done. VEEV/IRES was able to replicate, albeit at a severely delayed rate compared to the parental TC-83 virus. VEEV/mutSG/IRES with the adaptive mutations in nsP2 remained incapable of replication in these mosquito cells. Volkova *et al.* then sequenced VEEV/IRES harvested

from C7/10 cells and found that it was in fact deleting a large portion of the IRES, leaving only 13-15 nt. Since this virus still produced sgRNA, translation of the envelope proteins could occur through cap-dependant manner when the IRES was removed.

Due to the higher stability of VEEV/mutSG/IRES, it was chosen for the initial animal studies. An attenuation study utilized 6-day-old NIH Swiss mice. VEEV/mutSG/IRES was found to be significantly less lethal than TC-83 when injected IC into these newborn animals. This demonstrated that the IRES approach could significantly attenuate a virus in addition to restricting its host range. VEEV/mutSG/IRES was then used in a protection experiment wherein 5-6-week-old mice were vaccinated SC with either TC-83, VEEV/mutSG/IRES, or phosphate buffered saline (PBS). Four weeks post-vaccination, the subjects were challenged with VEEV strain 3908. TC-83 protected 100% of the animals, and the cell-adapted VEEV/mutSG/IRES protected 80% of the animals from the lethal challenge. VEEV/mutSG/IRES was also immunogenic in infant (6-day-old) mice, as the 12 animals that survived the IC injection from the attenuation experiment were challenged 5 weeks later and 10 of the 12 survived. Interestingly, though, pre-challenge sera from animals receiving VEEV/mutSG/IRES were below the limit of detection in a plaque reduction neutralization test at an 80% endpoint (PRNT<sub>80</sub>). Thus, the IRES-based alphavirus platform was shown to effectively limit host range and also to be both attenuated and protective in mice [67].

Guerbois *et al.* designed and tested a second VEEV vaccine using the IRES strategy [68]. VEEV/IRES/C leaves the sg-promoter intact; however, the C gene is placed after the E1 gene, under the translational control of the EMCV IRES [68] (Figure 1). In theory, this allows the virus to produce sgRNA for the cap-dependent translation of the glycoproteins. Translation of C, however, relies on internal initiation of the ribosome at the IRES. This strategy was designed to increase the immunogenicity of the virus by allowing the production of sgRNA, generating more glycoproteins, critical viral



antigens. The vaccine conferred 100% protection in mice against a lethal challenge. The vaccinated subjects also developed average PRNT<sub>80</sub> titers of 1:184, with 8 of 10 seroconverting. As expected, however, this vaccine was less attenuated compared to the VEEV/IRES. During an attenuation study, 50% of murine pups inoculated IC with VEEV/IRES/C succumbed to illness, whereas VEEV/IRES was fatal in only 25%. The second vaccine version was also incapable of orally infecting mosquitoes and even after intrathoracic (IT) inoculation little or no replication occurred [68].

The IRES-based vaccine platform has been adapted to multiple alphaviruses. The platform was first adapted to CHIKV and will be explained in great detail in the following sections of this dissertation [69]. Wang *et al.* also made a CHIKV vaccine based on chimeric VEEV or EEEV nonstructural genes and CHIKV structural genes [70]. A vaccine was also designed for EEEV using the EEEV strain FL93 backbone and the IRES strategy [71]. A second VEEV vaccine attempt was done using a subtype IE strain of VEEV, 68U201, and utilizing both IRES-based strategies [72]. Currently, another VEEV vaccine based on the ID ZPC938 strain has been developed and has shown promise as a vaccine against both endemic and epidemic VEEV (Rossi unpublished). WEEV and MAYV IRES-based vaccines are also in early stages of development and testing (Weaver laboratory unpublished).

## **Chikungunya Animal Models**

Initial work with CHIKV was focused on infant, (>2 weeks of age) Swiss outbred mice due to the lack of signs of disease in adult outbred mice [41]. Recently, other models have been investigated, yet at least in small animal models there is no single choice that mimics all aspects of human disease and immunity. Small animal models that

develop an arthritic phenotype are limited. Infant models, such as CD-1 mice, are still a large focus [73]. These animals develop muscle and joint histopathologic lesions similar to those found in humans. Newborn or 14-day-old outbred CD-1 mice inoculated SC develop multiple signs of illness. These animals develop pathologic lesions in the skeletal muscle, lethargy, and in some cases hind limb paralysis. They also develop calcification in the joints. However, due to the age restriction of these models, it is difficult to use them for vaccine studies.

Recently, work has been done on C57Bl/6 mice to try to develop an immunocompetent adult arthralgic model. Gardner *et al.* found that if they injected 5-6-week old animals on the ventral side of the foot proximal to its ankle, they could simulate arthritis. Infected mice develop a strong cellular infiltrate consisting of monocytes and macrophages at the site of injection. These animals reportedly develop arthritis and myositis in the isolateral leg opposite the site of injection [74]. Though this model is effective at elucidating the mechanism of arthralgic symptoms in humans, it remains highly insensitive. Also, although footpad swelling is quantitative, the arthralgic histopathology is subjective and is not as easily analyzed as a survival outcome model.

There was an obvious need to develop an animal model that can provide a severe or lethal phenotype after challenge. With a severe disease phenotype it would be easier to test the efficacy of vaccines and would be a more stringent method. Couderc *et al.* studied what sensitizes a mouse to CHIKV disease by measuring the effects of age and interferon (IFN) type 1 functionality on disease progression. Initially, they worked with C57Bl/6 inbred mice at different ages. Twelve, 9 and 6 day old mice were inoculated ID with  $10^6$  pfu, and there was a sharp difference in disease phenotype. At 12 days of age the animals demonstrated few signs of illness. Animals inoculated at 9 days of age developed morbidity and approximately 40% succumbed to a fatal illness. Animals given the virus at 6 days of age also developed morbidity; however, all of the animals

became moribund and were euthanized by day 13. Couderc *et al.* were able to claim that there is an age-dependent sensitivity in mouse models of CHIKV disease [75].

A critical gap in CHIKV animal models remained an adult, small mammal that exhibits severe signs of illness. Previous work has shown that Type I IFN is important in the control of alphavirus infection [76-78]. Knowing that a mouse defective in this receptor would probably develop a severe phenotype post-challenge, Couderc *et al.* began to develop a new model. They focused on 129 backbone mice that have a defective type 1 IFN receptor. These IFN $\alpha$ /bR KO mice, also named A129, were tested as homozygous and heterozygous KOs. The 129, A129<sup>+/-</sup>, and A129<sup>-/-</sup> mice had drastic differences post-challenge outcome with a La Reunion isolate of CHIKV. The wt mice were unaffected post-challenge, even with a dose of 10<sup>6</sup> pfu. The heterozygous A129 KOs were similarly unaffected when challenged with wt-CHIKV. However, the homozygous A129 KOs developed lethargy and loss of muscle tone by day 2 and succumbed to illness by day three. Other signs of illness in these animals were hunched posture, ruffling of fur, and drastic weight loss. The LD<sub>50</sub> was 3 pfu in the A129<sup>-/-</sup> mice. In addition to significant morbidity and mortality, the homozygous A129 animals developed high viral titers in the 8 tissues measured by day 3 [75].

Larger animal models also exist for CHIKV infection. CHIKV was first tested in Rhesus monkeys during the initial characterization work done by Ross *et al.* [41]. More recently, CHIKV infection of cynomolgus macaques has been described experimentally [79]. In one experiment, Labadie *et al.* inoculated the animals intravenously (IV) with varying doses of CHIKV and then observed the animals for signs of illness. A total of 13 animals ranging from 3-5 years old were used in the study. They inoculated 12 animals with doses ranging from 10<sup>1</sup>-10<sup>8</sup> pfu and used one animal as a sham-infected control. At the lowest dose, the animals developed no signs of illness; however animals receiving 10<sup>2</sup>-10<sup>6</sup> pfu all developed fever and most developed a morbilliform rash. Animals receiving yet a higher dose exhibited other signs of illness, such as subcutaneous edema

and joint effusion. The animals that received the  $10^8$  pfu dose had a 25% survival rate and the animals that succumbed to the infection had meningoencephalitis.

Labadie *et al.* also ran other experiments where they infected 13 cynomolgous macaques with  $10^3$  pfu either IV or ID. The animals developed a peak viremia by day 2, with an average of  $10^9$  RNA copies/ml. They became hyperthermic by day 2 and their temperatures generally remained above normal until day 7. Half of the animals also developed gingivorrhagia (bleeding of the gumline). Cell counts and other bloodwork were done on these subjects, and several interesting observations were made. The five animals tested all showed elevated aspartate transaminase (AST) and alanine transaminase (ALT) levels until day 15, which is indicative of liver damage. Platelet and leukocyte depletion were observed from days 2-6. Histopathology was also completed on animals that were given an intermediate dose. Splenic lesions were found at days 6 and 32 in the red pulp. At 44 days post infection lymph nodes still had expanded follicles. Necrotic lesions were also found in the liver, which may explain the increase of ALT and AST. Labadie *et al.* also found drastically increased levels of IFN $\alpha$ /b during the first 5 days of infection [79].

## Chikungunya Vaccine Development.

The first attempt at a CHIKV vaccine was completed at the Walter Reed Institute of Research [80]. White *et al.* used an African CHIKV strain designated 167. This virus was grown in green monkey kidney (GMK) cells and concentrated suspension cultures. Harvested virus was formalin-inactivated and inoculated IP into 3-4 week old Swiss Bagg mice. The mice were boosted on day 7. At day 14, the mice were challenged with 100-1,000 LD<sub>50</sub> of a homologous virus. The concentrated suspension-grown virus was more immunogenic than the GMK-grown virus, requiring about ¼ the dose to protect 50% of the mice from a lethal challenge [80].

The first attempt at a live-attenuated CHIKV vaccine was also done at the Walter Reed Institute of Research [81]. Levitt *et al.* had a small amount of the GMK-grown inactivated vaccine for at-risk personnel that had been tested in human volunteers and they wanted to increase the efficacy of the vaccine [82]. The initial virus used was a human isolate of CHIKV, termed 15561, from a 1962 outbreak in Thailand. The attenuation of the parent strain was completed through serial cell culture passages in MRC-5 cells, which are human embryonic lung cells. This virus was repeatedly plaque-purified and titered for 18 passages. On the 18th passage, Levitt *et al.* isolated three plaque clones that had favorable plaque morphology (homogenous 2-3 mm in diameter), clones 25-27. These three clones all were completely non-lethal when given IC to 120 1-3-day-old mice, whereas the parent strain was lethal in 73 of 120 mice. To assess efficacy, weanling 18-21-day-old CD-1 mice were vaccinated with 2.5, 4.5, or 6.5 log<sub>10</sub> pfu of the vaccine candidates. Clone 25 was the most efficacious, conferring 100% protection of against lethal challenge at 4.5 log<sub>10</sub>.

The researchers then further investigated the 181/clone 25 vaccine with non-human primate (NHP) testing [81]. The experiment used rhesus macaques and its goals were to observe viremia, antibody titers, and protection against virulent challenge. The

animals were split into 4 cohorts of 3 animals each. Three of the groups were given the vaccine at varying doses of either 3.5, 4.5 and 5.5 log<sub>10</sub>. The 4th group of animals was used as a sham-vaccinated control. Blood was collected daily from all animals for 7 days, and titrations were done on the serum samples. Levitt *et al.* did find a low level viremia in the vaccinated animals, generally peaking days at 2 and 3 post-vaccination. Then, on day 37 of the study, all NHPs were challenged intramuscularly (IM) in the hind leg with 5.0 log<sub>10</sub> pfu of the parent 15561 virus. The unvaccinated animals were all viremic on days 1-3 post-challenge, with an average peak titer of 4.7 log<sub>10</sub> pfu/ml. The 12 animals that received the vaccine remained aviremic for the duration of the study via plaque titration.

Turell *et al.* at Fort Detrick then wanted to examine the capability of the live-attenuated 181/25 vaccine to be spread by mosquitoes [83]. The ability of wt-CHIKV and the 181/25 vaccine strain to infect the Oahu and Gentilly colonies of *A. albopictus* and the Rockefeller colony of *A. aegypti* was assessed. When the 181/25 vaccine was injected IT, the mosquitoes were permissive to infection and the virus replicated efficiently. They also found that these IT-infected mosquitoes were able to infect mice through feeding in roughly 17-20% of attempts. Following artificial blood meals of 10<sup>7</sup> pfu/ml, *A. aegypti* became infected 32% of the time when feeding on the parent virus and 17% of the time while feeding on the 181/25 vaccine strain. These mosquitoes were then tested for transmissibility. Only those that fed on the parent strain showed any ability to transmit virus. Mosquitoes were also allowed to feed on viremic NHPs post-vaccination. Only 3 out of 627 mosquitoes became infected in this experiment [83].

Briefly, clinical trials are run in multiple phases with each phase testing a different aspect of the drug or vaccine. Phase I clinical trials focus on safety with a small group of human volunteers given either the experimental vaccine or a placebo. Phase II focuses on the efficacy of the new vaccine by testing on a larger group of people and measuring correlates of protection like neutralizing antibody titers and, if practical,

decreased disease incidence. Phase III trials are even larger, requiring participation of many medical doctors and subjects, and continue to focus on efficacy and safety with an emphasis given to obtaining information on how the treatment may be used in the safest fashion. In phase III (and if practical in phase II), vaccines are tested in a large group of naïve people from a locality which has the target agent actively circulating. Incidence of illness could then be compared between the experimental and control groups. Phase IV trials also utilize large groups of participants and generally occur after the drug/vaccine has been approved to look at long term side effects (referenced from the U.S. National Medical Library).

The 181/25 CHIK vaccine was evaluated in a phase I clinical trial, during which it was administered to 15 alphavirus-naïve people and 36 people who had been previously vaccinated with VEEV strain TC-83 [84]. The alphavirus-immune people developed no adverse effects following vaccination. In the alphavirus-naïve group, no definitive conclusions could be made to distinguish placebo- and CHIKV-vaccinated individuals after inoculation. The subjects vaccinated with CHIKV 181/25 produced a neutralizing antibody response by 30 days after vaccination [84].

The next step was to take the vaccine, now named TSI-GSD-218, into a phase II clinical, double-blind study. A group of 73 healthy adults participated in this study. One cohort of 59 people received a SC injection of the vaccine, and the remaining cohort of 14 people received a placebo in the form of cell culture fluid. The vaccine and placebo doses contained less than 0.02µg of neomycin and 2% human serum albumin. The 0.5ml vaccine dose containing  $10^5$  PFU was delivered IM into the deltoid muscle. The subjects were observed and interviewed on days 1-4, 10, 14, and 28 post-vaccination. During these interviews, the subjects were asked questions about any symptoms they had experienced, and blood draws and temperature checks were performed. The subjects also had their blood drawn at one year post-vaccination. At 28 days post-vaccination,

98.3% of the subjects had seroconverted with a PRNT<sub>80</sub> titer over 1:20. At one year post-vaccination, 85% of the vaccinated subjects remained PRNT-seropositive [85].

During the first 28 days post-vaccination, approximately 20% of subjects in the experimental and control groups complained of local symptoms at the site of inoculation. In the control group, 29% of people complained of flu-like symptoms, compared to only 22% of experimental subjects. In the experimental group, 5 of 59 people (8%) experienced transient arthralgia, compared to no subjects in the control group. The 5 subjects who complained of arthralgic symptoms all claimed mild to moderate unilateral pain in one or two joints [85].

The TSI-GSD-218 vaccine was not pursued further because, although it was immunogenic and relatively safe, it was apparently reactogenic and the commercial options for its use were limited. Recently, Gorchakov *et al.* examined the attenuation profile of the TSI-GSD-218 vaccine [86]. It was found that the attenuation of 181/25 relies solely on 2 point mutations in E2. The point mutations translate to 2 coding changes in E2 amino acids 12 and 82. When these mutations reverted to the parental sequence, the 181/25 virus became virulent [86].

Additional CHIKV vaccines are currently being developed and tested. In 2008, Wang *et al.* described a series of live-attenuated vaccines based on a chimeric approach [87]. This study focused on 3 types of chimeras. The structural genes were from a CHIKV La Reunion strain, which had been passaged 5 times in BHK cells. The nsP genes and the 5' and 3' UTRs were from one of three alphaviruses: VEEV vaccine strain TC83, EEEV strain BeAr436087, or SINV strain AR339. The most stringent model used to test the safety of these three vaccines was the 6-day-old CD-1 mouse inoculated either SC or IC. Mice that received the vaccines all survived the inoculations and exhibited no signs of illness, whereas wt-CHIKV proved lethal for 50% of the mice by day 6 following IC inoculation. At this time Wang *et al.* decided to focus on the VEEV/CHIKV and EEEV/CHIKV vaccines due to their high immunogenicity in pilot



studies. These chimeric viruses were produced due to the hypothesis that they could produce high levels of the target viruses structural protein but remain attenuated. The immunogenicity experiments focused on the use of the 3-week-old C57BL/6 mouse model. When  $5.8 \log_{10}$  pfu of either vaccine was delivered SC, mice generated average PRNT<sub>80</sub> titers greater than 1:200 by three weeks post-inoculation. This model did not allow for a lethal challenge at 6 weeks due to age-dependent resistance to fatal disease. However, animals that were vaccinated were protected against weight loss following virulent CHIKV challenge at 6 weeks. The sham-vaccinated animals lost about 5 grams on average, whereas the vaccinated mice maintained their weight [87].

A DNA-based CHIKV vaccine based on a consensus sequence of the E2, E1, and C proteins was produced by Muthumani *et al.* [88]. The consensus sequence was determined from 21 strains collected between 1952 and 2006. After the consensus sequence was generated, Muthumani *et al.* fused it to an IgE leader sequence to increase expression and secretion. The sequence was codon-optimized and the existing Kozak sequence was modified to increase ribosomal initiation [88]. In a separate study, the vaccine was tested in multiple animal models [89]. Mallilankaraman *et al.* vaccinated BALB/C mice IM 3 times at two-week intervals with 25ug of vaccine or control DNA. These animals were then challenged intranasally (IN) with  $10^7$  PFU of CHIKV strain PC-08, and the vaccine protected against the lethal challenge. The vaccine was then tested in rhesus macaques. The macaques were vaccinated with either the vaccine or empty vector at 0, 4, and 8 weeks with a dose of 1.0 mg IM. These animals all developed strong neutralizing antibody titers [89].

A virus-like-particle (VLP) vaccine for CHIKV has also been developed [90]. Akahata *et al.* used the glycoproteins of CHIKV strain 37997 in a lentiviral vector pseudotyped with a vesicular stomatitis virus G protein. Genetic material responsible for producing the VLP was electroporated into HEK293 cells, producing particles that incorporate the CHIKV glycoproteins. The vaccine induced neutralizing IgG when

NHPs were given 3 doses. Immune NHP serum was then passively transferred to mice, and was found to protect against a lethal challenge with the La Reunion strain of CHIKV. This vaccine has recently entered phase I clinical trials [90].

CHIKV E1 and E2 proteins expressed in insect cells have also been tested as a vaccine [91]. Metz *et al.* cloned in the E3/E2 and 6K/E1 gene combination downstream of a baculovirus promoter. These plasmids were transfected into *Spodoptera frugiperda* cells. The proteins were expressed using a Bac-to-Bac expression system, by Invitrogen, purified using spin columns, and used to vaccinate rabbits. The rabbits produced neutralizing antibody titers after vaccination with the purified E2. However, the E2 vaccine has yet to be tested in an animal model that allows for lethal challenge [91].

### **Chikungunya Transmission.**

CHIKV exists in two distinct transmission and maintenance cycles: an enzootic and epidemic cycle (Figure 2). The epidemic cycle occurs in Africa, India, and Southeast Asia and was briefly seen in Italy and France; it requires only a viremic human host and the vector mosquitoes. The epidemic cycle revolves around *A. aegypti* and, more recently, *A. albopictus* feeding on humans, which can act as amplifying hosts to continue the cycle. In the original work done by Dr. Lumsden and Dr. Ross, *A. aegypti* was suspected to be the vector of CHIKV [40,41]. However, due to the recent emergence of CHIKV and the epidemic characteristics they observed, Lumsden and Ross were obviously only observing the epidemic cycle of CHIKV. Others have been able to consistently collect CHIKV-positive *A. aegypti* in other outbreak areas from Africa, India, and southeast Asia [92,93]. Definitive proof of the *A. aegypti* mosquito's ability to transmit the virus was provided by a study in which a human was directly infected by an experimentally infected *A. aegypti* [94]. In the recent outbreaks, *A. albopictus* has proven

to be a potent vector for CHIKV [95]. This new component of the epidemic cycle is believed to be caused by an A226V substitution in E1 which has been shown to greatly enhance the infectivity of the virus to this new vector [96,97]. Generally, epidemic outbreaks occur after heavy rain increases the chance of spillover from the enzootic cycle.

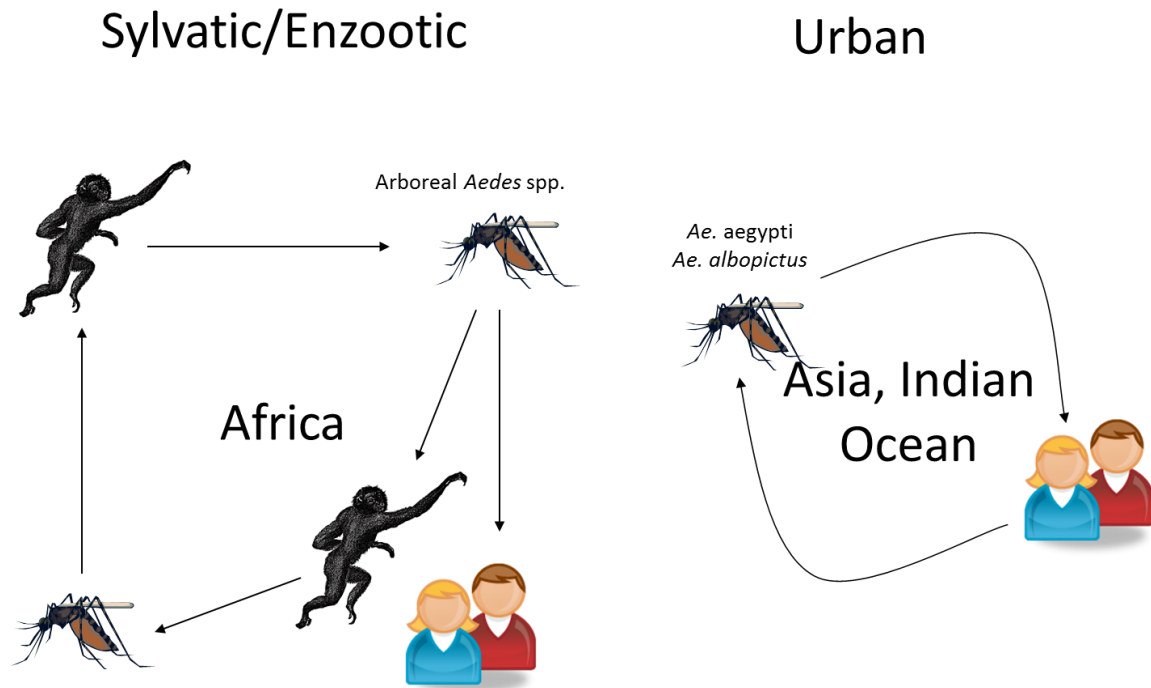


Figure 2: Transmission cycle of CHIKV

Sylvatic/enzootic and urban transmission cycles of CHIKV. Figure courtesy of Dr. Scott Weaver.

The enzootic cycle, which is believed responsible for viral maintenance, has only been observed in Africa. This sylvatic cycle primarily involves *Aedes* species, such as *A. taylori*, *A. fucifer*, *A. africanus*, and *A. luteocephalus* [98,99]. These mosquitoes are known to feed on NHPs. It was shown early in the history of CHIKV research that NHPs have a high seroprevalence against CHIKV and can be experimentally infected with the virus [100]. These NHPs are the amplifying hosts for the sylvatic *Aedes* species mosquitoes to feed upon and propagate the transmission cycle. During this cycle, people can be directly infected by some of these enzootic vectors due to the human proximity to

wooded areas. The *A. furcifer* mosquitoes are known to enter villages where they can feed upon a naïve human [101]. Once a human is infected and conditions are favorable to *A. aegypti* or *A. albopictus* feeding, the outbreak cycle can begin. Initially, Lumsden and Ross believed *Culex* mosquitoes were possible vectors, but they were later proven incapable of experimentally transmitting the virus to humans [92].

### **Chikungunya Fever Outbreaks and Distribution.**

While the first studied outbreak of CHIKF occurred in 1952-1953 in Tanzania, it is believed to have existed before that time [102]. Carey made a retrospective examination of historical reports of dengue and CHIKF cases and believed misdiagnosis had occurred. His work implies that CHIKV outbreaks could have occurred as early as 1779 [102]. From the first proven outbreak until 1992, there were multiple outbreaks and isolations of CHIKV. The first outbreaks occurred in Tanzania, Uganda, and the Democratic Republic of Congo. Between the 1960s and 1990s, many other African countries such as Zimbabwe, Senegal, Nigeria, South Africa, Kenya, Burundi, Gabon, and Malawi experienced outbreaks of this disease [103]. In 1958 the first non-African outbreak was observed in Thailand, and from that time until 1989 CHIKV was frequently detected in a myriad of southeast Asian countries such as Pakistan, Myanmar, Vietnam, India, Cambodia, Malaysia, and Indonesia [104-109].

Recently CHIKV has entered the public eye due to a series of outbreaks, which have their origins in eastern Africa. In 2004, a series of outbreaks occurred on the coast of Kenya [110]. Later, several other outbreaks occurred in islands of the Indian Ocean, most notably the French territory of Reunion island. The island saw roughly 300,000 cases between 2005-2006, which is 38% of the population. Approximately 2,200 people

required medical care and were hospitalized [111]. Then, in 2005, India started reporting large outbreaks of CHIKV infection [112]. During this time Southeast Asia also started to report outbreaks of the CHIKV [113]. Interestingly, autochthonous transmission also took place in France and Italy, indicating the expansion of this virus into novel regions [114,115]. There are no known cases of CHIKV transmission in the United States, although infected returning travelers have developed disease while in the U.S. [51]. CHIKV transmission is still very active, and there are frequent alerts initiated from the International Society of Infectious Disease of confirmed and suspected CHIKV cases. During the process of writing this dissertation there have been multiple, short communications from a series of locations such as the Philippines (multiple separate incidences), Papua New Guinea, Indonesia, and India.

The first phylogenetic analysis grouped CHIKV into 3 geographical genotypes: Asian, West African, and the East/Central/South African (ECSA) [116]. To conduct this analysis, Powers *et al.* used 18 different CHIKV sequences along with sequences of related alphaviruses. A 1050 basepair (bp) PCR amplicon fragment of E1 was analyzed and sequences were aligned and analyzed phylogenetically using both distance matrix and maximum parsimony algorithms. The samples generally grouped according to the location of the isolate. Powers *et al.* were also able to show the close relation of ONNV, another Old World alphavirus, to CHIKV. More recently, a more in-depth study was done looking at full genome sequences of a very large number of historic and recent isolates of the virus. Since this work was done after the outbreaks starting in 2004, it was able to effectively determine which virus genotype(s) were responsible for the new, large outbreaks [117]. The study used full length nsP and sP ORF sequence of 80 viruses in a maximum clade credibility tree. The older isolates were easily grouped by their suspected geographical clade. However, many of the new isolates from the recent outbreaks formed another distinctive clade, the Indian Ocean outbreak group. The first viruses in this group were a pair of isolates found in Kenya collected during the initial

phases of the epidemic. Viruses collected from many other sites such as India, Reunion, Mauritius, Seychelles, Japan, Malaysia, Comoros, Japan, Singapore, and Bangladesh were all grouped in this newly formed clade. During this time, other isolates were collected that represented their geographical clades such as samples from Malaysia in 2006 that were found to be closely related to other viruses of the Asian genotype. Using the tree, Volk *et al.* were able to estimate that the new clade diverged from the ECSA clade in roughly 2003. (Figure 3) Using a Bayesian MCMC method, CHIKV was found to undergo roughly  $4.3 \times 10^{-4}$  substitutions per year, although the rate in the epidemic lineage was much higher. Common mutations found in the newly formed genotype involved two codons in C and one codon in E1. The E1 mutation, as previously discussed, enhances CHIKV replication and infection rates in *A. albopictus* [96,97]. Volk *et al.* also developed trees using only E1 sequences, but found the topology of the tree did not resolve properly compared to the full genome sequence analysis. For instance, the ECSA group would not group together as it did using full-length sequence. Volk *et al.* made the assertion that full genome sequence is required to produce reliable phylogenetic models [117].

A need for a vaccine represents not only the gap in knowledge but the goal of my dissertation. I will present work to address the multiple concerns of developing any vaccine, especially a live-attenuated one. Some of the important gaps that will be addressed is whether a live-attenuated vaccine can be produced in a safe fashion using small animal models and whether it will remain protective against a wild-type CHIKV infection. I will also expand the knowledge of a commonly used A129 mouse model for CHIKV infection. My goal is to produce a highly efficacious and extremely safe vaccine which is stable and unlikely to be accidentally transmitted.



## **CHAPTER 2 METHODS**

The following chapter will cover the experimental designs and protocols used to achieve the goals of this study. The purpose of this chapter is to give a broad understanding of all techniques used, and specific details or adaptations will be covered in the results chapters.

### **Production of Infectious Clones**

What follows is an overview of the production of infectious clones. The first step was developing a strategy to produce the desired plasmid. To design the required primers, template sequences were introduced into a freeware software program called Amplify 3, (<http://engels.genetics.wisc.edu/amplify/>). In addition to amplifying the desired section of the template plasmid, these primers could also be used to add restriction enzyme sites, introduce point mutations, or add overhangs for fusion PCR. Generally primers were selected for their proximity to naturally occurring restriction sites in the target sequence. Once the primers were designed in silico they were synthesized by Sigma-Genosys, St. Louis MO. Stocks of lyophilized primers were diluted to 100  $\mu$ M, and working stocks were further diluted to 5-10  $\mu$ M.

Some fragments were unable to be joined with a simple restriction digest and ligation. This could be due to a myriad of reasons such as a lack of opportune restriction sites, requirement for multiple point mutations, or the need to join two distinct sequences directly together. If this was the case, fusion PCR primers were designed. A fusion PCR primer consisted of annealing and non-annealing portions. The primer's annealing portion (its 3' end) would bind to the template and act as a standard primer, but the non-annealing portion (its 5' end) could contain a sequence that didn't match that of the template but was included to achieve several cloning goals. For example, the non-



annealing portion could match the sequence of a second template to allow subsequent joining of the two templates through fusion PCR. Alternately, the non-annealing portion could anneal directly to another fusion primer used on a separate PCR fragment to introduce small segments of DNA, such as restriction sites or to introduce large groups of mutations over a small area. Refer to figure 4 for a graphical explanation.

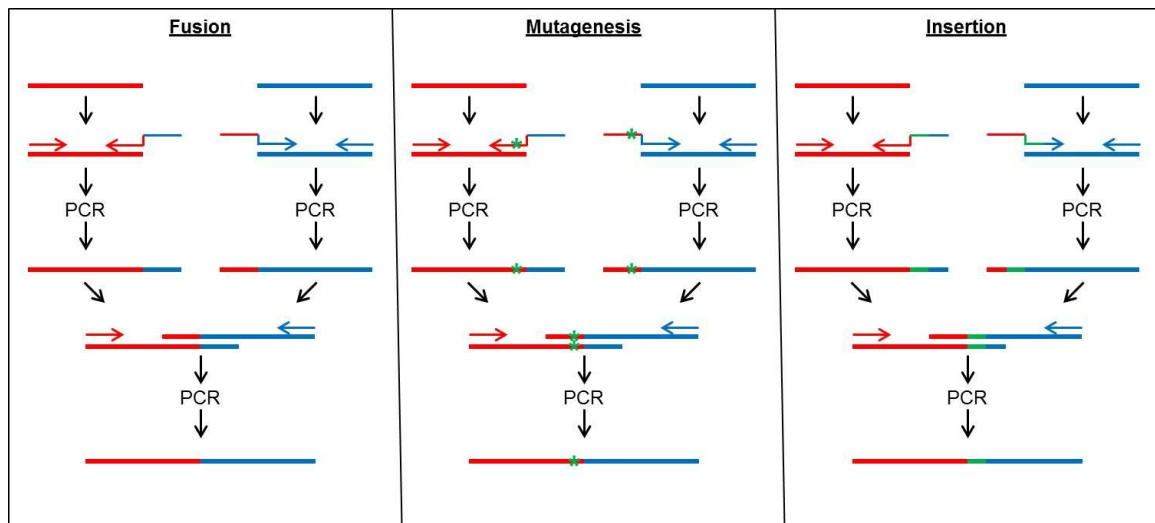


Figure 4: Fusion PCR

Graphical representation of the strategies and uses of fusion PCR. Red = template 1, blue = template 2, green = insertion or mutagenesis element.

To produce the desired dsDNA fragments, PCR was performed using Phusion Taq polymerase from Finnzymes (Espoo, Finland). This reaction could be performed with either standard or fusion primers. The manufacture's protocol was used with slight modifications. A 50  $\mu$ l reaction would be produced using 10  $\mu$ l of 5x high fidelity buffer, 1  $\mu$ l of 10mM dNTP mix, 2  $\mu$ l each of a forward and reverse primer, 1-3  $\mu$ l of the template DNA (~5ng), 0.5  $\mu$ l of enzyme, and the remaining volume filled with nuclease free water. The reactions were then placed into a 2720 thermocycler from Applied Biosystems (Carlsbad, CA) and a hot start PCR was performed. The reaction conditions for the standard PCR amplification can be found in figure 5.

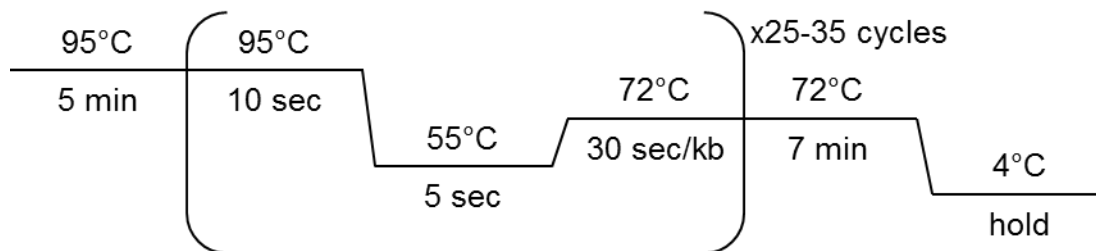


Figure 5: Standard PCR cycle parameters

Conditions for standard amplification PCR.

After the PCR was completed the amplicon DNA was isolated via agarose gel electrophoresis. Briefly, 8  $\mu$ l of a 6x loading dye from New England Biolabs (NEB) (Ipswich, MA) was added to the 50  $\mu$ l sample. Using Lonza agarose and tris acetic acid and EDTA buffer (TAE), a 1.2% agarose gel was made. The agarose and TAE were combined at the proper ratio and heated to liquify the agarose. Once the gel was cool enough to handle, ethidium bromide from Life Sciences (Pittsburg, PA) was added. The 1 mg/ml ethidium bromide was diluted 1:10,000 in the gel for a final concentration of 100ng/ml. The gel was cast in a Thermo Scientific gel apparatus (Waltham, MA). After the gel solidified it was submerged in TAE. The samples and a properly sized DNA ladder from Promega (Madison, WI) were loaded into the gel. An electric current ranging from 45-115 volts was run through the gel to separate the DNA fragments by size. After the gel was resolved an image was captured using a FlourChem Q camera from Cell Bioscience (San Jose, CA) and the correct bands were excised using a UV light table and scalpel. These DNA fragments were purified away from the agarose using a Qiaquick Gel Extraction Kit from Qiagen (Venlo, Limburg) using the manufacturer's protocol. The resulting DNA was resuspended in 30  $\mu$ l of nuclease-free water.

After the desired fragments had been generated and purified, they needed to be sequenced. To sequence the fragments, a shuttle vector, pRS2, was used (produced and provided by Dr. Frolov). First, restriction enzymes from NEB were used to digest the proper fragments fragment and the pRS2 vector in separate reactions. These reactions involved adding 1-2  $\mu$ l of any restriction enzyme, 4  $\mu$ l of bovine serum albumin (BSA)

and 4  $\mu$ l of the required buffer to the 30  $\mu$ l of gel purified DNA. The 40  $\mu$ l reaction was incubated at 37°C for 1-2 hours depending on the buffer efficiency. The digestion reaction for the vector was similar except that it included 1  $\mu$ l of calf intestine phosphatase from NEB to prevent self ligation. After the reaction was complete, the digested DNA was electrophoresed and extracted as described earlier to purify the desired fragment.

After the desired fragment and vector were digested and purified they needed to be ligated together. This was achieved by using Stratagene T4 DNA ligase (La Jolla, CA) in a 20  $\mu$ l reaction. The reaction generally contained a 3:1 insert to vector ratio of DNA. A typical reaction was 2  $\mu$ l of 10x buffer, 1  $\mu$ l of ligase, 12  $\mu$ l of insert, and 5  $\mu$ l of digested vector. Negative controls consisted of the same reaction except the insert DNA was replaced by nuclease free water. The incubation was allowed to proceed at 4°C overnight or at 12°C for 4 hours. After the incubation period, the ligation reaction was transformed into OneShot TOP10 chemically competent *E. coli* from Invitrogen (Carlsbad, CA). The manufacturer's "freeze thaw" protocol was followed using 2-10  $\mu$ l of the ligation reaction depending on the complexity of the reaction (the more fragments being simultaneously ligated, the higher the volume used). The 200  $\mu$ l of transformed cells were plated on dried ampicillin LB plates from Teknova (Grimstad, Norway). The bacteria were incubated overnight at 37°C. Screening was done directly to individual colonies using colony PCR. A colony was carefully touched with a p-10 pipette tip (leaving the colony essentially intact on the plate) and the bacteria were added directly to a standard PCR reaction by pipetting up and down 15 times, primers were selected depending on desired fragment and located in table 1. The resulting fragment was electrophoresed and purified as described earlier and then sequenced to confirm the identity of the insert. Sequencing was done with a Big Dye kit from Applied Biosystems (Foster City, CA). A 10  $\mu$ l reaction was made by adding 1  $\mu$ l of primer, 2  $\mu$ l of the supplied buffer, 1  $\mu$ l of Big Dye, 4  $\mu$ l of DNA and 2  $\mu$ l of water. The sample was placed

into a thermocycler with the Big Dye program (see figure 6). The sequencing reaction was cleaned using EdgeBio Sequencing Cleanup (Gaithersburg, MD) columns according to the manufacturer's protocol. The samples were sequenced in-house using a Applied Biosystems 3500 Genetic Analyzer.

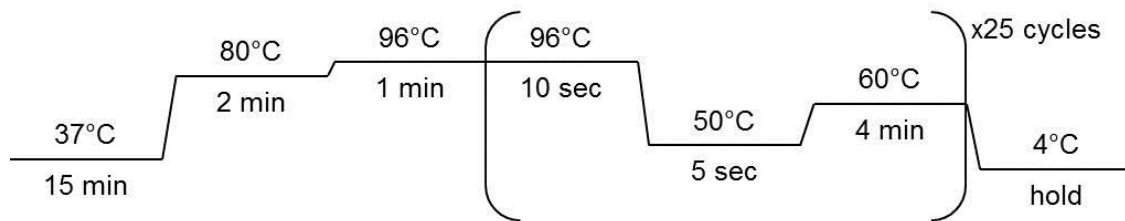


Figure 6: Big Dye PCR cycle parameters

Conditions for Big Dye sequencing PCR.

Once a positive colony was detected via colony PCR, a 3ml overnight culture was grown from the original colony which was marked on the original plate. This liquid culture was then split in two parts to both generate a freezer stock of bacteria for future use and to isolate plasmid using a Qiaprep Miniprep kit from Qiagen according to the manufacturer's protocol. To confirm the identity of the insert for a second time, the plasmid was linearized using a unique restriction site, electrophoresed, purified, and sequenced as described above.

Once the fragments were successfully produced and sequenced in a shuttle vector, the final cloning steps were performed. Generally, several fragments needed to be combined prior to ligation with a final linearized vector plasmid. If these fragments could not be digested and ligated together directly, fusion PCR was used. A graphical representation can be seen in figure 7, but briefly, the initial PCR was done using the fusion primers. The fusion primers had annealing and non-annealing portions (refer to figure 4). The non-annealing portion acted as an annealing primer on the secondary fragment. Separate, standard PCR reactions were run using these primers, and the fragments were harvested using previously described methods. The separate fragments

were then placed into a second reaction. This reaction was done as a standard PCR, however equal amounts of both fragments were added as templates. Because of the non-annealing primer sequences from the first round of PCR, each fragment now had an overhang, which allowed for annealing to the other fragment. Two “flanking” primers were added to the reaction to allow the polymerase to fill in the entire sequence into a single dsDNA fragment. The fragment was then digested and ligated into the final vector plasmid as described previously. The identity of the plasmid was verified via restriction digest prior to being transformed and sequenced as described previously.

## **Virus Rescue**

A large-scale plasmid preparation was completed using a standard CsCl<sub>2</sub> purification protocol. Briefly, 100 µl of the remaining liquid culture that tested positively was used to seed a 250 ml culture. The large culture medium used was terrific broth from Cellgro (Manassas, VA). After an overnight incubation, the medium was centrifuged at 7,600xg for 10 minutes. The pellet was resuspended in 8 ml of buffer 1, containing 1 M tris, 5 M NaCl, and 0.5 M EDTA. Then, 16 ml of buffer 2 was added to the suspension. Buffer 2 contained 1 M NaOH, 10% SDS, and water. The third buffer, containing KAc, glacial acetic acid, and water, was added at a volume of 12 ml. The bottles were then placed on ice for 15 minutes and centrifuged at 25,900xg for 10 minutes. The supernatant was collected, and 20-25 ml of 100% isopropanol from Sigma was added. The solution was placed at -20°C for 15 minutes. The total nucleic acids were precipitated by centrifuging the solution at 1,600xg for 10 minutes. The pellet was dissolved in 2 ml of TE buffer. Then, 2 ml of 5 M LiCl was added and the solution was placed on ice for 10 minutes. The solution was centrifuged at maximum speed for 10 minutes, and the supernatant was collected. Next, 8 ml of 100% ethanol from Sigma was

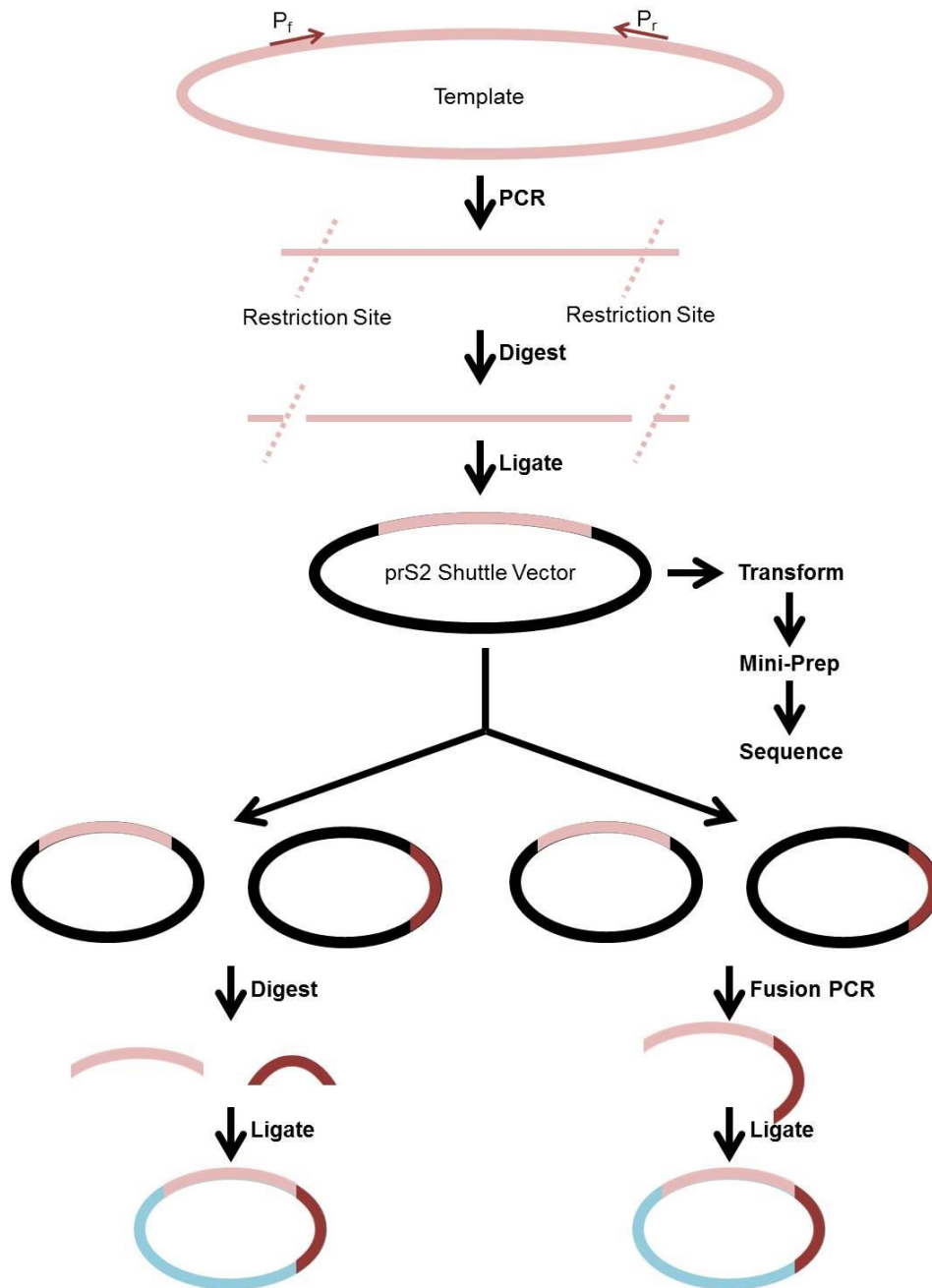


Figure 7: Overview of cloning strategy

Basic strategies for generating CHIKV infectious clones. Pink = viral sequence 1, red = viral sequence 2, black = shuttle vector, blue = final vector.

added and the solution was held at -20°C for 15 minutes. The DNA was then pelleted at 1,600xg and the ethanol was removed by pipetting. The DNA pellet was then resuspended in 1 ml of TE. Then, the DNA was combined with 4.8 g of CsCl<sub>2</sub>, 1 ml of TE, and 40 µl of EtBr in a Beckman ultracentrifuge tube. A balance tube was also made with identical components except that plain TE was used in place of the DNA. Both tubes weighed 9.1 g. The tubes were properly sealed either by melting or pop cap and centrifuged at 292,000xg for a minimum of 4 hours. After centrifugation, the sample tube was gently handled and, using a syringe, the bottom band containing the complete DNA was aspirated through the side of the tube. The band was then added to 1 ml of TE and 3.5 ml of ethanol. The solution was placed at -20°C for 30 minutes and then centrifuged at 3,500xg for 10 minutes. The pellet was dissolved in 0.4 ml of TE and put on ice for 10 minutes. A phenol/chloroform extraction was then completed. Briefly, 0.4 ml of Amresco (Solon, OH) phenol/chloroform was added and the solution was vortexed. Then, it was centrifuged at 12,400xg for 5 minutes. The upper phase was collected and the phenol/chloroform extraction was repeated once more. The upper phase was then had 60 µl of 5 M NaCl and 0.94 ml ethanol added to it. The sample was kept at -20°C for 15 minutes. The DNA was pelleted by a 13,000g centrifugation for 10 minutes and was washed with 0.5 ml of 70% ethanol. The DNA is then resuspended in TE to a final concentration of 1 µg/µl according to a spectrophotometer.

Once the large-scale plasmid preparation was complete, 1 µg of the infectious clone plasmid was linearized using techniques described previously. RNA was transcribed in vitro using the SP6 mMESSAGE mMACHINE kit from Ambion. This technique was done according to the manufacturer's protocol. The RNA was then used for an electroporation. For each electroporation, two T-150 flasks of Vero cells were grown to 95% confluency. These cells were harvested through trypsinization and pelleted at 1,600xg for 10 minutes. The cells were then washed with 7 ml of PBS and pelleted at 1,600xg for 5 minutes. This washing step was repeated two more times, and

on the final time the cell pellet was resuspended in 0.7 ml of PBS per sample and kept on ice. The cell suspension was then added to the 10  $\mu$ l transcription reaction ( $\sim$ 4  $\mu$ g of RNA) and mixed three times. The sample was quickly placed into a 4 mm electroporation cuvette from Molecular BioProducts (San Diego, CA) and the cuvette was placed in the receptacle of the BTX 830 electroporator from Harvard apparatus (Holliston, MA). The machine was run using a program that entails three 250 V, 10 ms pulses at one second intervals. The electroporated cells were allowed to settle for 10 minutes, then were added to a T-75 flask along with 10 ml of DMEM containing 5% FBS. The flask was observed 4 hours later to confirm that the cells survived and adhered. After 50% CPE was observed (generally 24-36 hours post-electroporation), the medium was collected and centrifuged at 1,600xg for 10 minutes. The virus-containing supernatant was then harvested and frozen in 1 ml aliquots.

### **RNA Radiolabeling and Electrophoresis**

A 6-well plate with 90-95% confluent Vero cell monolayers was infected at an MOI of 20. At 4-8 hours post infection, the original medium was removed and replaced with 0.8 ml of medium containing 5  $\mu$ g of actinomycin D from Sigma and 20-40  $\mu$ Ci/ml of 3H 5,6 uridine from Moravsek Radiochemicals (Brea, CA). Two to four hours after the addition of the radiolabeled media, the cells were collected in TRIzol from Life Technologies. The RNA was harvested from the TRIzol according to the manufacturer's protocol. A sodium phosphate buffer was generated by titrating 0.2 M  $\text{Na}_2\text{HPO}_4$  with 0.2 M  $\text{NaH}_2\text{PO}_4$  until the solution reached pH 7.0. This sodium phosphate buffer was then combined with DMSO and Sigma Glyoxal at a ratio of 10:3:1, respectively, in a 25  $\mu$ l volume. This buffer was added to 10  $\mu$ l of the radiolabeled RNA. The solution was



incubated at 50°C for one hour. During this incubation, a 1% agarose gel was made using the pH 7.0 sodium phosphate buffer and Lonza agarose. The gel was placed in a Model HRH gel apparatus from International Biotechnologies from (New Haven, CT) with an attached pump to circulate buffer. A syringe was filled with the DEPC-treated running buffer (Sigma) from the apparatus and used to clean any residual debris from the wells of the gel. The RNA samples were then combined with 10x RNA loading dye and loaded into the wells. The dye consisted of 0.1 M EDTA, 80% glycerol, and 0.02% bromophenol blue. The gel was run at 75 V until the samples entered the gel, and then the gel was run at 150 V for 4 hours. The gel was then removed from the running apparatus and washed in 100% methanol from Sigma for 30 minutes on a rocking table. This methanol wash was repeated one more time, and the gel was then placed in 2.5% diphenoxylate (PPO) from Sigma suspended in methanol. The gel was left in the PPO/methanol solution overnight, and the next day the solution was poured off. The gel was washed with deionized water two times for 30 minutes each to precipitate the PPO in the gel. The gel was then sandwiched between Whatman paper and saran wrap and dried by placing it on the gel dryer. Finally, the dried gel was exposed on Kodak X-OMAT AR film at -80°C overnight, and the film was exposed using an x-ray developer.

## **Basic Cell Culture**

African green monkey cells (Vero) type E6 C1008 were originally obtained from the American Type Cell Culture (Bethesda, MD). Cells were maintained in T-150 flasks made by Corning (Corning, NY) with 25 ml of medium. The cell culture medium, Dulbecco's Modified Eagle Media (DMEM) produced by Gibco, (Grand Isle, NY), was supplemented with penicillin and streptomycin antibiotics produced by Gibco added at a concentration of 1:100 and fetal bovine serum (FBS) by Hyclone (Logan, UT) at varying

concentrations. The cells were incubated at 5% CO<sub>2</sub> and 37° C until needed. Once the cells reached confluency, they were trypsinized using 2ml of the Gibco dissociation reagent. The flasks of cells with the trypsin were incubated at 37°C and 5% CO<sub>2</sub> for a period of 5 minutes. The trypsin was then deactivated by adding 8 ml of the DMEM medium containing 5% FBS. The resuspended cells were then passed by placing 1 ml of the 10 ml into a fresh T-150 and adding 25 ml of fresh 5% FBS-containing DMEM. Some confluent flasks were used to seed ten 12-well plates, six 6-well plates, or twenty 96-well plates for the next day's use.

Insect cells used were C6/36 *A. albopictus* mosquito cells 1660, also obtained from American Type Cell Culture and were maintained in 10% FBS- and 10% typtose phosphate-containing DMEM and incubated at 32°C in an incubator. Unlike the Vero cells, C6/36 cells were not exposed to trypsin during passage. Instead, they were manually detached with a sterile scraper. Splitting ratios were the same as those described for Vero cells.

### **Viral Titrations/PRNT<sub>80</sub> /CPE assay**

Viral titrations were completed on 90-95% confluent monolayers of Vero cells. The cells were seeded in 12-well Costar plates (Corning, NY) one day prior to the experiment. The virus samples were serially diluted 1:10 using 96 well plates. In short, the 96 well plate was marked and then the wells were filled with 180 µl of 2% FBS-containing DMEM. Then, 20 µl of sample was added to the first well and mixed thoroughly with the pipette. Next, 20 µl was taken from that first well and deposited into the 2nd well and the mixing procedure was repeated. This was repeated until the virus was at the final desired dilution factor. After all the samples were diluted, the semi-confluent plates were removed from the 37°C 5%CO<sub>2</sub> incubator and the plates were

labeled. The medium was removed from the plates and the diluted virus was added to wells starting from the highest dilution factor and continuing to the lowest. The plates were returned to the 37°C 5% CO<sub>2</sub> incubator for one hour. During this time, an overlay was produced. The overlay was four parts DMEM containing 5% FBS and one part 2% Agar produced by Lonza (Rockland, ME). The agar was melted and added to the medium, and the solution was kept at 56°C until needed. After the one hour incubation, 2 ml of overlay were added to each well. The overlay was then allowed to solidify at room temperature, and then the infected plate was returned to the 37° C 5% CO<sub>2</sub> incubator for 2-3 days depending on the virus being titrated. If individual plaque isolations were necessary, the plaques were visualized using a light table and isolated using a cut p-1000 pipette tip. The plaque/agar plug was then be placed in .75 ml of TRIzol and RNA was isolated according to the manufacturer's protocol. If plaque isolation was not required, 1ml of Ricca (Arlington, TX) 10% formaldehyde was added to each well and incubated for a period of one hour at room temperature. The agar was then removed and the wells were stained with Sigma crystal violet in 25% methanol for a period of five minutes. The crystal violet was then washed and the plaques were counted.

The PRNT protocol was done in similar fashion as the titrations with respect to the plates and plating procedures. In short, the collected mouse sera to be tested for neutralizing antibodies were heat-inactivated in a 56° C water bath for one hour. The virus being tested was diluted to 800 pfu/ml. In the first well, 22 µl of the sera were added to 200 µl of medium, producing an initial dilution factor of 1:10. The well was mixed and then serial 1:2 dilutions were done to a final dilution factor of 1:640. After the sera were diluted, an equal volume of virus was added to each sample of diluted sera. The sera/virus suspensions were incubated at 37°C, 5% CO<sub>2</sub> for one hour. Following incubation, 100 µl of the sera/virus suspensions were plated starting with the highest antibody concentration and following down to the lowest, using a fresh tip for each well. In conjunction, control titration was done with 2% FBS DMEM medium instead of sera.

The plates are overlaid and incubated as stated previously. After the plates were fixed and stained, the lowest antibody dilution factor that inhibited 80% of the plaques when compared to the control titer was recorded as the PRNT<sub>80</sub> value.

Cytopathic effect assays were completed in 96 well plates for mosquito homogenates. In short, the mosquitoes were frozen in 2% FBS-containing DMEM with amphotercin B from Sigma. The mosquitoes were then homogenized using a steel ball bearing in an Eppendorf (Hamburg) round-bottom tube in a TissueLyser II from Qiagen. The homogenate was centrifuged at 10,000 x g for 10 minutes to clear away debris and the supernatant was serially 1:10 diluted up to 1:1000. The diluted homogenates were added to Vero monolayers in a 96-well plate and incubated for one hour. After the incubation, 5% FBS DMEM was added and the plates were observed for 24-48 hours for the development of cytopathic effects.

### **Replication Kinetics**

Replication kinetics were completed in Vero cells. They were done using 35 mm, 6-well plates at 95% confluency. Initially the medium was removed and 0.2 ml of 2% FBS DMEM containing 10<sup>5</sup> pfu of virus was added to each well for a multiplicity of infection (MOI) of 0.1. The virus was incubated with the cells at 37° C for one hour. The plates were then washed three times with PBS from Gibco, and then 2.1 ml were added to each well. The initial time-point was immediately collected by removing 0.1 ml for t=0. At various other time-points, 0.1 ml was removed and 0.1 ml of fresh medium was replaced. Samples were stored at -80° C and subsequently titrated on Vero cells as described above.

## **Passages**

Viral passaging was completed on both Vero and C6/36 cells in their respective incubation and media conditions listed above. In short, cells were grown in T-25 flasks from Corning and allowed to reach 95% confluency. The cells were then infected at an MOI of 0.1 with 2 ml of medium/virus for 1 hour in their respective incubators. Then, medium was added to the flasks and left to incubate for 30 hours before samples were harvested. The procedure was repeated as required.

## **Animal Work**

### **ETHICS STATEMENT**

All of the following procedures were compliant with the “Guide for the Care and Use of Laboratory Animals” put forth by the National Institutes of Health. All procedures were also reviewed and approved by the University of Texas Medical Branch and University of Wisconsin Institutional Animal Care and Use Committees (IACUC). All work done with animal subjects was completed under Animal Biosafety Level (ABSL) 2 or 3 depending on the agent being used. Personnel performing experiments at the University of Texas Medical Branch were formally trained in the following techniques by Animal Resource Center (ARC) trainers and were observed by the onsite veterinarian for approval. All experiments that follow are approved under Dr. Scott Weaver’s IACUC protocol. What follows is a brief description of the techniques used.

### **ANIMAL MODELS USED**

Multiple mouse models were used during the course of experiments. Outbred CD-1 mice were used as neonates (<10-days-old) and adults. Both were obtained from Charles River (Wilmington, MA). To obtain infant mice, timed pregnant mothers were purchased and animals were born in our facilities. We used C57BL/6J inbred mice obtained from Jackson Labs (Bar Harbor, ME) in our initial vaccine efficacy studies. Multiple knockout (KO) mice were also used to test the virulence of vaccine candidates. These mice included mitochondrial antiviral signaling (MAVS)- and STAT1-KO mice, which were obtained from Jackson Labs and Taconic (Germantown, NY), respectively.

The A129 animals that were used in the bulk of these experiments were bred on site. The original breeding pairs were obtained from Dr. Lynn Soong’s breeding colony located at the University of Texas Medical Branch, Galveston, Texas. Briefly, animals were housed by sex until they reached 4-5 months of age. Breeding groups were then

housed together as either single breeding pairs or harem breeding. Harem breeding, consisting of two females and one male, was used to lower the number of cages needed for the process. The animals were left in the cages for 6-7 days to copulate. After this, the male was removed from the cage. If copulations were successful, the females would give birth approximately 21 days later. The mother and pups were continually observed for the next 21 days, at which time the pups were weaned and caged by sex.

### **VIRULENCE AND EFFICACY TESTING**

During a virulence experiment, several cohorts of animals were infected with one of the following: a negative control of saline, a positive control of the La Reunion wt-isolate, our vaccine candidates, and in some cases, the 181/25 army vaccine. In adult mice these viruses were inoculated either subcutaneously (SC) in the back or intradermally (ID) in the footpad with a dose ranging from  $10^4$ - $10^5$  total PFU. A neurovirulence test was completed on 6-day-old CD-1 mice with animals receiving an IC inoculation of  $10^4$  PFU. Animals were observed for signs of morbidity and sacrificed as needed. Euthanization of adult animals was completed via CO<sub>2</sub> asphyxiation followed by cervical dislocation. Animals under 2 weeks of age were rendered unconscious with isoflurane, from Piramal Healthcare (Digwal Village, India), and then decapitated with surgical scissors. Disease signs that were measured included weight loss, footpad swelling, and mortality. Footpad measurements were done using a digital caliper at the site of injection, which was the distal portion of the animals' footpad. Tissues were collected and analyzed in some cases as described in more detail later in this chapter.

Efficacy testing was done in adult animals. Animals were vaccinated with one of the following: saline, our vaccine candidates, or the 181/25 army vaccine. Animals received a vaccine dose of  $10^4$  pfu ID in the footpad or SC in the back, depending on the experiment. These animals were observed for a period of 28-30 days. In some

experiments, sera were collected from these animals by retro-orbital bleeds to measure PRNT<sub>80</sub> titers as described above. During the retro-orbital bleeds, the animals were rendered unconscious using isoflourane. The animal was then removed from the container and handled in a way to force the eye to protrude. A heparinized glass capillary from Fisher (Waltham, MA) was then placed behind the eye and gently manipulated to extract whole blood. The whole blood was then left at room temperature for one-to-two hours. The blood was then centrifuged at 1600 x g on a table-top centrifuge for 10 minutes. The serum in the supernatant was then collected and placed in a separate tube for storage at -80°C. While the animals remained unconscious they were challenged by inoculating 10<sup>2</sup>-10<sup>4</sup> PFU of wt virus, SC. The animals were then observed for a minimum of 14 days to measure morbidity and mortality.

#### **TISSUE COLLECTION**

Tissue collection was required for multiple aspects of the study. All tissue collection was completed in a biosafety cabinet. Separate tools were used for each animal. After each use, the surgical tools were washed with Metrex Cavacide (Romulus, MI), 70% ethanol, and in some cases 1% sodium hydroxide (NaOH). The tools were then autoclaved prior to storage for subsequent use. Adult mice were euthanized as described above. They were then washed with ethanol wipes from Fisher and placed on fresh paper towels. The animal was opened by cutting into the peritoneal cavity with surgical scissors. Then, a single transecting cut was made along the medial line of the animal up to the thoracic cavity. The spleen, GI tract, liver, and kidneys were then harvested. Next the diaphragm was removed from the subject's thoracic cavity. This was completed using iridectomy scissors. After the removal of the diaphragm was complete, the thoracic cavity was entered by a single medial cut through the sternum of the animal. The ribcage was separated and the lungs and heart were removed. The animal's left leg (containing the site of any footpad injection) was then removed. This was completed



using large scissors and cutting through the hip joint. The skin was then removed from the leg and, if muscle was needed for titrations, a small part of the hamstring was removed with a clean pair of iridectomy scissors. The brain of the animal was then removed. The animal was positioned so the dorsal aspect was facing up and the ventral side of the animal was facing towards the back of the BSC. The animal's spinal column was cut and a single shallow cut transecting the medial line of the skull in a posterior to anterior fashion was made. On the posterior side of the skull two lateral cuts were made at the base of the skull. The calvarium was then opened using forceps while gently holding the skull in place. The brain was gently removed using the forceps. In infant mice the animals were decapitated as stated previously, and the brain was subsequently collected in a similar fashion as adults.

Tissues needed for titrations were placed into pre-labeled 2ml round-bottom tubes. The tubes contained 0.5ml of DMEM with 2% FBS and a stainless steel ball bearing from Glenn Mills Inc. (Cliffton, NJ). These tissues were weighed against blank tubes containing only the medium and ball bearing. The tissues were then homogenized by placing the tubes in the TissueLyser II from Qiagen and shaking them at a frequency of 26 Hz for 5-10 minutes, depending on the tissue. The homogenate was then centrifuged at 15,000 x g on a tabletop centrifuge for 10 minutes. The supernatant then could be titered as described above. In some cases, the tissues were placed in 10% formaldehyde from Ricca for histopathological analysis, which will be described later.

#### **BRAIN PASSAGE**

Virus was passaged through neonatal A129 mouse brains 5 times. The animals were purpose-bred as stated earlier in this section. At 2 days of age the mothers were moved to a separate cage and the required pups were combined for randomization. The required number of pups per cohort was placed in a cage with a lactating mother. Animals were then injected one at a time intracranially (IC) with  $10^4$  pfu in a 10  $\mu$ l dose.

After 30-36 hours the brains were harvested, placed in the round-bottom tubes, triturated and titrated. When the next cohorts of mice were ready, the samples were thawed and centrifuged to remove any particulate matter. Using the titration data, the sample was diluted to  $10^6$  pfu/ml, and  $10^4$  pfu was injected in a 10  $\mu$ l dose into each of the next group of animals. The process was done in duplicate for each virus.

### **TRANSCARDIAL PERFUSION**

This technique was performed to remove viremic blood from the tissues being collected and assayed. Due to the high risk of aerosolization it was necessary to wear a positive air pressure respirator (PAPR) from MAXAIR (Irvine, CA) even when in the ABSL2. A raised platform surrounded by a large basin was constructed in the laboratory to catch the liquid waste produced by the procedure. The animal was rendered unconscious by isoflourane and then placed on the platform. The animal was fitted with a nose cone to provide constant anesthesia. The subject's limbs and tail were secured to the platform with tape. The animal was then opened using two lateral ascending cuts from the peritoneal cavity to the thoracic cavity. The animal's diaphragm was removed as stated prior. After this, the subject's nose cone was removed. The thoracic cavity was then opened using two lateral cuts and pinned the freed ventral side of the animal above its head. Next the heart was gently removed from the pericardium. A butterfly needle from Jorvet (Loveland, CO) was attached to a 30 ml syringe from BD Syringe (Franklin Lakes, NJ) containing 30 ml of warm saline. The air was pushed out of the needle and the needle was inserted into the left ventricle. Using iridectomy scissors, a small incision was made in the animal's right atrium. Then, using constant pressure, 30 ml of saline was pushed through the animal at approximately 2-3 ml/min. The process was repeated with a second 30 ml syringe. Then, the subject's tissues were collected as stated previously.

## **IN-VIVO IMAGING**

The A129 mice that were observed using the in vivo imaging system (IVIS) were 9-12-weeks-old. Depending on the experiment, animals were treated with a vaccine or negative control one month prior to the experiment. Three-to-five days prior to the experiment, the animals were prepared by shaving their bodies. The animal's ventral/dorsal sides were shaved using hair clippers from Wahl (Sterlin, IL). A small strip of fur was left on the animal's dorsal side by its front limbs for warmth. Extra bedding was also provided to increase comfort. Animals were observed during this time for any small abrasions that may have occurred during the process. If any wounds were present they were treated with an antibiotic gel. On the first day of the experiment the mice were injected with wt-CHIKV expressing firefly luciferase (FfLuc) (provided by Dr. Klimstra), SC in the footpad. Luciferin substrate from GoldBio (St Louis, MO) was diluted in double distilled water to a final concentration of 15mg/ml and filtered. The next day animals were transported to the IVIS room and injected intraperitoneally (IP) with approximately 170-180 ul of luciferin. The animals were returned to their cages for 5-7 minutes. Then they were rendered unconscious by isoflourane and placed into the imaging box. The box was attached to the isoflourane for continuous anesthesia and moved into the IVIS machine. Using LivingImage software from Perkin Elmer (Waltham, MA), multiple pictures were taken. Animals were returned to their cages and observed until they regained consciousness. Animals were not allowed to be unconscious for more than 20 minutes.

## **HISTOPATHOLOGY TISSUE PREPARATION**

If a study required histopathology, small changes were done to the tissue collection protocol. Tissues were retrieved and bilateral tissues were separated right from left. For example, the animal's right kidney was used for histopathological analyses and the left kidney was saved for titrations. Non-bilateral tissues were cut into halves and

treated similarly. The tissues for histopathology were placed in 50 ml conical vials containing 35 ml of 10% neutral buffered formalin. The tissues were submerged in the fixative and allowed to fix overnight. The formalin was replenished the next day. Tissues were then put into cassettes and placed back in the formalin. If the sample contained bone, such as whole leg, tissue was placed in a cassette and then immersed in a decalcifier agent from VWR international (Radnar, PA). The legs were decalcified for 2-3 days and then transferred back to formalin. Tissues were embedded in paraffin wax and sectioned by the University of Texas Medical Branch Histology Core lab. Then hemotoxylin and eosin staining was performed. The paraffin was removed by a 15-minute xylene incubation. The sections were then slowly rehydrated using varying concentrations of ethanol and deionized water. The hemotoxylin stain from Richard Allan Scientific (RAS) (Kalamazoo, MI) was then applied for 3 minutes. Excess was washed off using distilled water. Then the sections were placed in Clarifier I from RAS for 5 minutes and again rinsed using distilled water. The slides were then stained with RAS eosin stain for 30 seconds. They were then dehydrated using varying washes of ethanol/water and finally washed with xylene. The slides then had cover slips added and were allowed to dry overnight.

### **MOSQUITO MANIPULATION**

The mosquitoes used were from an *Aedes albopictus* colony maintained at UTMB. The colony was established in 2003 from collections done in Galveston. Female mosquitoes were harvested 4 days post-eclution. Manipulations were done in the ACL-3 facility on a chill table from Bioquip (Rancho Dominguez CA). The mosquitoes were intrathoracically (IT) injected with 1 µl doses containing approximately 10 pfu of CHIKV. The mosquitoes were then held at 27°C for 7 days. During this time they were provided 10% sucrose. Mosquitoes were then frozen and collected for titrations as described above.

## CHAPTER 3 PRODUCTION AND INITIAL TESTING OF VACCINE CANDIDATES

### Rationale

Initially a series of vaccine candidates for CHIKV needed to be designed and produced. It was decided that our vaccine should be a live-attenuated because CHIK-endemic and -epidemic areas tend to be resource-limited with large populations, and the live-attenuated strategy offers the potential advantage of a single-dose, highly and rapidly immunogenic vaccine. Another desirable trait for a potential CHIKV vaccine is the lack of transmissibility by the arthropod vector. This would prevent accidental transmission to viremic vaccinees and the accidental establishment of a CHIKV infection cycle in a non-endemic area, where the epidemic vectors are present but CHIKV has not yet been detected. To this end, the IRES-based vaccine strategy was adapted from VEEV and applied to CHIKV. The initial proof of concept for the IRES strategy utilized the TC-83 vaccine strain of VEEV [67]. The resulting virus was highly attenuated but with limited immunogenicity. This original TC-83/IRES strain was subsequently modified to increase immunogenicity. We decided that the CHIKV vaccine should be designed using a recently circulating wt-CHIKV for multiple reasons. The wt-CHIKV clone, OPY-1 produced by Tsetsarkin *et al.* is a representative of the Indian Ocean outbreak clade from La Reunion against which the vaccine would need to protect [118]. Also, applying the IRES strategy to a vaccine strain has been shown to produce an overly attenuated phenotype [67]. Therefore, I hypothesized that utilizing a wt-CHIKV strain as the backbone would produce more a more immunogenic vaccine. The resulting vaccine would also be designed to protect against the current outbreak viruses, whereas if the 181/25 vaccine was used as a backbone it would be designed against an older Asian genotype virus.

The initial vaccine candidate, which will be named from this point forward CHIKV/IRESv1, was based on the original TC-83 construct produced by Volkova *et al.* The genomic organization remained similar to the wt-CHIKV strain; however a series of point mutations was added to the sg-promoter to ablate its function. The IRES was then added between the nsP and the structural gene cassette. In a second strategy, CHIKV/IRESv2, the sg-promoter remained intact and the capsid gene was moved to the 3' end of the genome and placed under IRES translational control. Some experiments will include only CHIKV/IRESv1, because it was chosen as the primary vaccine candidate due to its genetic stability and safety. Due to the non-chronological nature of this report, some studies will also include CHIKV/IRESv2 and/or CHIKV/IRESv2b. What follows is the results of the recovery and initial characterization of the CHIKV/IRES vaccine candidates.

## **Results**

### **PRODUCTION OF CHIKV/IRESv1**

The backbone of CHIKV/IRESv1 was the OPY-1 plasmid, an isolate collected from a human infection in 2006 on La Reunion island[118]. A basic overview of the cloning strategy for CHIKV/IRESv1 is depicted in figure 8. Several fragments were produced. The first required fragment, fragment 1, was generated to mutate the sg-promoter. All primer sequences can be found in table 1. The region of the upstream restriction site Bsu361 was selected for the forward primer, 'forward BSU361 primer'. The reverse primer, 'reverse mutated promoter primer II', included the mutated promoter sequence, which can be found in figure 9, and an added SpeI site for later cloning steps. This fragment containing the mutated sg-promoter between the Bsu361 and SpeI restriction sites was produced through a standard PCR reaction as stated in the materials and methods section using the OPY-1 plasmid as a template.

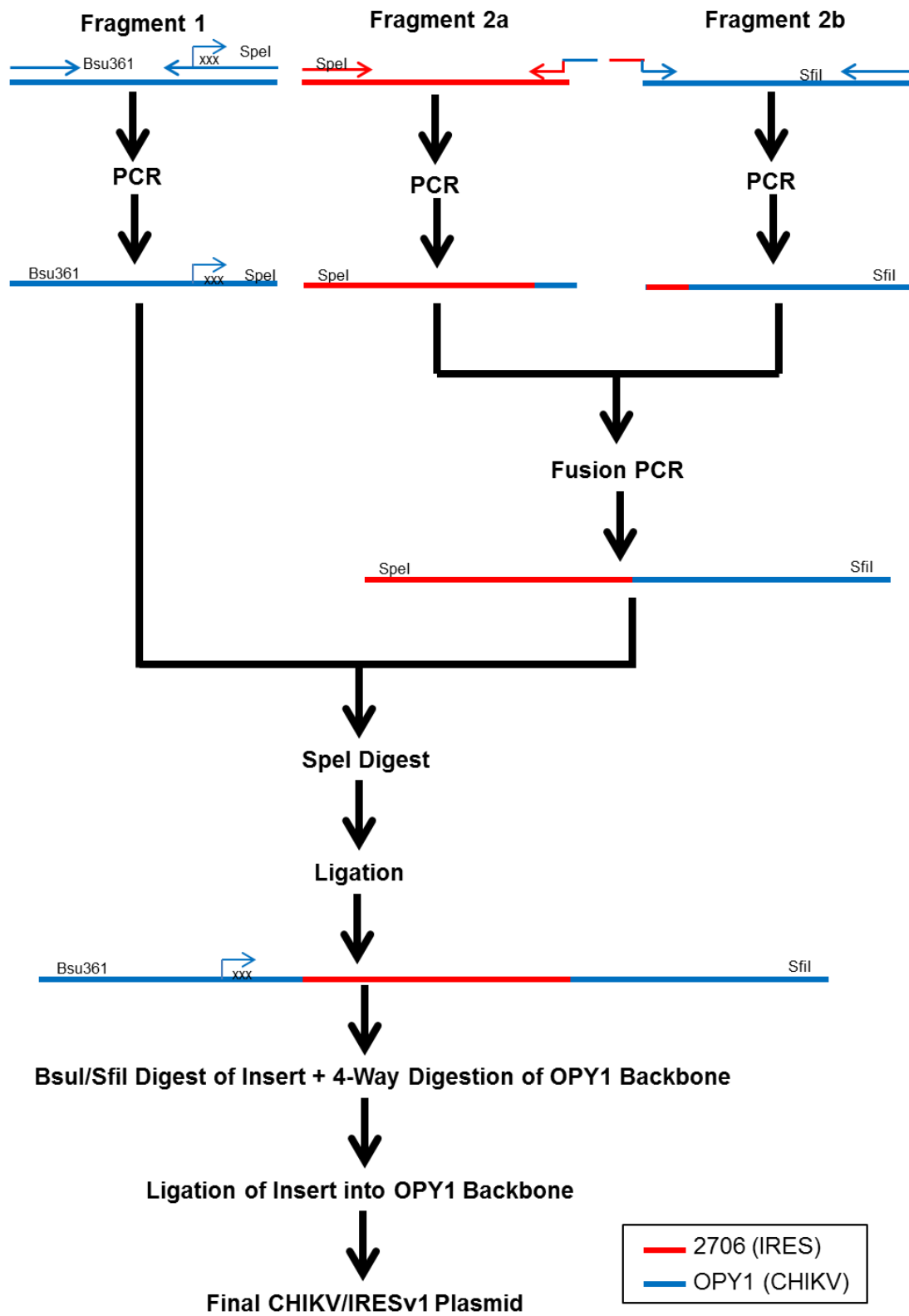


Figure 8: CHIKV/IRESv1 cloning

Overview of cloning strategy for CHIKV/IRESv1 infectious clone. xxx = mutated promoter region.

Name	Sequence (5'-3')
CH2(-) 635	GCGTTGTACATGAACGG
CH1(+) NEW 1	ATGGCTGCGTGAGACAC
CH2(+) NEW 614	ACAACCCCGTTCATGTA
CH4(+) NEW 1360	ACACACGGTCTACAAGAGGC
CH5(+) NEW 1892	GTGCCCTCAGGCTATG
CH6(+) NEW 2414	ACCAGTCGACGTGTTG
CH7(+) NEW 3002	GGAAATTTTAAGGCAACWATTAAGG
CH7(-) NEW 3200	GGTGAGTATGCTCTGTCTTCTTT
CH8(+) NEW 3513	CATTGGTGGCCGAAC
CH9(+) NEW 4065	GAGCAGGGTGTGCACC
CH10(+) NEW 4604	CGMGTCACCCCTGACAG
CH11B(+) NEW 5348	GACGAGAGAGAAGGGAA
CH13(+) NEW 6114	ACATGGTGGACGGGTC
CH14(+) NEW 6580	AAGGCCTAAGGTGCAGG
CH15(+) NEW 7052	TTCATCGGCGACGAC
CH16(-) NEW 8081	TTCATGTGCACSGGTATCTG
CH17A(+) NEW 8021	TGGCCTTTAAGCGGTC
CH18(+) NEW 8730	TTGGACCAAGCTGCG
CH19(+) NEW 9378	GAAAAACCAAGTCATCATGC
CH19(-) NEW 9419	GTCGGATGGTCAGGATACAG
CH21+ 10000	CACGTAACAGTGATCCCG
CHIK1133R	CAGCTTCTGTGCATCCTC
CHIK2528R	ATTGAAGAAGCCGCACTG
CHIK3498R	CTAATGAGTGTGGTAGTCTCC
CHIK4084R	ATGCGTTTWACCCGGTAC
CHIK4627R	TATCCTTTTCTGCCTGCC
CHIK5251R	WGGTRCGGTGYTCATTACC
CHIK5810R	CACTYTCCTGGAGTTTCTTAAG
CHIK6285R	CTCATCTGTGTGACGTTGC
CHIK7182R	GTGCAGTATAAACCCCTCCRC
CHIK9037R	GGCATGTGYACCTCTATCTC
CHIK10574R	AAATTGTCCTGGTCTTCCTG
CHIK11787R	GAAATATTAAAAACAAAATAACATC
FORWARD BSU361	CCACGGATCCACAGTAGATATGAAAAGGGACGT
REVERSE SFII PRIMER	CCACGAATTCTTCATGTGCACGGGTATCTGCGCGCA
FORWARD CAPSID FUSION	CACGATGATAATATGGCCACAACCATGGAGTTCATCCCAACCCAAAC
REVERSE IRES FUSION	GTTTGGGTTGGGATGAACTCCATGGTTGTGGCCATATTATCATCGTG
REVERSE MUTATED PROMOTER PRIMER II	CCACCTCGAGACTAGTTTATTACTTCGGTCTCCATAAAGCGTAATCAC G GGTCTCTGAGCTTCTCGAAG
FORWARD IRES PRIMER II	CCACCTCGAGACTAGTAACGTTACTGGCCGAAGCC
FORWARD MUTATED PROMOTER PRIMER	GTGATTACGCTTTATGGAGGACCGAAGTAATAAGGGCCACAGCTACC TATTTTGCAGAAGCCGA
REVERSE PROMOTER PRIME	TACCTATTTAGGACCGCCGTACAAAGTTATGAC
REVERSE MUTATED PROMOTER PRIMER	TTATTACTTCGGTCTCCATAAAGCGTAATCACGGGTCTCTGAGCTTC TCGAAG
FORWARD IRES PRIMER	TCTAGAAACGTTACTGGCCGAAGCC
CHK F MUTSG PRIMER	GTGATTACGCTTTATGGAGGACCGAAGTAATAAACTAGTACAGCTACC TATTTTGCAGAAGCCGA

Table 1: Cloning and sequencing primers

Sequence of primers using for the construction and sequencing of CHIKV.



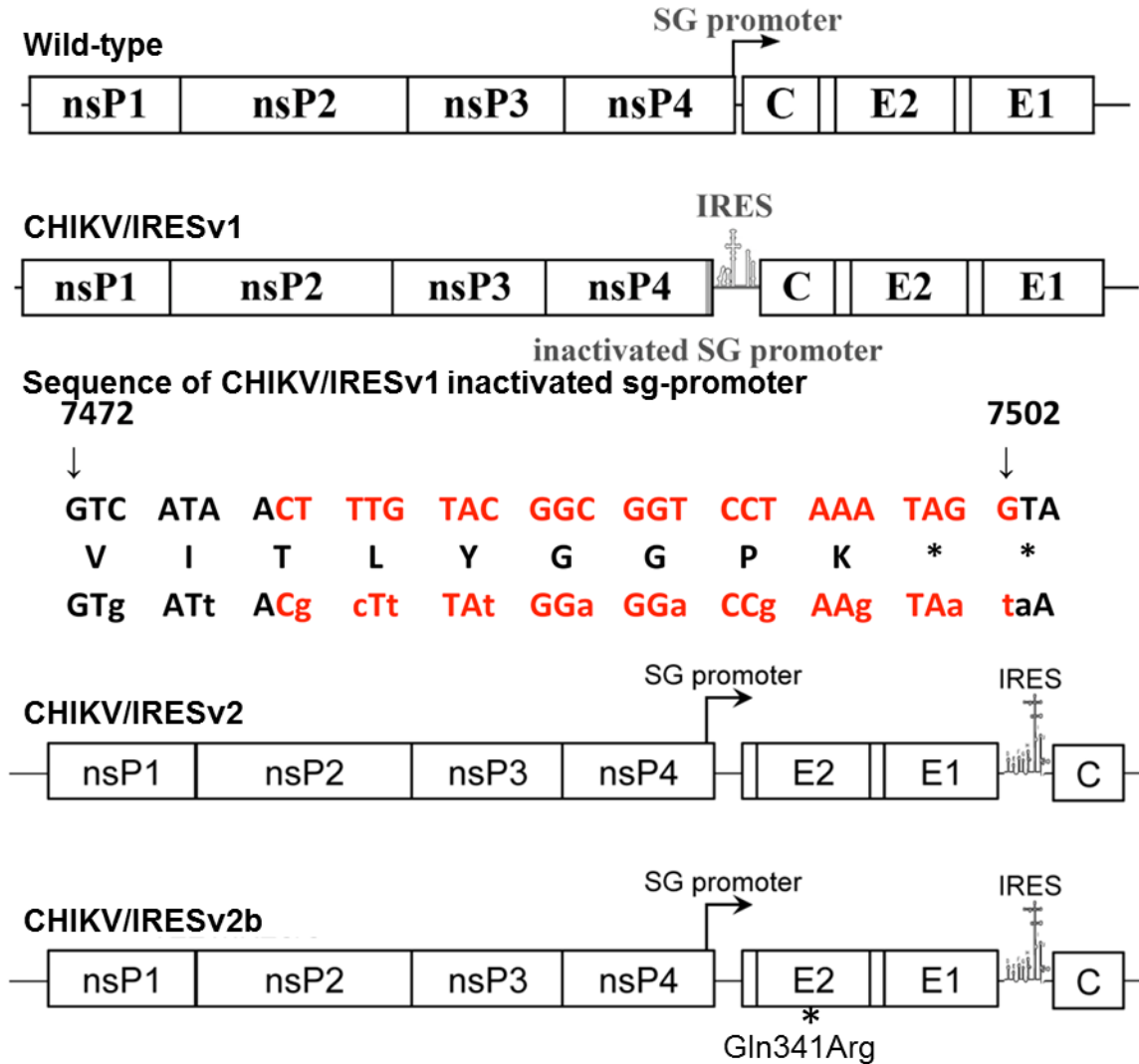


Figure 9: Schematic of CHIKV/IRES vaccine candidates

Diagram of wild-type CHIKV, CHIKV/IRESv1, CHIKV/IRESv2, and CHIKV/IRESv2b. Inactivation of the sg-promoter in CHIKV/IRESv1 is shown with synonymous mutations represented in lower-case letters. Figure adapted from Plante *et al.* and Guerbois *et al.*[68,69]

The fragment, fragment 2, was the IRES and capsid fusion DNA. The IRES and capsid sequences were joined though fusion PCR due to the lack of convenient restriction sites. The template for producing the IRES-containing DNA, fragment 2a, was the 2706 clone provided by Dr. Iyla Frolov. This clone is the first generation IRES construct of TC-83 [67]. The forward primer used was the ‘Forward IRES primer II’, which included a 5’ SpeI site added for later ligation to fragment 1, and it annealed to the first 19 nucleotides of IRES. The reverse primer, ‘Reverse IRES fusion primer’, was a fusion

primer that annealed at its 5' end to the 3' end of the IRES sequence and the next four codons of the original EMCV sequence that follows the IRES. These 12 nt were previously shown not to affect the virus [67]. The 3' end of 'Reverse IRES fusion primer' annealed to the 5' end capsid. This PCR product was ~0.6kb and its production was verified via gel electrophoresis.

The second fusion fragment, fragment 2b, was produced using the OPY-1 plasmid as a template. The 5' end of the forward primer, 'Forward Capsid Fusion Primer', annealed to the 3' end of fragment 2a. The 3' end of the 'Forward Capsid Fusion Primer' annealed to the 5' end of the capsid gene. The reverse primer, 'Reverse SfiI', was designed to be downstream of the SfiI site in capsid so that site could be used for subsequent cloning steps. This PCR product was ~0.5 kb and its production was also verified via gel electrophoresis.

Once fragments 2a and 2b, containing the IRES and capsid, respectively, were generated, they needed to be joined together to form fragment 2. This was accomplished using both fragments as the template DNA for a fusion PCR reaction. The 3' end of the IRES fragment (fragment 2a) was able to anneal directly to the 5' end of the capsid fragment (fragment 2b). The flanking primers for the fusion reaction were the 'Forward IRES primer II' and the 'Reverse SfiI primer'. The resulting ~1kb fragment contained the 561 nucleotides of IRES and ~500 nucleotides of capsid joined directly together.

At this point, two fragments had been produced: fragment 1 with nsP4 and the mutated sg-promoter, and fragment 2 with the IRES and capsid. To verify the successful production of these fragments, further sequencing was done. This was accomplished using the prS2 shuttle vector. For fragment 1, the PCR product and prS2 were each digested with BamHI and then ligated together for 18 hours. In the case of fragment 2, EcoRI was used. The resulting plasmids were transformed into the TOP10 *E. coli* as described in chapter 2. The transformed bacteria were grown on CARB/LB plates and the resulting colonies were tested for the presence of the PCR insert via colony PCR.

The colony PCR utilized the m13f and m13r primers, which anneal to the prS2 plasmid. Four colonies each were checked for both fragments 1 and 2. Three of the 4 tested colonies were positive and one was selected for sequencing in each case. The separate fragment sequencing reactions were completed with either the m13f or m13r for the forward or reverse sequences, respectively, and were completed as described in the methods section. Both fragments 1 and 2 were found to have the correct sequence.

The final cloning steps involved multiple digestion and ligation reactions. The complete insert (CI) fragment was produced by digesting fragment 1 with BamHI and SpeI, fragment 2 with SpeI and EcoRI, and prS2 with BamHI and EcoRI. These fragments were then 3-way ligated and checked by transformation and digestion as described in the methods. The validation digestion then could be used in the cloning steps to insert the CI fragment into the OPY-1 vector. The validation digestion was completed with BSU361, which cuts near the 5' end of fragment 1, and SfiI, which cuts near the 3' end of fragment 2. Now that this CI fragment was validated and ready for ligation, the OPY-1 vector needed to be prepared. The vector was cut 2 separate times to allow for directionality. A 897 bp fragment and a 11.4kb fragment were produced by cutting the OPY-1 plasmid with AgeI and BSU361 for the former and AgeI and SfiI for the later. The two vector fragments and the CI fragment were then ligated, transformed and minipreped as described previously. Six colonies were chosen for minipreps and were then checked via restriction digestion. The restriction digest included BSU361, AgeI and SfiI. The original OPY-1 plasmid produced a 1.4kb fragment of interest (CI fragment), whereas a positive CHIKV/IRESv1plasmid would produce a 2kb fragment. Of the 6 colonies tested, 4 were positive.

## **PRODUCTION OF CHIKV/IRESv2**

The second generation clone, CHIKV/IRESv2, was then produced. The main purpose of this clone was to remove the capsid gene from its initial position while

introducing a start codon for the E3 protein gene. The sg-promoter remained intact, and the capsid gene was placed at the 3' end of the infectious clone and remained fused directly to the IRES. This strategy was designed to retain sg-RNA and leave the glycoproteins under the control of cap-dependent translation, while causing capsid to be restricted to IRES-dependent translation to maintain incompetence for mosquito infection.

The first cloning fragments used fusion PCR to cleanly delete the capsid gene from OPY-1. To accomplish this, a forward primer '7215NheF' was designed to bind nsP4, and a reverse primer 'UTR3r' was designed to bind to the subgenomic UTR and had a non-annealing 3' portion corresponding to the E3 while introducing a start codon upstream. Using these primers with the OPY-1 plasmid, fragment 1a was produced. To make fragment 1b, the forward primer 'UTR3D' was designed to bind to the 5' end of E3 while introducing a start codon. The non-annealing 3' portion of 'UTR3D' then corresponded to the 3' end of the subgenomic UTR. The reverse primer used to produce fragment 1b was '8516SphR', designed to end downstream of the SphR site in E3. The template for fragment 1b was also OPY-1. The PCR reactions were completed and produced the two independent fragments; 1a was 337bp and 1b was 191bp. To join these fragments, they were placed in the same PCR reaction to act as template along with the two flanking primers, '7215NheF' and '8516SphR'. This produced fragment 1, which was a 522 bp fragment joining nsP4 and the subgenomic UTR directly to E3 and introducing a start codon into E3.

The next fragment needed was the IRES/capsid fusion. New primers were designed to work with the CHIKV/IRESv1 plasmid as a template. The forward primer, 'BsrIRESd', and the reverse primer, 'EcoRR', were designed to flank the entire IRES and capsid sequence from the CHIKV/IRESv1 clone. These primers included the addition of a BsrI site at the 5' and an EcoRV site at the 3' end, plus extra nucleotides at each end to

allow the restriction enzymes to bind to the introduced restriction sites more efficiently on the PCR product.

Two clones were then produced, incorporating the two fragments. The 7015 clone included fragment 1 introduced into OPY-1. To make this clone several digestions were run. Two separate vector fragments needed to be made along with the fragment 1 insert. The vector fragments were produced by two separate digestion reactions. The first digestion used MluI and SphI on the OPY-1 plasmid. This produced 9 fragments, the largest of which was used for further cloning. The second vector fragment was produced by digesting OPY-1 with MluI, NheI, and SacII. SacII was included to allow the desired MluI-NheI fragment to be easily distinguished from the undesired fragments on a gel. The resulting 1.8 kb fragment was harvested. Fragment 1 was then digested with NheI and SphI. These fragments were all collected and cleaned via gel electrophoresis. The three fragments were then ligated overnight and transformed as described above. This clone was then miniprepmed and the second intermediate clone was produced.

The other clone, 7016, also utilized two vector fragments and an insert of fragment 2. There were 3 digestion reactions used to produce the desired fragments. The first vector fragment utilized EcoRI and NaeI on the OPY-1 plasmid DNA, producing a ~3,700 bp fragment. The second vector fragment utilized the BsrGI and EcoRV on OPY-1 and the small 761 bp fragment was harvested. The fragment 2 insert was then digested with BsrGI and EcoRI. These three fragments were then utilized in an overnight ligation reaction and amplified via a miniprep.

The 7015 and 7016 clones were sequenced to verify that all the restriction sites remained intact and that the cloning had functioned properly. The 7015 clone was sequenced with a single primer '7215NheF' due to the small size of the added sequence. The 7016 clone was sequenced with 'CHK 16(-)' and 'CHK 17a (+)'. The sequences of both 7015 and 7016 were as expected and the final cloning steps were then begun.

The final digestion reactions brought the 7015 and 7016 clones into the original OPY-1 clone, producing the CHIKV/IRESv2. This was accomplished by digesting 7015 with AgeI, BglI, NaeI, and SalI. The AgeI and SalI ~4.4kb fragment was isolated for further cloning. The 7016 insert fragment was digested using BamHI and SalI, and the largest 4.6kb fragment was isolated. The OPY-1 vector was prepared by digesting OPY-1 with AgeI, BamHI, BglI and KasI. The BamHI and AgeI 5.6kb fragment was isolated. These three fragments were ligated together overnight as previously described. After transformation, the clone were verified through colony PCR and found to be correct.

#### **RECOVERY OF CHIKV/IRESv1 AND CHIKV/IRESv2**

Both the CHIKV/IRESv1 and CHIKV/IRESv2 were seeded into a large scale culture by inoculating successful miniprep cultures into 250 ml of terrific broth. These cultures were then CsCl<sub>2</sub> prepared for large-scale plasmid collection. The protocol is found in the methods section. The large scale preps produced 320 µg of plasmid for CHIKV/IRESv1 and 270 µg of plasmid for CHIKV/IRESv2, which were resuspended to a final concentration of 1 µg/µl in nuclease-free water. The plasmids were linearized with NotI and RNA was transcribed with the mMessage SP6 kit according to the manufacturer's protocol. The resulting RNA was electroporated into Vero cells and virus was collected at 48 hours post-electroporation. A single step replication curve was completed using the CHIKV/IRESv1, 181/25 army vaccine, and the wt-CHIKV strain. The 181/25 and wt-CHIKV had a similar replication kinetics, while the CHIKV/IRESv1 was delayed as shown in figure 10.

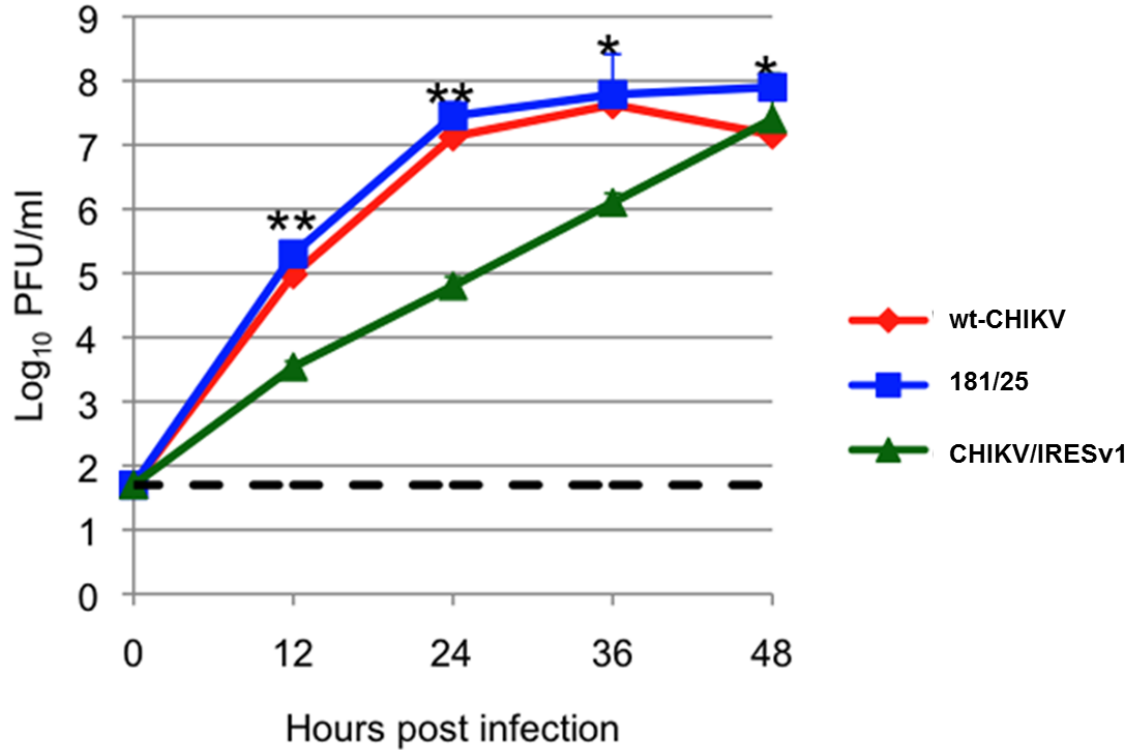


Figure 10: Replication kinetics of CHIKV/IRESv1, 181/25, and wild-type CHIKV

Replication kinetics of CHIKV/IRESv1, 181/25, and wt-CHIKV in Vero cells. Figure from Plante *et al.* [69] \*p<0.05 \*\*p<0.001

#### IN VITRO STABILITY OF CHIKV/IRESv1 AND CHIKV/IRESv2

The next step was to measure the stability of these constructs after cell culture passages. To accomplish this, the viruses were passaged on a Vero cell monolayer in t-25 flasks 10 times with an initial MOI of 0.1. The virus was harvested 30-36 hours post infection (at 50% CPE) and blind passaged in a fresh flask of Vero cells by removing 0.1 ml and adding 0.9ml of media for the 1 ml infection volume. After the 10<sup>th</sup> passage the virus was collected, titrated, and consensus-sequenced. Neither CHIKV/IRESv1 nor CHIKV/IRESv2 acquired any apparent changes in plaque morphology following the 10 Vero passages. CHIKV/IRESv1 maintained a similar titer compared to its original electroporated stock. However, CHIKV/IRESv2 was found to have a 6-fold higher titer after 10 passages in comparison to its original stock (data not shown).

The original and passage 10 viruses were consensus-sequenced to detect any changes. The CHIKV/IRESv1 consensus sequence had no mutations in any of the opening reading frames. However, the poly-A tract in the IRES sequence itself that had multiple peaks, suggesting a mixed population with different size poly-A tracts. Plaque clones of this passage 10 CHIKV/IRESv1 virus were then sequenced. Ten plaques were picked and (nt 8005) region was directly sequenced. Eight of the ten plaque clone sequences showed 7 adenosine nucleotides (cloned wt sequence is 7) and 2 plaque clones had an extension. Refer to figure 11 for chromatograms. An IRES containing 10 adenosines was placed into the infectious clone and basic cell culture analysis was done. The mutation was found to revert to the wt 7 adenosine sequence after electroporation (R. Gorchakov, unpublished).

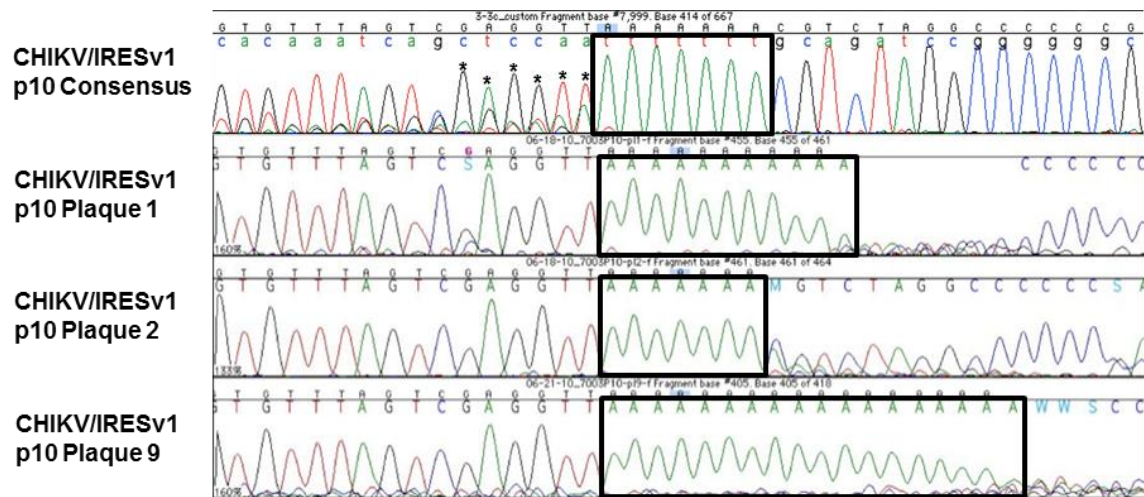


Figure 11: Chromatogram of CHIKV/IRESv1 poly-A tracts

The parent CHIKV/IRESv1 has 7 adenosines, while CHIKV/IRESv1 passage 10 has an indeterminate number of adenosines. Passage 10 plaque 2 has the parent sequence of 7 adenosines, while plaques 1 and 9 have 11 and 18 adenosines, respectively. \* = Mixed peak with strong readable adenosine signal.

CHIKV/IRESv2 was also sequenced after 10 passages. The sequence electropherograms indicated a mixed population with mutations found in a portion of the RNA in the nsP2 and E2 genes; refer to table 2. The mutation with the strongest chromatogram peak represented a suspected heparin sulfate binding substitution since it



was an addition of a (+) charge AA in E2. Due to the attenuating nature of a similar mutation in the army vaccine, this mutation was introduced into the original clone, CHIKV/IRESv2, producing CHIKV/IRESv2b (refer to figure 9). The mutation was added via PCR mutagenesis by Rodion Gorchakov and was rescued as described previously.

NT Position	Original NT	Mutated NT	AA Position	AA Change
3950	A	T	nsP2 757	Thr→Ser
8783	A	G	E2 341	Gln→Arg
8807	A	T	E2 349	His→Leu

Table 2: Mutations acquired by CHIKV/IRESv2 during passage in Vero cells.

List of consensus mutations detected in CHIKV/IRESv2 after 10 passages in Vero cells.

#### **PRODUCTION OF GENOMIC AND SG-RNA BY CHIKV/IRESv1 AND CHIKV/IRESv2b**

The vaccine candidates were tested to measure the RNA species produced *in-vitro*. A wt-CHIKV virus produces both genomic and sg-RNA. However, the ablation of the sg-promoter in CHIKV/IRESv1 should inhibit the formation of sg-RNA. The CHIKV/IRESv2b (CHIKV/IRESv2 was not studied at this point) should, however, produce a sg-RNA species similar to wt-CHIKV. To test these hypotheses, [5,6-<sup>3</sup>H] uridine was introduced into virus cultures as described in the methods section. The RNA was harvested 8 hours post-addition of the radiolabeled uridine, then run on gel electrophoresis and imaged by exposing the dried gel to film. Refer to chapter 2 for complete protocol. Refer to figure 12 for the image. The wt-CHIKV and the CHIKV/IRESv2b produced both genomic and sg-RNA species as expected. The CHIKV/IRESv2b virus sg-RNA was larger than the wt-CHIKV due to the added IRES sequence. The CHIKV/IRESv1 did not produce the sg-RNA as expected.

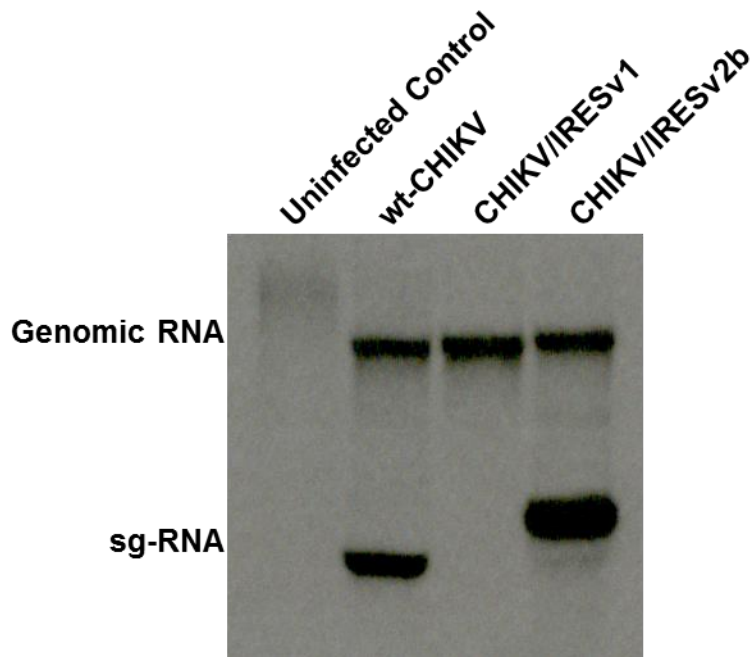


Figure 12: RNA production by wt-CHIKV, CHIKV/IRESv1, and CHIKV/IRESv2b

Production of genomic and sgRNA by wt-CHIKV, CHIKV/IRESv1, and CHIKV/IRESv2b after infection in Vero cell culture.

### **MOSQUITO INFECTIVITY OF CHIKV/IRESv1**

Several experiments were then done to test the ability of CHIKV/IRESv1 to replicate in mosquitoes *in vitro* and *in vivo*. The first set of experiments focused on cell culture passaging the virus in C6/36 cells. CHIKV/IRESv1 and the wt-CHIKV were inoculated onto a cell monolayer at an MOI of 0.1. The medium was collected at 24 hours post-infection, titered, and inoculated onto a fresh monolayer of C6/36 cells for a series of 5 passages. The wt-CHIKV virus maintained relatively consistent titers; (table 3). However, CHIKV/IRESv1 was only found at low levels in the first passage, and never thereafter. The presence of virus after the first passage was attributed to virus not removed during the washing procedure.

<b>Virus</b>	<b>p1</b>	<b>p2</b>	<b>p3</b>	<b>p4</b>	<b>p5</b>
<b>wt-CHIKV</b>	5.0 <sup>7</sup>	4.0 <sup>7</sup>	3.0 <sup>7</sup>	4.2 <sup>7</sup>	3.7 <sup>7</sup>
<b>CHIKV/IRESv1</b>	4.0 <sup>2</sup>	0.0 <sup>0</sup>	0.0 <sup>0</sup>	0.0 <sup>0</sup>	0.0 <sup>0</sup>

Table 3: Titer of wt-CHIKV or CHIKV/IRESv1 following passage in C6/36 cells  
24-hour post infection titer of wt-CHIKV or CHIKV/IRESv1 passaged in C6/36 cells.

The CHIKV/IRESv1 and wt-CHIKV were tested further by intrathoracically injecting them into *Ae. albopictus* mosquitoes, the most permissive route of infection. The virus was initially diluted to 10<sup>4</sup> pfu/ml to ensure that a 1µl inoculum would infect the mosquitoes with 10 pfu. The mosquitoes were reared and injected as described in chapter 2. Seven days later, the mosquitoes were harvested and initial testing for viral titer was done using a CPE assay, (figure 13). All mosquitoes injected with wt-CHIKV were positive for virus with this assay, whereas the mosquitoes injected with the CHIKV/IRESv1 showed no evidence of infectious virus by CPE.

To verify that CHIKV/IRESv1 does not replicate in these mosquitoes, RNA was TRIzol extracted from 20 of the CHIKV/IRESv1, 10 of the wt-CHIKV and 5 control mosquito homogenates. Using the Titan RT-PCR kit by Roche with a pair of capsid primers, table 1, a 1 step RT-PCR was performed. The wt-CHIKV samples produced positive bands, and both the PBS control and CHIKV/IRESv1 mosquitoes produced no PCR products; refer to figure 14.

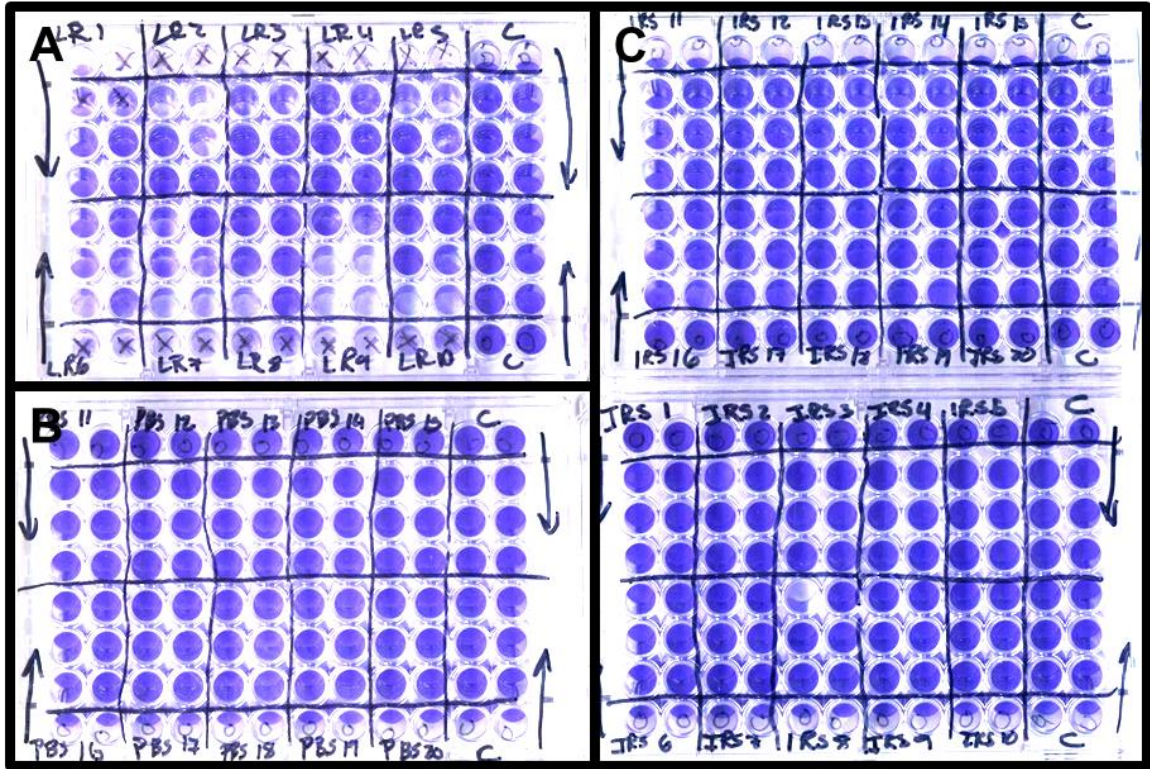


Figure 13: CPE assay assessing the infectivity of CHIKV/IRESv1 and wt-CHIKV in *Aedes albopictus*

CPE assay of *Ae. albopictus* mosquitoes infected IT with either (A) wt-CHIKV, (B) PBS, or (C) CHIKV/IRESv1. On each 96-well, plate columns 11 and 12 are uninfected controls.

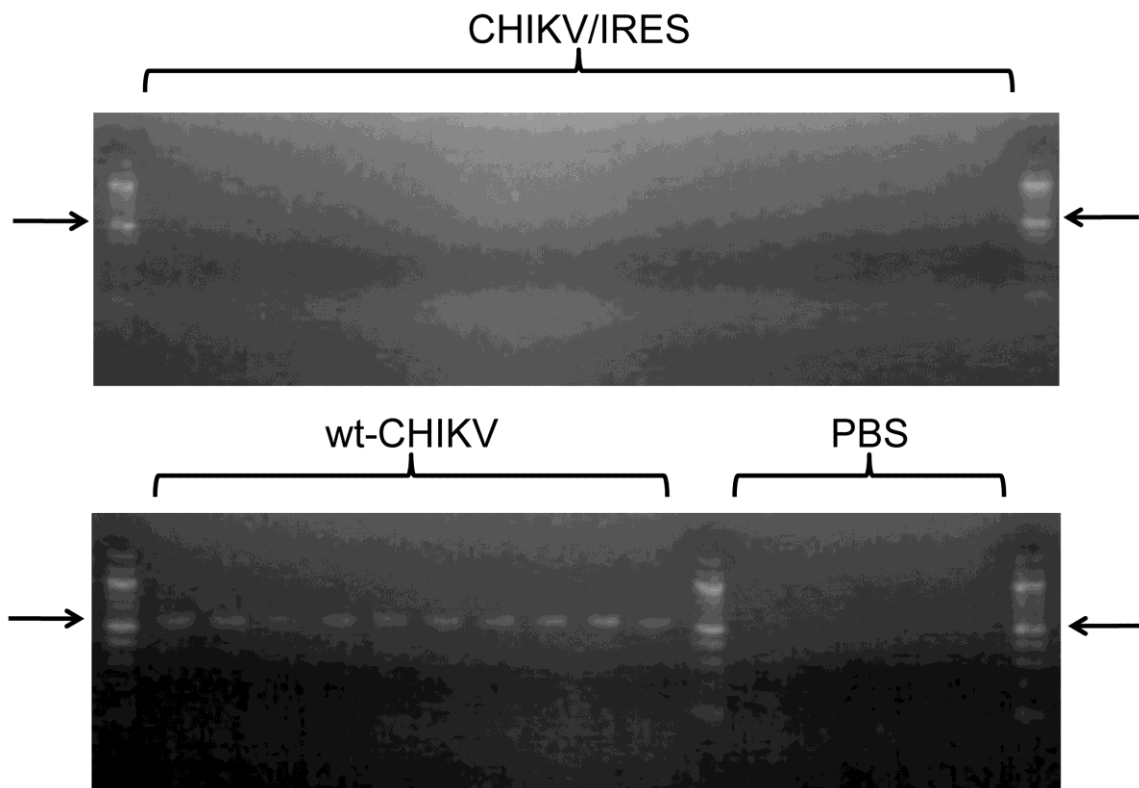


Figure 14: RT-PCR assessing the infectivity of CHIKV/IRESv1 and wt-CHIKV in *Aedes albopictus*

RT-PCR assay of *Ae. albopictus* mosquitoes infected IT with either CHIKV/IRESv1, wt-CHIKV, or PBS. Figure from Plante *et al.* [69]

## Summary/Conclusions

In these initial studies a series of vaccine candidates utilizing the IRES-based vaccine strategy were produced. Initially, two methods developed by Dr. Ilya Frolov using TC-83 were transferred into the wt-CHIKV backbone. The cloning of the vaccine candidates was relatively straightforward. The template DNA used was kindly provided by Drs. Ilya Frolov and Stephen Higgs [67,118]. The initial post-electroporation titer of CHIKV/IRESv1 was only  $3.0 \times 10^5$  pfu/ml. Several changes to the electroporation settings were made to reach our peak post-electroporation titer of  $2.6 \times 10^6$ . These settings were then utilized for CHIKV/IRESv2 and CHIKV/IRESv2b. These second

generation vaccine constructs replicated to higher titers of 2.6 and  $5 \times 10^7$  pfu/ml, respectively. These high titers allowed for collaboration with Inviragen to begin production of a master seed stock for CHIKV/IRESv1, testing in NHPs, and planning for clinical trials.

To test the potential for these vaccine candidates to be produced by cell culture techniques in an industrial setting, it was important to measure their stability during Vero cell passages. Approximately 4-5 passages are needed to produce master and working seed vaccine lots, as well as a final vaccine lot. To ensure adequate stability, the vaccines were tested for stability after 10 passages. The CHIKV/IRESv1 was found to have no consensus mutations in either of the two open reading frames, and was also found to remain at a relatively constant titer throughout the passages. This was one of the main reasons that CHIKV/IRESv1 became the main topic of this dissertation and the focus of further preclinical development. As stated previously, there was a small insertion mutation in the poly-A sequence of the EMCV IRES itself. However it was always found in mixed minority populations. Further studies involving cloning of the most common insertion, 10 adenosines instead of the wt 7-adenosines showed rapid reversion to the wt 7-adenosines post-electroporation (R. Gorchakov, unpublished). The factors that constrain the length of this polyA tract in the IRES deserve further study.

The passaging and sequencing of the CHIKV/IRESv2 vaccine, on the other hand, did expose some instability. The virus was found by the end of the passaging experiment to replicate to a 6-fold higher titer, suggesting that some adaptive mutations probably occurred. In the consensus sequencing it was found that three separate mutations were beginning to appear in mix populations. These three mutations did result in amino acid changes: A3950T resulted in nsP2-Thr757Ser, A8783G resulted in E2-Gln341Arg, and A8807T resulted in E2-His349Leu, table 2. The second mutation was the only one that had a higher chromatogram peak than the wt sequence. This hints at the possibility of a mix population at these points. It also represented a positive charge change, which

suggests a heparin sulfate binding mutation. It has been shown previously that positive charge substitutions in the E2 protein of alphaviruses can increase the binding affinity of the virus to heparin sulfate [6,119,120]. Work done by Gorchakov *et al.* also showed that a suspected heparin binding mutation is largely responsible for the attenuation of the 181/25 army CHIK vaccine [86]. This result suggested that the A8783G mutation might further increase the attenuation of these CHIKV/IRES vaccine candidates. This Gln342Arg E2 substitution was therefore cloned into the CHIKV/IRESv2 plasmid through a double nucleotide change in its codon for increased stability.

The different versions of the CHIKV/IRES capitalize on different aspects of the virus's ability to replicate its structural proteins. In theory, CHIKV/IRESv1 eliminates the production of the sg-RNA and forces the structural genes to be translated via internal initiation of the genomic RNA. The second version vaccines, (CHIKV/IRESv2 and CHIKV/IRESv2b) however, allow the production of the sg-RNA and thereby allow for cap-dependent translation of the glycoproteins, followed by IRES-dependent capsid translation. It was important that these RNA species were produced by these viruses. Originally, the CHIKV/IRESv1 was tested along with the wt-CHIKV and the 181/25 vaccine [69]. It was found to be unable to produce a sg-RNA, as expected. Later, when CHIKV/IRESv1 and CHIKV/IRESv2b were tested in NHPs, an experiment was needed to show the RNA species of both vaccine candidates. The viruses were used to infect cell culture and their RNA species were measured via radiolabeling. This was represented in figure 12. It showed the expected results of a sg-RNA that is larger than the wt-CHIKV.

One of the main original purposes of the IRES vaccine platform was to host-restrict viral replication. Because most alphaviruses replicate in mosquitoes and vertebrate hosts, it is important for any live-attenuated vaccine to eliminate infection of the vector to limit the possibility of accidental transmission. The EMCV IRES element has been shown to translate inefficiently in insect cells [121]. The version one vaccine should thus be unable to translate any of the structural genes in a mosquito. The version

2 vaccine candidates would only restrict the translation of capsid. At the time that these experiments were done, CHIKV/IRESv1 had already been selected for further preclinical development and thus only it was tested for its ability to replicate in mosquitoes both *in vitro* and *in vivo*. In cell culture passages in the *A. albopictus* cell line C6/36, CHIKV/IRESv1 was found to be unable to survive to the second passage. It was found in the medium at a low level after the first passage. Probably indicating that during the initial infection, some virus bound to the cells was not effectively washed away. After demonstrating that the virus was unable to replicate to a measurable titer in C6/36 cell culture passages, its ability to replicate *in vivo* in *A. albopictus* was tested. Mosquitoes were infected via an intrathoracic injection, the most permissive route of arbovirus infection of mosquitoes that bypasses the barriers to infection encountered through feeding. The injected mosquitoes were found to be negative for CHIKV/IRESv1 through CPE and RT-PCR assays 10 days later, indicating that the vaccine was incapable of infecting mosquitoes.

These initial steps thus resulted in production of several vaccine candidates. As stated previously, the CHIKV/IRESv1 showed the most promise in terms of stability and attenuation (STAT1<sup>-/-</sup> mouse virulence, chapter 4) and was therefore selected for further preclinical development. The vaccines replicated in mammalian cell culture to adequate titers for industrial production. CHIKV/IRESv1 showed great stability in Vero cell culture passage and produced the expected RNA species. Finally, the host range restriction of the CHIKV/IRESv1 to only vertebrate hosts should minimize risk for accidental spread. Because CHIKV does not currently circulate in the New World, this is an important safety feature.



## CHAPTER 4 SAFETY STUDIES

### Rationale

After the production and initial testing of the CHIKV/IRES vaccine candidates, the next step in the pipeline involved safety testing. The vaccine candidates were tested for virulence in several mouse models. During the initial testing, the CHIKV small animal models available were severely limited. These limitations made it hard to measure signs of illness that resemble human pathology. However, due to the traits of safety testing, a prolonged seroconversion period was not required. This allowed for use of younger animal models than were possible for immunogenicity and efficacy testing.

Each small animal model that will be discussed in this chapter has strengths and weaknesses. The neonatal CD-1 model allows for replication of wt-CHIKV; however, the model is not sensitive and even mildly attenuated viruses may not replicate in a measurable fashion. However, this model is useful for initial safety testing due to the ease of obtaining the mice and the straightforward measurements that can be obtained from them [73]. To have a more sensitive model, KO mice were required. Generally, ablating the type I IFN pathway leads to a fatal phenotype in adult mice infected with wt-CHIKV. To this end, several KO mice were initially used, such as STAT1<sup>-/-</sup> and A129. The results of these experiments helped determine the main mouse strain to be used as the optimal model for the majority of work described in this dissertation.

The homozygous A129 model developed by Couderc *et al.* was the most effective “vaccine” model for several reasons [75]. The type I interferon receptor KO is presumably not represented in a human population. The disease phenotype experienced by these mice is also not similar to the signs and symptoms experienced by a human. However, the A129 model does allow for the delineation of subtle differences in the

virulence of different CHIKV strains. The A129 model also allows for increasing and/or decreasing the sensitivity of the model depending on the age of the mice. Meaning that the mouse is more permissive to CHIKV infection as a young subject. CHIKV is also able to generate a high titer, systematic infection in this model.

The CHIKV/IRES vaccine candidates were tested against the wt-CHIKV and the 181/25 vaccine. The 181/25 vaccine was used as a benchmark for attenuation. The goal for the CHIKV/IRES vaccine candidates was to slightly exceed attenuation of the 181/25 vaccine. The 181/25 vaccine performed well in small animal models, and was also shown to have a highly attenuated phenotype in NHP [81]. However, as previously stated, it performed only moderately well when tested in humans in a phase II clinical trial, with some reactogenicity seen in vaccinees [85]. If the CHIKV/IRES vaccine candidates demonstrate a higher level attenuation in small animal models, it would add confidence for future testing in humans. Though these small animal models which I used do not translate directly to human studies, the use of the 181/25 vaccine, which has been used in humans, allows us to infer the performance of CHIKV/IRESv1 will respond in humans.

## **Results**

The initial virulence experiment was done using CHIKV/IRESv1. This experiment used neonatal CD-1 mice to observe the differences in viral replication in tissues. Six-day-old CD-1 mice were injected with a 100 $\mu$ l inoculum SC in the animals' between the animals shoulders. The inoculum contained 10<sup>6</sup> pfu/ml, allowing for a 10<sup>5</sup> pfu dose. There were 4 cohorts of 12 neonatal mice: wt-CHIKV, 181/25, CHIKV/IRESv1 and a PBS control group. Timed pregnant CD-1 mice were obtained and their birthed pups were randomized. A single lactating mother supported the 12 experimental animals in each cohort. The pups were observed for four days. During that

time, three animals were harvested daily. Blood, brain, and the knee (whole knee tissue cut approximately 5mm on either side of the knee joint) were harvested from these animals. The tissues were then titrated as described previously.

The results of these titrations can be found in figure 15. wt-CHIKV was detected in all three tissues tested. The viremia peaked by day 2 at  $\sim 4 \log_{10}$  pfu/ml. The knee tissue peaked at  $\sim 4.5 \log_{10}$  pfu/g day 2. The highest viral load measured in the brain was  $\sim 4 \log_{10}$  on day one. The 181/25 vaccine was also detected in all tissue types tested. Peak viremia of  $\sim 4 \log_{10}$  pfu/ml was measured at day one. The viremia was drastically lower by day 2 and was below the limit of detection by day 3. One of the 3 subjects had a positive viremia at day 4. Interestingly, the 181/25 vaccine replicated to higher levels than wt-CHIKV in the knee tissue at all time points tested. The peak viral load in the brain was seen at day 2 at  $\sim 4 \log_{10}$ . The CHIKV/IRESv1 vaccine remained undetectable by tissue titrations at all time points tested.

Fearing that CHIKV/IRESv1 was overly attenuated, a second smaller experiment was done using CHIKV/IRESv2. In this experiment viremia was the focus. The experiment was done to the previous specifications using neonatal CD-1 mice. This experiment also included another virus cohort termed the “4x” mutant, which was a wt-CHIKV La Reunion with 4 of the 5 coding mutations that were found in the 181/25 vaccine. The 4x mutant did not include the mutation believed at the time to be the primary attenuating mutation of 181/25 [86]. This virus acted as a second positive control. The 181/25 and wt-CHIKV viruses produced viremias similar to those recorded in the previous experiment; table 4. The 4x mutant produced a viremia similar to that of wt-CHIKV. However, the CHIKV/IRESv2 was not detected in any of the sera tested. A similar experiment was done using C57Bl/6 mice, and no viremia could be detected for CHIKV/IRESv1 or CHIKV/IRESv2 via plaque titration (data not shown).

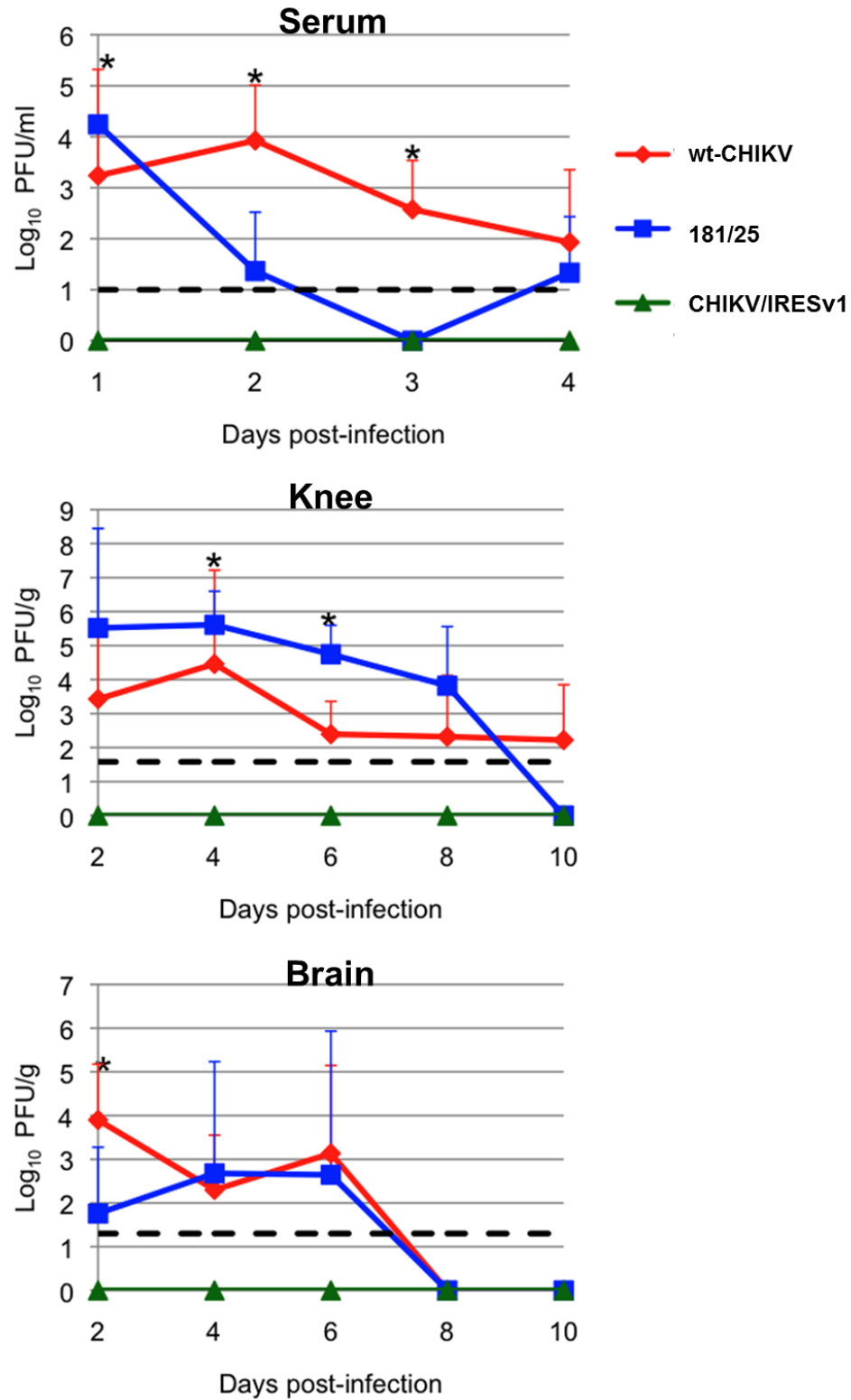


Figure 15: Replication in neonatal CD-1 mice

Replication kinetics of wt-CHIKV, 181/25, and CHIKV/IRESv1 in 6-day-old CD-1 mice. \* =  $p < 0.05$ . \*\* =  $p < 0.001$ . Statistical Analysis conducted by one-way ANOVA. Figure from Plante *et al.*[69]

1 Day Post-Infection			2 Days Post-Infection		
Virus	No. of Positive / Total	Mean Viremia (Log <sub>10</sub> pfu/ml)	Virus	No. of Positive / Total	Mean Viremia (Log <sub>10</sub> pfu/ml)
wt-CHIKV	3/4	5.1	wt-CHIKV	4/4	4.6
CHIKV/IRESv2	0/4	<0.9	CHIKV/IRESv2	0/4	<0.9
4x Mutant	4/4	4.7	4x Mutant	4/4	3.2
181/25	3/3	4.2	181/25	1/3	2.2

3 Days Post-Infection			4 Days Post-Infection		
Virus	No. of Positive / Total	Mean Viremia (Log <sub>10</sub> pfu/ml)	Virus	No. of Positive / Total	Mean Viremia (Log <sub>10</sub> pfu/ml)
wt-CHIKV	4/4	3.4	wt-CHIKV	2/4	2.9
CHIKV/IRESv2	0/4	<0.9	CHIKV/IRESv2	0/4	<0.9
4x Mutant	4/4	3.9	4x Mutant	2/4	2.5
181/25	0/3	<0.9	181/25	1/3	2.1

Table 4: Viremia in neonatal CD-1 mice

Viremia developed by neonatal CD-1 mice infected with either wt-CHIKV, CHIKV/IRESv2, the 4x mutant, or 181/25.

The next step was to use a model with a higher sensitivity. To this end, a survival experiment was planned using 8-10-week-old STAT1<sup>-/-</sup> KO mice. Cohorts ranged from 3-4 mice and were injected with either wt-CHIKV, 181/25, CHIKV/IRESv1, or CHIKV/IRESv2. These animals were given a 10<sup>5</sup> pfu SC dose in the back. Animals were observed for 2 weeks for mortality. The mice infected with the wt-CHIKV succumbed to lethal infection by day 6. The CHIKV/IRESv1- and 181/25-inoculated animals remained healthy throughout the experiment. The CHIKV/IRESv2-infected animals, however, also completely succumbed to lethal infection by day 10; (figure 16).

The next series of experiments focused on the A129 model developed by Couderc *et al.* [75]. Some of the initial A129 experiments were done in collaboration with Dr. Harry Partidos *et al.* from Takeda Vaccines in Wisconsin, Madison due to the unavailability of the animals at UTMB at that time. Later experiments were completed at UTMB. The first experiment utilized a footpad ID injection of 10<sup>4</sup> pfu in 10-week-old animals. Three cohorts of 6 mice were used: CHIKV/IRESv1, 181/25, and PBS. These animals were observed for two weeks. During the observation period, the subjects had their temperature, weight and viremia measured; (figure 17).

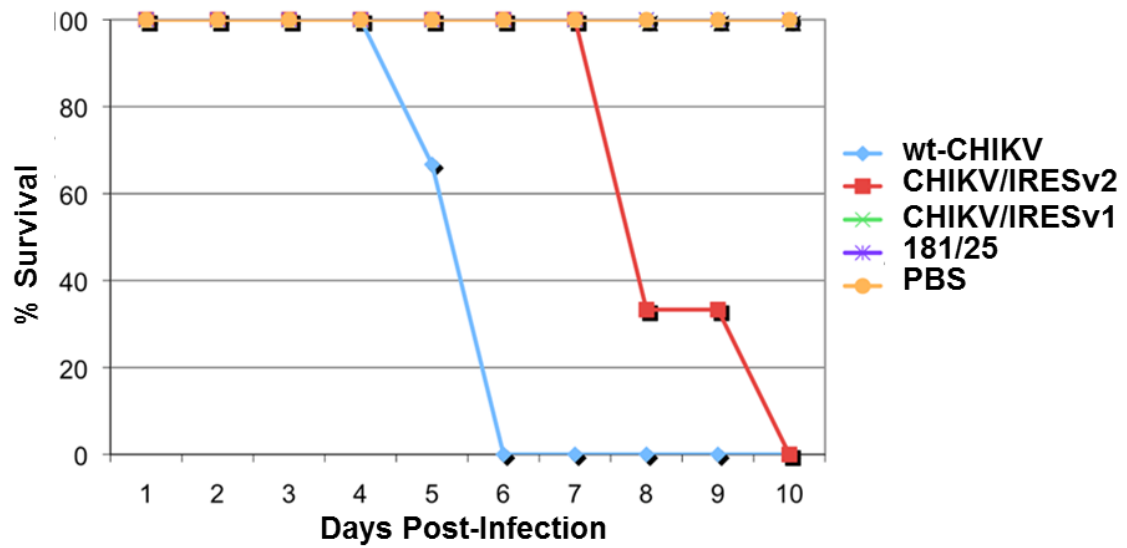


Figure 16: Virulence in STAT1 KO mice

% Survival of STAT1 KO mice infected with either wt-CHIKV, CHIKV/IRESv1, CHIKV/IRESv2, 181/25, or PBS. Survival between all groups varied significantly ( $p=0.000$ ), and the only two cohorts to exhibit mortality (wt-CHIKV and CHIKV/IRESv2) also differed from each other significantly ( $p=0.030$ ). Survival analysis conducted using the Kaplan Meier log rank test.

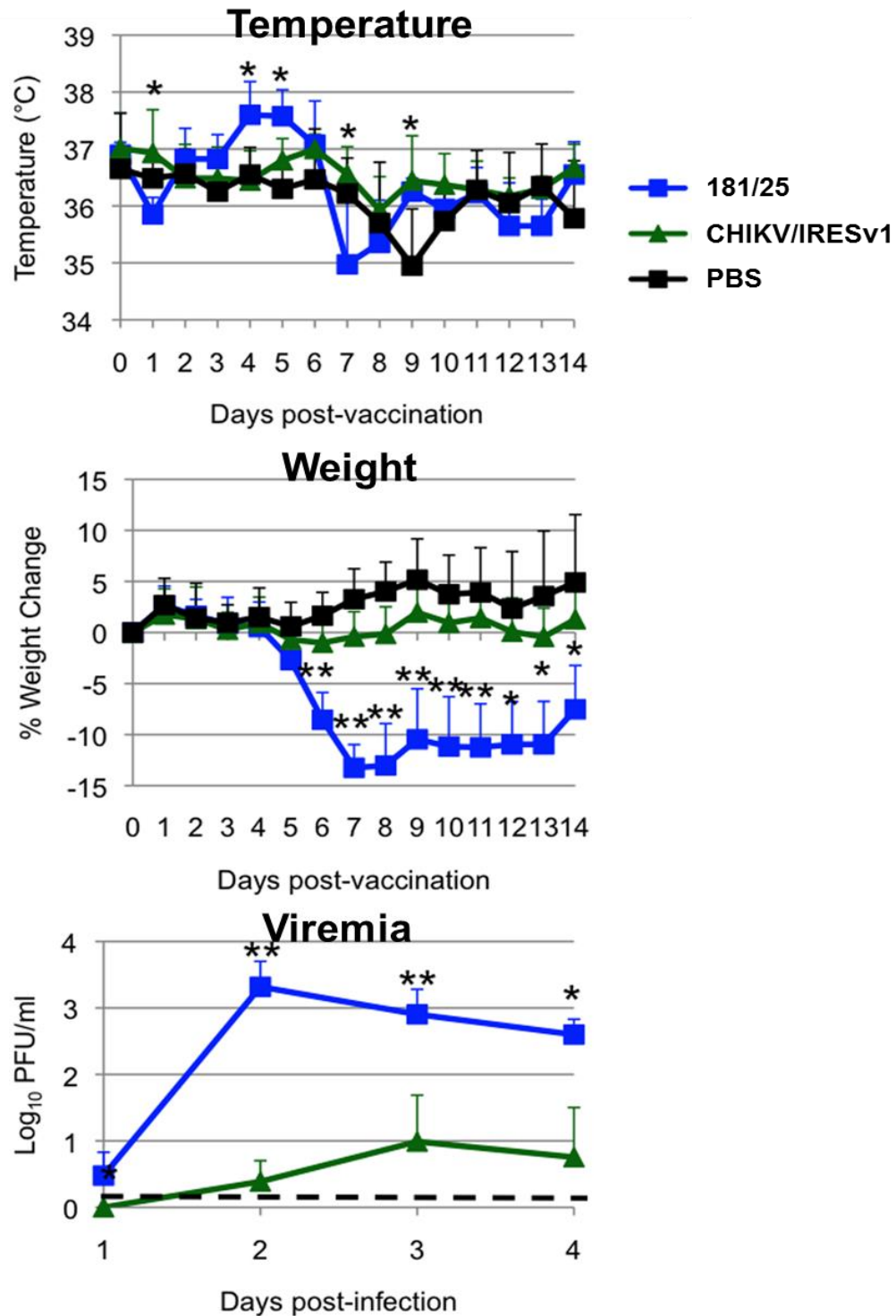


Figure 17: Temperature, weight change, and viremia in 10-week-old A129 mice

Footpad inoculation of CHIKV/IRESv1 and 181/25 viremia and impact on weight change and temperature in 10-week-old A129 mice. \* =  $p < 0.05$ . \*\* =  $p < 0.001$ . Statistical Analysis conducted by one-way ANOVA. Viremia was determined via qRT-PCR using previous studies to correlate RNA copies to infectious units. Figure from Plante *et al.* [69]

The animals that received the 181/25 vaccine did suffer slight morbidity, including a significant hyperthermia by days 4 and 5, followed by a moderate hypothermia on day 7. Animals that received the CHIKV/IRESv1 maintained a relatively constant temperature during the course of the experiment. The next form of morbidity measured was weight loss. Animals were weighed individually, and their average percent change can be found in figure 17. Animals that received the 181/25 vaccine did suffer from statistically significant weight loss by day 6 post infection,  $P < .001$  by one way ANOVA. However, these animals never exhibited other signs of illness such as ruffled fur, hunched posture, or lethargy. The weight of these animals did appear to be rebounding by the end of the observation period. CHIKV/IRESv1-infected mice did not lose a significant amount of weight. The animals were bled daily for the first 4 days and their sera were analyzed using qRT-PCR. The 181/25 animals had a peak viremia by day 2 at  $\sim 3.2 \log_{10}$  pfu/ml. The CHIKV/IRESv1-infected animals did have low level viremia that peaked at day 3 at  $\sim 10$  pfu/ml (using qRT-PCR results with RNA copies correlated to infectious units on the basis of previous results).

To further define the virulence difference between the 181/25 vaccine and the CHIKV/IRESv1 vaccine candidate, an experiment was done using 3-week-old A129 mice; figure 18. These animals were also injected with  $10^4$  pfu in the left rear footpad in cohorts of 5, and weights and survival outcomes were recorded. The CHIKV/IRESv1-infected mice had a slight decrease in weight at day 5, but other than that gained weight in a stable fashion throughout the study. The CHIKV/IRESv1 mice did not exhibit any signs of morbidity. In comparison, the 181/25-infected mice were healthy for the first 5 days of the experiment, but at day 6 they began to lose weight and showed hunched posture. The animals degenerated through day 7 and by day 8 were found dead or were euthanized.



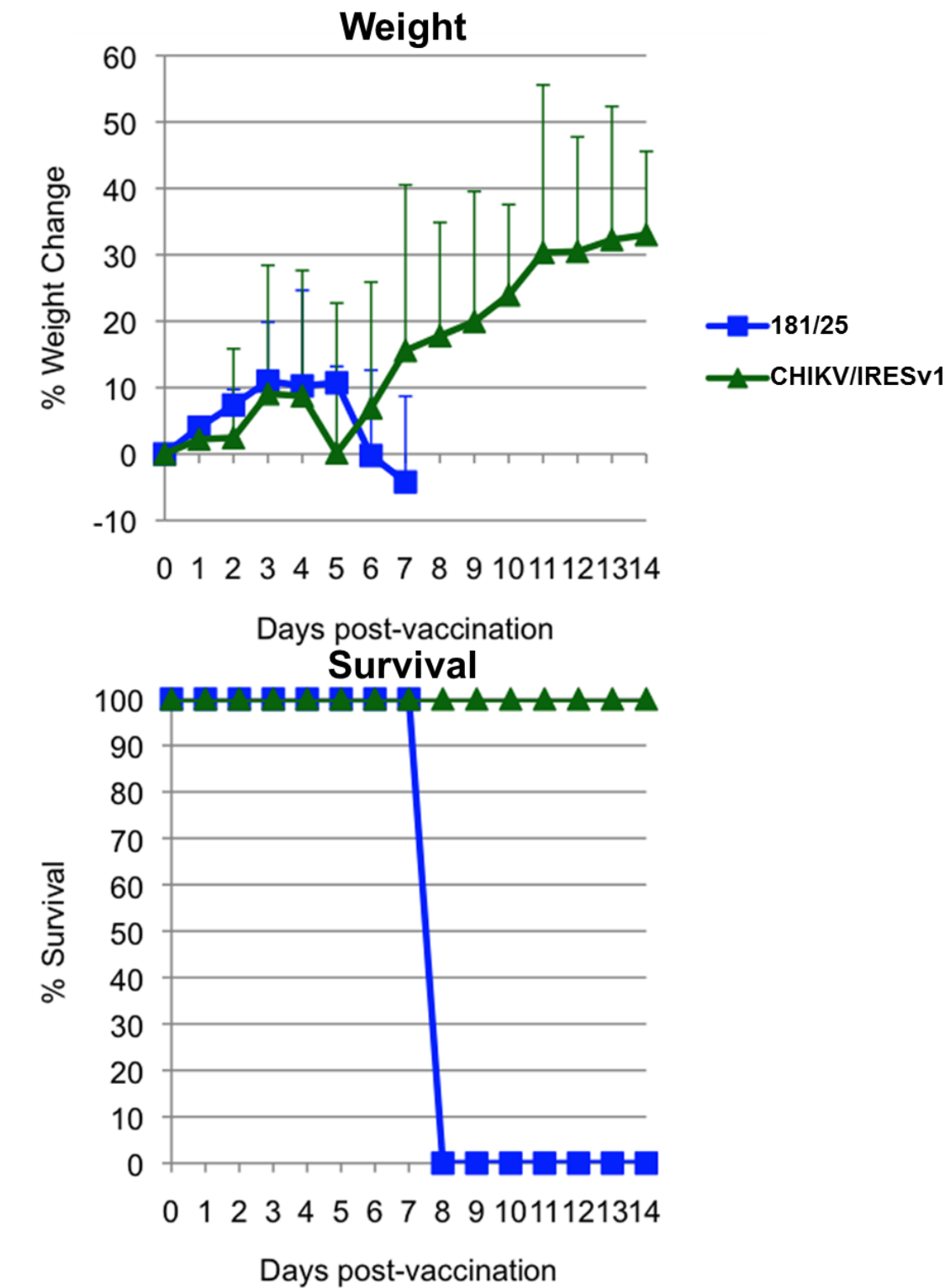


Figure 18: Survival and weight change in 3-week-old A129 mice following vaccination

Survival and weight change in 3-week-old A129 mice infected with CHIKV/IRESv1 or 181/25. Figure from Plante *et al.* [69]

Another study was designed to assess the virulence of CHIKV/IRESv2 and CHIKV/IRESv2b in the A129 mouse model. Due to the virulent nature of CHIKV/IRESv2 in the STAT1 model, it was believed that the vaccine would also be virulent in the A129 mice. CHIKV/IRESv2b was hypothesized to be less virulent. Three cohorts of 5 female 9-10-week-old A129 mice were purpose-bred and used in the experiment. These animals were infected with  $10^4$  pfu or a PBS control in the left rear footpad and were observed for a period of 2 weeks. The CHIKV/IRESv2 was virulent in this mouse model. The subjects began to suffer weight loss by day 4. These animals also exhibited ruffled fur and hunched posture by day 5, and degenerated until, by day 8, they were either found dead or were euthanized. The animals that received the CHIKV/IRESv2b suffered no measurable morbidity during the course of the experiment (Figure 19).

Finally, the potential neurovirulence of CHIKV/IRESv1 was tested in neonatal CD-1 mice. This was accomplished by ordering timed pregnant mothers and inoculating the neonatal mice with a 10  $\mu$ l volume of a  $10^6$  pfu/ml solution, effectively dosing with  $10^4$  pfu. The three cohorts (wt-CHIKV, CHIKV/IRESv1, and PBS) each contained 10 neonatal mice and a lactating mother. Animals were observed and euthanized once they became moribund. Data are represented in figure 20. The wt-CHIKV-infected animals suffered 60% mortality by day 8. The remaining wt-CHIKV-infected animals survived to the end of the study 14 days post-infection. All of the animals that received either the CHIKV/IRESv1 vaccine candidate or PBS survived to the end of the experiment.

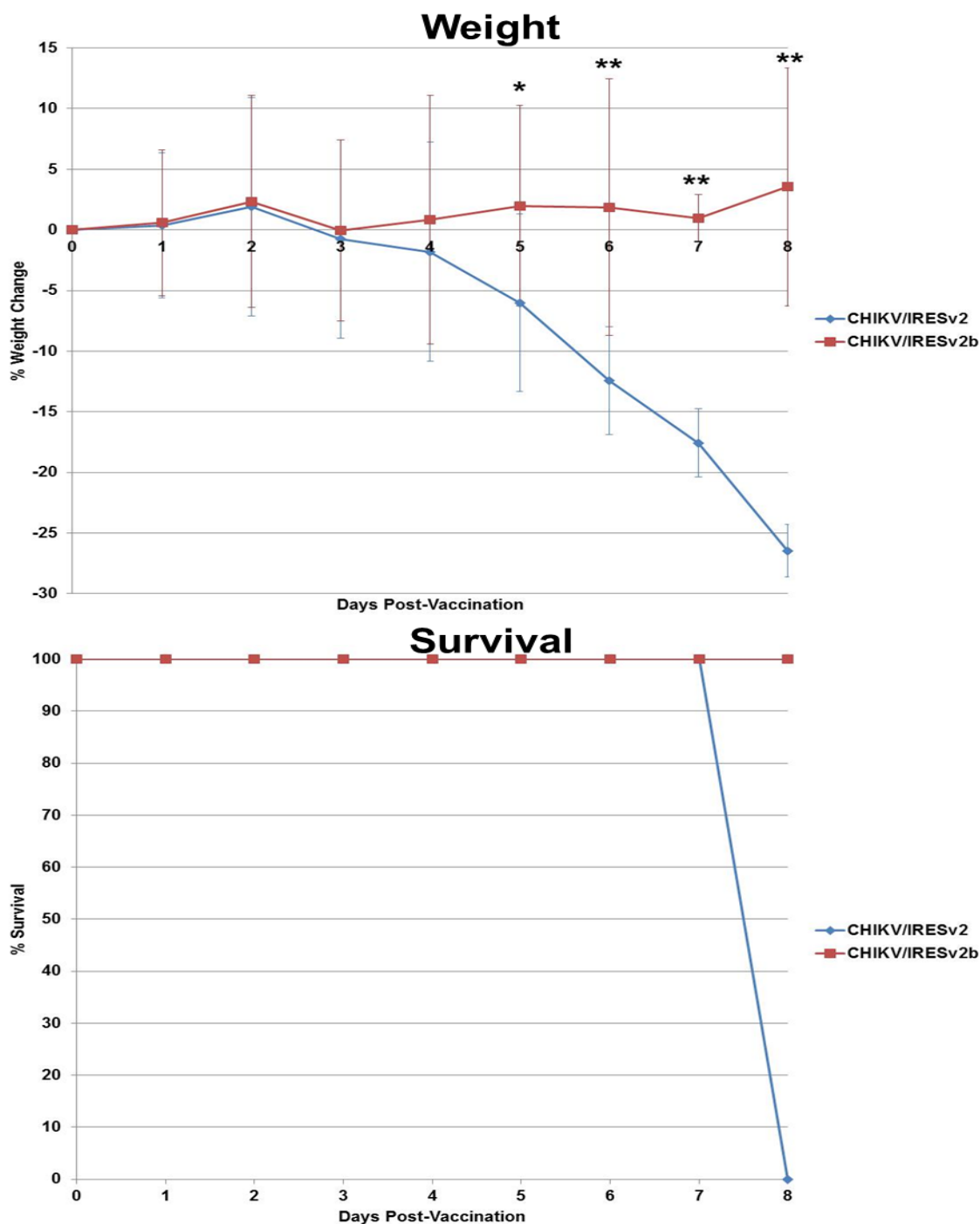


Figure 19: Survival and weight change in 10-week-old A129 mice following infection with 2<sup>nd</sup> generation vaccines.

Survival and weight change in 10-week-old A129 mice infected with  $10^4$  pfu via the footpad with CHIKV/IRESv2 or CHIKV/IRESv2b. Animals were under pain level E conditions and were allowed to succumb to illness directly. \* =  $p < 0.05$ . \*\* =  $p < 0.001$ . Analysis of weight change conducted by unpaired, two-tailed Student's T-test. Analysis of survival conducted by Kaplan Meier log rank test ( $p=0.005$ ).

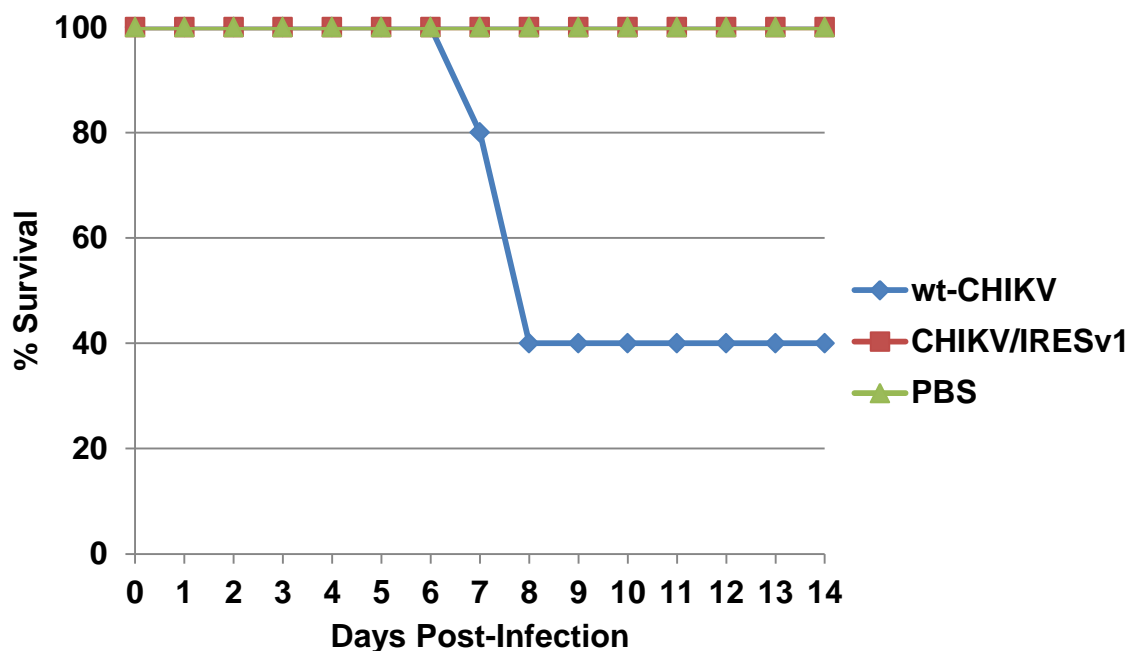


Figure 20: Survival in neonatal CD-1 mice

Survival of neonatal mice injected intracranially with either wt-CHIKV, CHIKV/IRESv1, or PBS. Analysis of survival conducted by Kaplan Meier log rank test ( $p=0.051$ ).

## Summary/Conclusions

These experiments were done to determine whether the vaccine candidates were safe enough for continued preclinical development. To do this, multiple animal models were infected with the CHIKV/IRES vaccine candidates, wt-CHIKV, and/or the 181/25 vaccine. As stated previously, the CHIKV/IRESv1 vaccine was the primary focus of these studies. However this is the first time any of these viruses were tested in an animal model. The TC-83 equivalent of the CHIKV/IRESv1 vaccine was overly attenuated in mice, meaning that although the vaccine was safe it did not confer the immunogenicity that was required for efficacy [67]. However, unlike VEEV strain TC-83, the CHIKV/IRES backbone was a wt-CHIKV strain and there was therefore some concern that the CHIK/IRES vaccine candidates could be too virulent for further development. These tests were designed to test that hypothesis.

In the original infant CD-1 experiments, CHIKV/IRESv1 was unable to replicate to measurable titers in leg tissue, brain, or sera. wt-CHIKV and the 181/25 vaccine, on the other hand, were positive in these tissues post-infection. This realization was both encouraging as well as discouraging. It was difficult to know if a live-attenuated vaccine that was unable to replicate to measurable titers could confer protection against challenge. Thus, a small study was done to examine CHIKV/IRESv2 in the CD-1 model, and it was similarly unable to produce a measurable viremia in 6-7-day old animals.

Knowing that the neonatal CD-1 mouse model was relatively insensitive to CHIKV disease, it was decided that the use of a more sensitive KO mouse model might provide a clearer picture of the attenuation of the CHIKV/IRES vaccine candidates. The STAT1<sup>-/-</sup> KO mice were commercially available, so the CHIKV/IRESv1 and CHIKV/IRESv2 vaccine candidates, wt-CHIKV and the 181/25 vaccine were administered to these animals. Interestingly, CHIKV/IRESv1 and 181/25 produced no detectable disease after infection. The wt-CHIKV was acutely lethal and killed the mice quickly. CHIKV/IRESv2 virus was also lethal by day 8. This study removed the CHIKV/IRESv2 from our focus going forward. The previous stability experiments after cell passaging, however, did allow us to produce the CHIKV/IRESv2b vaccine candidate. Our results suggested that the E2 gene mutation introduced to the CHIKV/IRESv2 backbone attenuates this version 2 vaccine.

Following its observed attenuation in the neonatal CD-1 and STAT1 KO models, studies utilizing CHIKV/IRESv1 and the A129 mouse model were undertaken. CHIKV/IRESv1 remained attenuated in this better described animal model as well. Later studies also included the use of CHIKV/IRESv2 and CHIKV/IRESv2b in this model to test whether they were virulent. Similar to the results with the STAT1 KO model, CHIKV/IRESv2 was virulent in A129 mice, while as predicted, the CHIKV/IRESv2b was better attenuated. These results led to the selection of CHIKV/IRESv1 and CHIKV/IRESv2b as the most promising vaccine candidates for

testing in cynomolgous macaques, where both proved safe, immunogenic and efficacious.

Though these studies used versions 1, 2, and 2b of the CHIKV/IRES vaccine, the focus remained on CHIKV/IRESv1. To this end, the neurovirulence of CHIKV/IRESv1 in the less sensitive CD-1 mouse model was tested. The overly sensitive KO small animal models were not used for neurovirulence testing. This experiment showed that CHIKV/IRESv1 had no measurable impact when injected IC, while wt-CHIKV caused 60% mortality in the animals infected.

Though the work completed and discussed in this dissertation is academic in nature, the data are being used by the collaboration between UTMB and Takeda for vaccine development. We showed that CHIKV/IRESv1 is highly attenuated in immunocompetent and immunocompromised animals. CHIKV/IRESv2 was also highly attenuated in immunocompetent mice, but exhibited residual virulence in the more sensitive KO mouse models. The adapted version 2b, however, remained attenuated in immunocompromised mice.

These studies demonstrate that the IRES-based vaccine platform can be adapted to CHIKV to produce a safe vaccine. This was demonstrated using multiple small animal models of varying ages. We also completed a neurovirulence assay which will prove important in later development stages. The next goal will be to test the vaccines protective properties/

## CHAPTER 5 EFFICACY

### Rationale

The common trend of modern vaccine development for CHIKV as was described in the background chapter is the use of multiple dose DNA, subunit, or VLP vaccines that emphasize safety. Obviously these methods have some benefits over the live-attenuated vaccine strategy, namely the lack of potential for reversion to virulence. Yet, live-attenuated vaccines do have a strong benefit when it comes to rapid and long lasting immunity. Our goal was to generate a safe vaccine that requires only a single dose, and that produces a strong immune response that could confer rapid protection for emergency use during an epidemic. Live-attenuated vaccines are also generally inexpensive to produce, an important feature for a vaccine needed in resource-limited nations with poor infrastructure.

To assess the efficacy of the CHIKV/IRES vaccine candidates, a series of studies was needed to demonstrate whether they could confer protection against challenge with wt-CHIKV. This period of study focused almost exclusively on CHIKV/IRESv1, with one small study measuring the efficacy of CHIKV/IRESv2b. The primary animal model used in these experiments remained the A129 type I IFN receptor KO mouse. Collaborative studies at the Tulane National Primate Research Center were also completed with cynomolgous macaques.

The hypothesis for the vaccine candidates is that a protective response could be induced by a single dose. In the following experiments, I looked at multiple signs of virulence following wt-CHIKV challenge in naïve and vaccinated animals. This resulted in multiple avenues for measuring vaccine-conferred protection as well as characterizing the effects of wt-CHIKV infection of A129 mice in more detail than was previously

published. Once again, the goal for the CHIKV/IRES vaccine is to be less virulent than the 181/25 vaccine (as demonstrated in chapter 4) while retaining the ability to protect against disease. It has been previously shown that the 181/25 vaccine is very efficacious in small animal models and NHPs, and in Phase II clinical trials it elicited extremely high levels of neutralizing antibody in humans. What follows are experiments that establish the efficacy of our CHIKV/IRESv1 vaccine candidate.

## **Results**

Early in the production and testing of the CHIKV/IRES vaccine candidates, the challenge animal model utilized in Dr. Weaver's laboratory focused was the vaccination 3-week-old C57Bl/6 mice followed challenge with a neuroadapted CHIKV strain (Ross) 3 weeks after vaccination [122]. Thus, cohorts of 9-10 three-week-old C57Bl/6 mice were vaccinated SC with  $10^5$  pfu of CHIKV/IRESv1, CHIKV/IRESv2 or 181/25, or a PBS negative control. Three weeks post-vaccination, the animals were bled and their sera were heat inactivated prior to PRNT to determine whether neutralizing antibodies were produced. The animals given any of the three vaccines all seroconverted; (table 5). The vaccines produced similar PRNT<sub>80</sub> titers, while, as expected, the PBS sham vaccination produced no measurable neutralizing antibodies.

The animals were then challenged with the neuroadapted CHIKV and observed for 14 days for survival. Some of the PBS-vaccinated animals began to exhibit signs of illness by day 7, such as ruffled fur and hunched posture. One animal succumbed to infection by day 9, with 6 more animals dying or requiring euthanasia by day 10. The remainder of the animals survived through the duration of the experiment with no signs of illness. The vaccinated animals all survived the challenge (figure 21).



Mouse #	PRNT <sub>80</sub> Titer		
	CHIKV/IRESv1	CHIKV/IRESv2	181/25
1	80	40	80
2	40	80	80
3	40	80	80
4	80	160	80
5	40	40	40
6	160	80	80
7	20	80	40
8	20	40	40
9	80	80	80
10	N/A	80	N/A
% Seroconversion	100	100	100
PRNT <sub>80</sub> Average±Standard Deviation	62±44	76±35	67±20

Table 5: Neutralizing antibody production in C57Bl/6 mice one month post-infection

Induction of neutralizing antibody by CHIKV/IRESv1, CHIKV/IRESv2, or 181/25 in C57Bl/6 mice. CHIKV/IRESv1 and 181/25 had only 9 animals, hence the 'N/A' on row 10 in those columns.

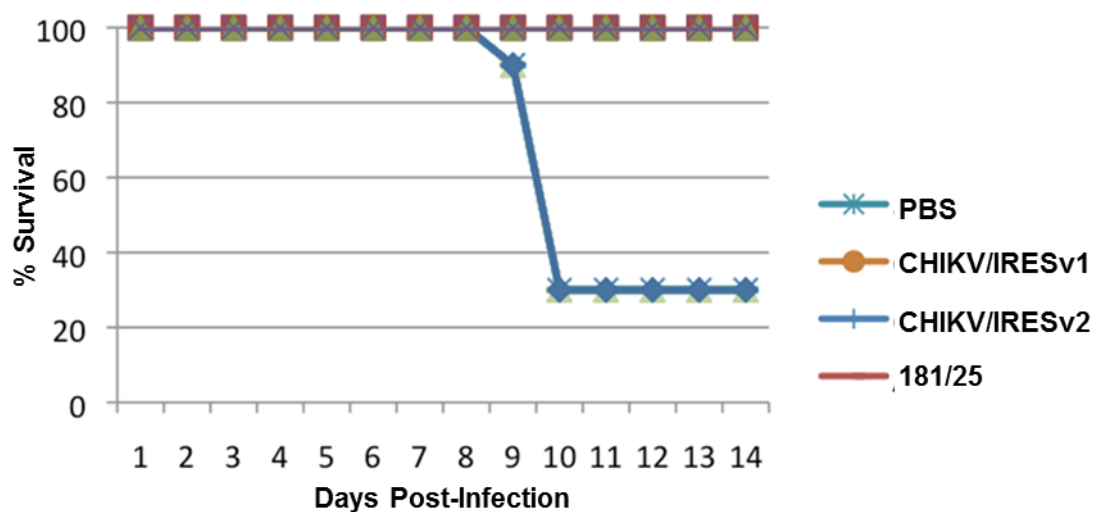


Figure 21: Survival of C57Bl/6 mice challenged with neuroadapted CHIKV

Survival of C56Bl/6 mice vaccinated with either PBS, CHIKV/IRESv1, CHIKV/IRESv2, or 181/25 and challenged with neuroadapted CHIKV. Statistical significance assessed via Kaplan Meier log rank test ( $p=0.000$ ).

The next series of experiments focused on the use of A129 mice in collaboration with Takeda. Three groups of 10-week-old A129 mice were given either PBS or  $10^4$  pfu of CHIKV/IRESv1 or 181/25 CHIKV via the footpad. These animals were observed and at day 2 post infection had their vaccinated footpads measured as stated in the methods

section; refer to the left columns of figure 22. The animals vaccinated with CHIKV/IRESv1 did exhibit slight swelling of the footpad ( $P < 0.05$  by student unpaired t-test). Twenty eight days later, the animals were bled and PRNT<sub>80</sub> assays were run. Each of the 7 animals that received the CHIKV/IRESv1 vaccine had  $\geq 1:320$  titers. The 4 animals that received the 181/25 vaccine also seroconverted, with 3 exhibiting PRNT titers  $\geq 1:320$  and one animal having a neutralizing titer of 1:160. The 4 animals that received the PBS vaccination were all negative for neutralizing antibodies.

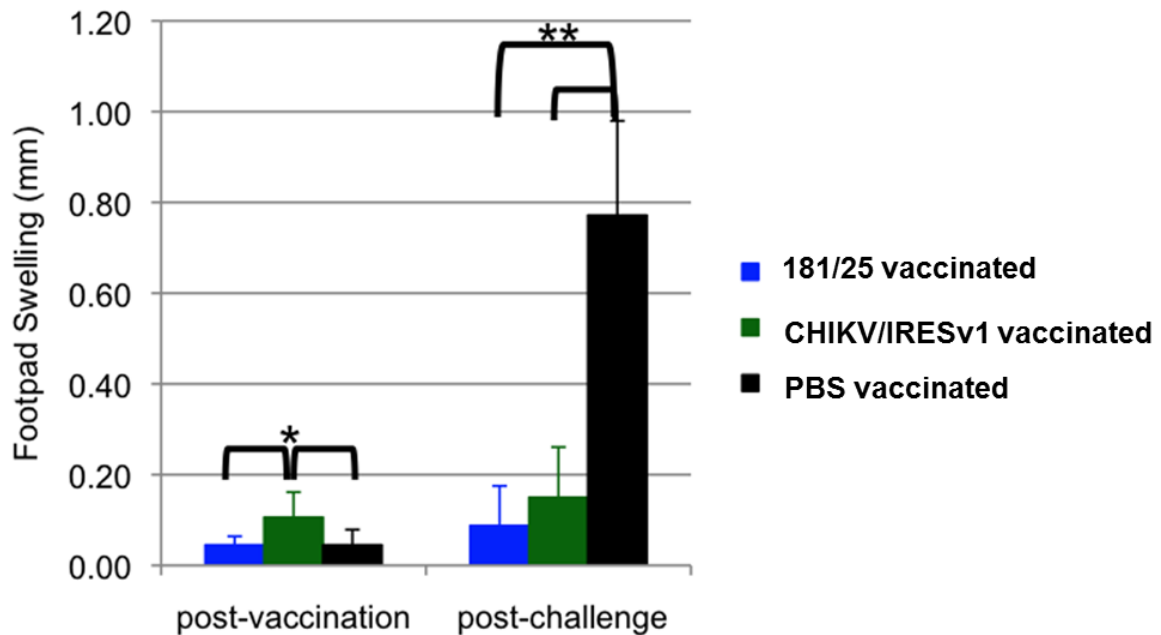


Figure 22: Footpad swelling post-vaccination and post-challenge

Footpad swelling in 10-week-old A129 mice vaccinated with either 181/25, CHIKV/IRESv1, or PBS and challenged with wt-CHIKV. \* =  $p < 0.05$ . \*\* =  $p < 0.001$ . Statistical Analysis conducted by unpaired, two-way Student's T test. Figure from Plante *et al.* [69]

Following the serum collection on day 28 post-vaccination, the mice were challenged with 100 pfu of wt-CHIKV virus via a footpad inoculation and were observed for weight change, morbidity and mortality for 2 weeks. By day 2, the sham-vaccinated animals started exhibiting signs of illness such as lethargy, ruffled fur, and hunched posture. At 2 days post-challenge the animals' footpads were measured for swelling; refer to the right columns of figure 22. The subjects that received the PBS vaccination developed a large amount of swelling, which was statistically different ( $p < 0.001$  by

students unpaired t-test) from the vaccinated groups, and succumbed to illness by day 3. All animals that were given either of the vaccines survived for the duration of the experiment. Interestingly, the animals that were vaccinated with CHIKV/IRESv1 did suffer slight weight loss on days 8 and 9. During this time period, the weight loss was significantly greater than that in the 181/25 vaccinees as measured by 1-way ANOVA ( $p < .05$ ). The animals in this cohort did recover after day 9, (figure 23).

Another experiment was designed to compare the histopathological changes caused by either CHIKV/IRESv1 or sham PBS vaccination, either with or without wt-CHIKV challenge. This experiment was designed to further our knowledge of wt-CHIKV infection of this KO model while simultaneously characterizing the protection against challenge elicited by the CHIKV/IRESv1 vaccine. The study used 10-week-old A129 mice in 2 cohorts of 3 animals. One group was given  $10^4$  PFU of CHIKV/IRESv1 and one group was given PBS in the footpad. At 4-days post-vaccination one animal was sacrificed from each cohort and all major organs (liver, lung, brain, heart, kidney, spleen, and the animal's left hind leg) were fixed and prepared for sectioning as described in the methods section. The remaining animals were then observed until day 26, when they were challenged with 100 PFU of wt-CHIKV in the footpad. These animals were sacrificed 4 days post-challenge, and tissues were again collected and fixed for sectioning. The only remarkable histopathological lesions seen were found in the spleens of unvaccinated, wt-CHIKV infected animals, (figure 24). The splenic architecture was disrupted in the non-vaccinated, wt-CHIKV challenged animals. Also there was noticeable necrosis and deposition of proteinacious debris. Interestingly, the legs that were swollen in the sham vaccinated animals that were challenged with wt-CHIKV showed only edema with no cellular infiltrate, myositis, or arthritis at day 4 post-challenge. Animals that were vaccinated with CHIKV/IRESv1 had no splenic lesions, demonstrating that CHIKV/IRESv1 can protect against tissue damage as well as lethal outcome.

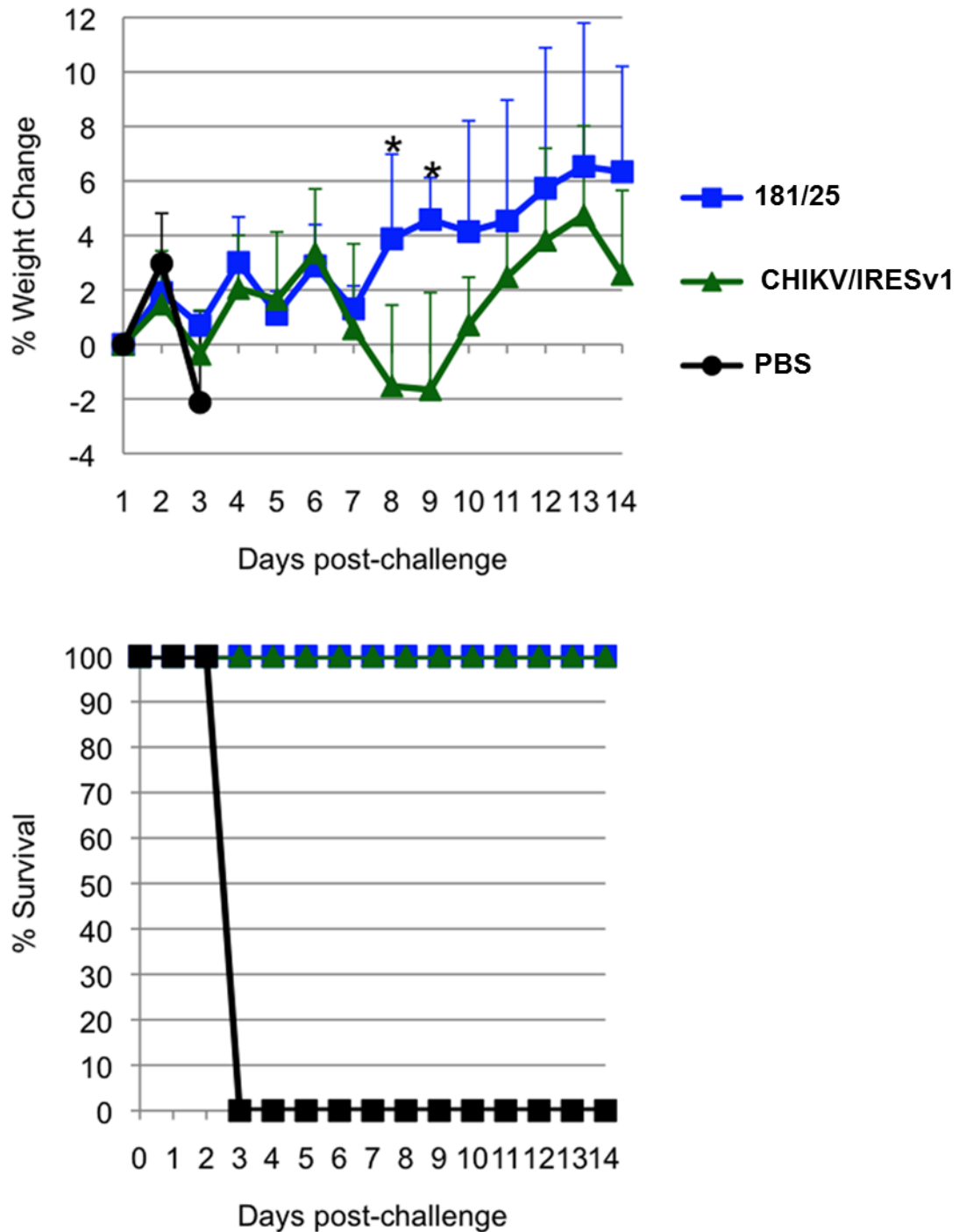


Figure 23: Survival and weight change in 181/25 or CHIKV/IRESv1 vaccinated, wt-CHIKV challenged A129 mice

Impact of wt-CHIKV challenge on A129 mice vaccinated with either 181/25, CHIKV/IRESv1, or PBS. \* =  $p < 0.05$ . \*\* =  $p < 0.001$ . Statistical Analysis conducted by unpaired, two-way Student's T test. Survival analysis conducted via Kaplan Meier log rang test ( $p=0.000$ ). Figure from Plante *et al.* [69]

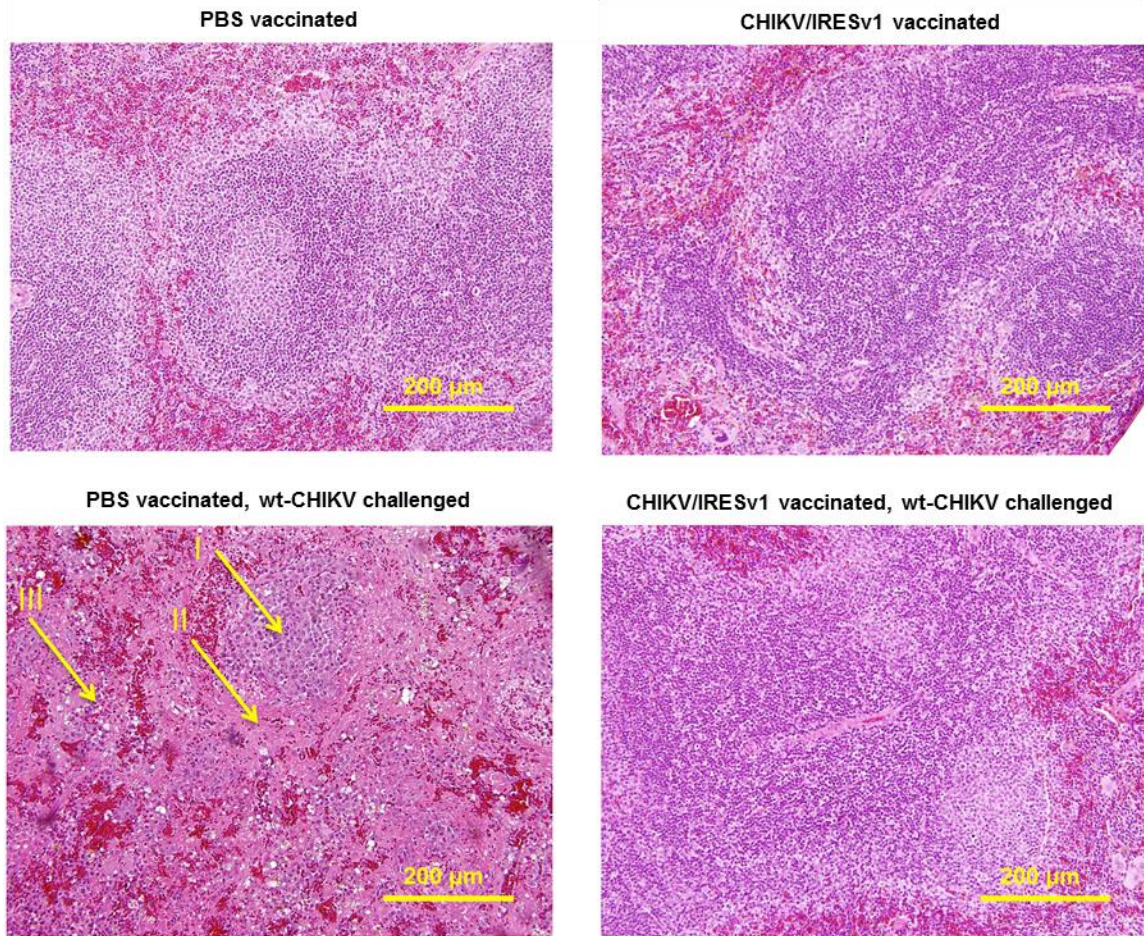


Figure 24: Splenic pathology in A129 mice

Pathology in spleens of 10-week-old A129 mice vaccinated with either PBS or CHIKV/IRESv1 and challenged with wt-CHIKV. I = follicle. II = proteinaceous debris. III = Monocytoid cell. Figure from Plante *et al.* [69]

The next goal was to test the protective capabilities of the attenuated CHIKV/IRESv2b vaccine candidate. A small experiment was designed for the animals that survived the virulence experiment described in chapter 4. These two cohorts of animals (n=5) of PBS and CHIKV/IRESv2b vaccinated mice were challenged with 100 pfu of wt-CHIKV in the footpad 28 days post-vaccination. The animals were observed for mortality for 2 weeks after challenge. All animals that received the sham vaccination died by day 4 after challenge, while the animals that were vaccinated with CHIKV/IRESv2b all survived lethal challenge, refer to figure 25.



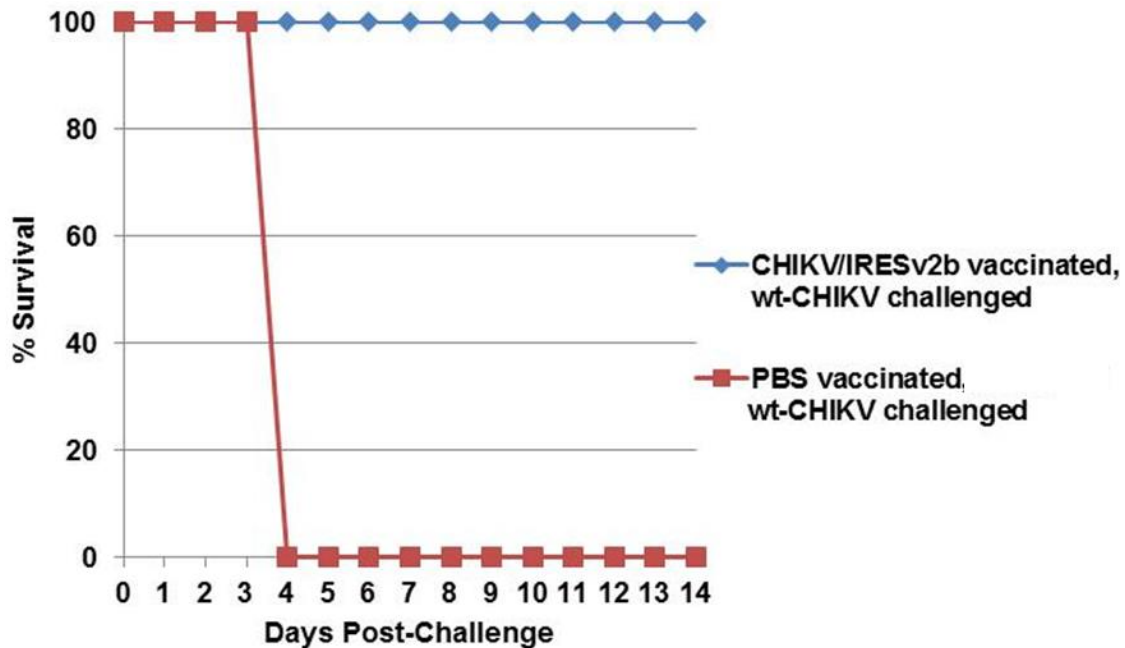


Figure 25: Survival of wt-CHIKV challenge in CHIKV/IRESv2b-vaccinated A129 mice  
 Survival of A129 mice vaccinated with either CHIKV/IRESv2b or PBS and challenged with wt-CHIKV. Survival analysis conducted via Kaplan Meier log rang test (p=0.000).

To test the duration of immunity, several experiments were designed and completed, generally focusing on the humoral response. The first experiment used CD-1 mice and the goal was to determine whether a humoral response could be detected in a mouse model that did not appear to support CHIKV/IRESv1 replication. The goal was also to test the duration of this immune response, and to measure the effects of a second vaccination 30 days after the first vaccination. Five cohorts of 5 mice were vaccinated with either PBS (1 cohort), CHIKV/IRESv1 (2 cohorts), or CHIKV/IRESv2b (2 cohorts). One of each vaccinated mice cohorts were then boosted 30 days after the initial vaccination with the homologous vaccine, and the others were given a PBS “boost.” Sera were collected once every 30 days for 150 days post-vaccination. The CHIKV/IRES vaccines were shown to produce relatively low neutralizing antibody titers at day 30, with PRNT<sub>50</sub> values of roughly 1:50 for both vaccines. The titers gradually increased with time, peaking at day 150. The boost seemed to have little effect on increasing the neutralizing antibody titers in response to CHIKV/IRESv1. However, the

CHIKV/IRESv2b boost did significantly increase neutralizing antibody titers, suggesting that future work should focus on use of this vaccine candidate as a booster. (Figure 26)

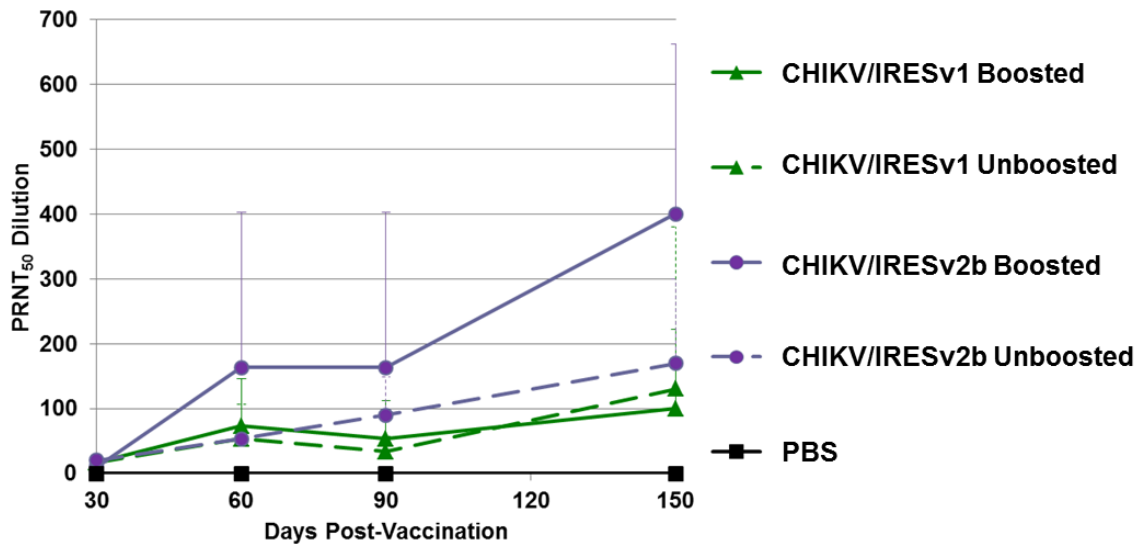


Figure 26: Long-term antibody production in CD-1 mice

Longitudinal neutralizing antibody production in CD-1 mice vaccinated with either CHIKV/IRESv1 or CHIKV/IRESv2b, with or without a boost. PRNT<sub>50</sub> values used due to lower neutralizing titers in this animal model.

Knowing that immunocompetent mice maintained neutralizing antibodies over an extended duration, I was interested in testing the longevity of protection afforded by CHIKV/IRESv1 in the immunocompromised mouse model afforded by neutralizing titers. To this end, a collaborative experiment was done with Takeda wherein 6 A129 mice received  $10^4$  pfu of CHIKV/IRESv1 via the footpad. Animals were observed post-vaccination, and no remarkable changes appeared. The animals were bled and sera were collected at days 21, 42, 59, and 92 post-challenge. The sera were tested for neutralizing antibody as described previously. At day 92 the animals were challenged by a 100 pfu footpad inoculation of wt-CHIKV, then observed for footpad swelling, weight change, temperature, and survival. The animals that received the vaccine were protected against the lethal challenge, while all animals that received the sham vaccination succumbed to illness by day 5 after challenge; (figure 27). We believe the delayed time of death in this

study is due to the advanced age of the animals at the time of challenge. Prior to death, the sham-vaccinated, wt-CHIKV-challenged animals suffered swelling of the inoculated footpad and hyperthermia at day 3, followed by two days of hypothermia prior to death. The sera of these animals were tested for neutralizing antibody titers and all animals that were vaccinated reached the upper limit of our test by day 56, and remained there until day 92 when they were challenged. The sham vaccinated animals were all negative for neutralizing antibody titers; refer to figure 28.

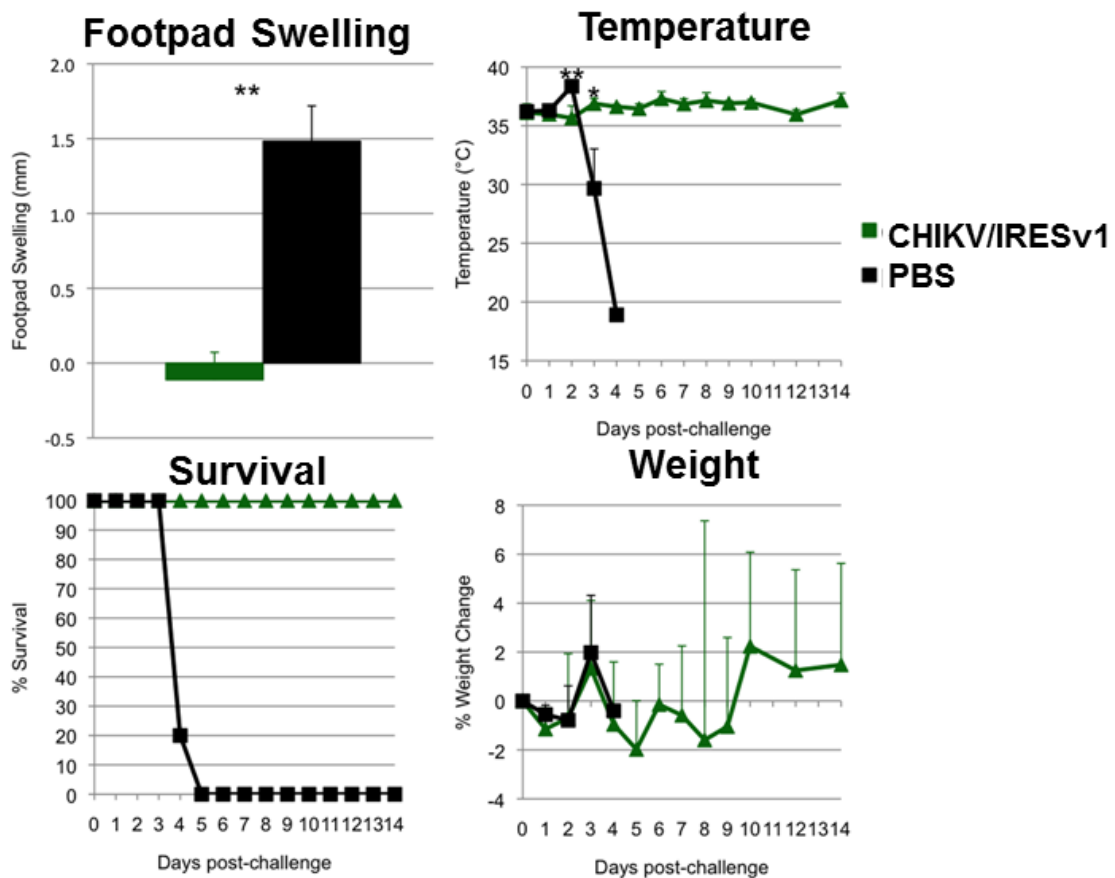


Figure 27: Longitudinal efficacy in A129 mice

Longitudinal efficacy of CHIKV/IRESv1 to protect against signs of wt-CHIKV challenge in A129 mice. Multiple aspects of disease were measured, such as footpad swelling, temperature change, weight change, and survival. Animals that received CHIKV/IRESv1 were protected against the negative impacts of the wt-CHIKV challenge. \* =  $p < 0.05$ . \*\* =  $p < 0.001$ . Statistical Analysis conducted by unpaired, two-way Student's T test. Survival analysis conducted via Kaplan Meier log rang test ( $p=0.000$ ). Figure from Plante *et al.* [69]



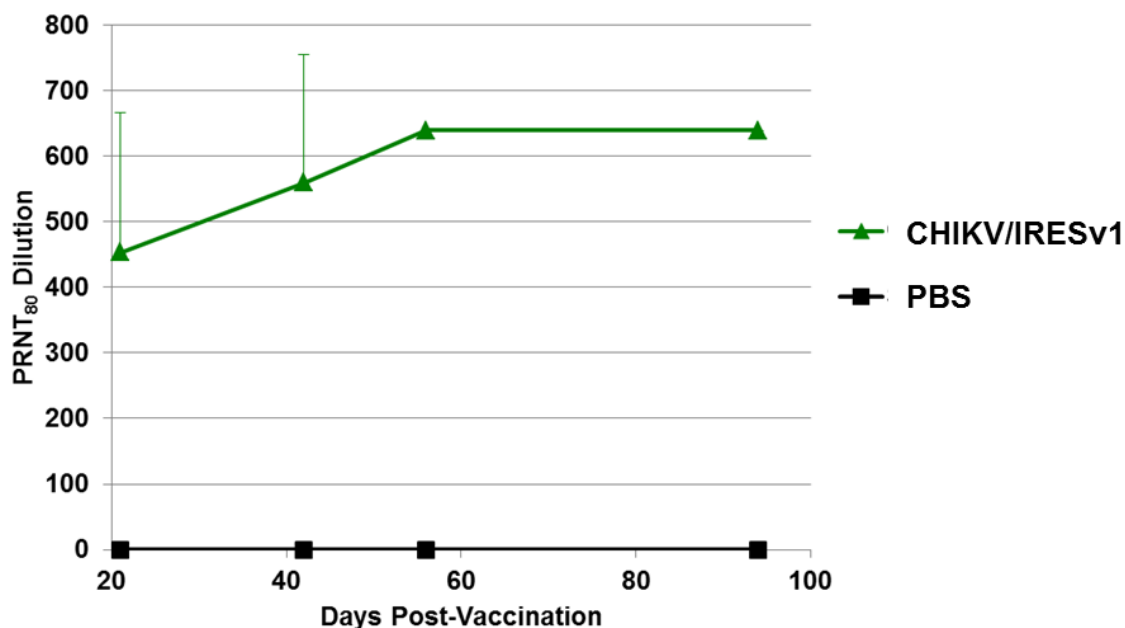


Figure 28: Longitudinal production of neutralizing antibody in A129 mice

Long term antibody production by CHIKV/IRESv1 in A129 mice.

## Summary/Conclusions

The experiments described in this chapter were designed to test the immunogenicity and efficacy of novel CHIKV/IRES vaccines. To this end multiple animal models were used and different aspects of protection against a wt-CHIKV challenge were measured. The humoral response was the primary focus of these studies, although the use of type I IFN receptor KO mice was necessary to sensitively show efficacy, demonstrating the importance of the IFN pathway in CHIKV infection in the small animal model. We believe that these studies show conclusively that the CHIKV/IRES vaccine platform can be adapted to produce a protective vaccine with a single dose.

Initially we tested the virus in immunocompetent mice. The C57Bl/6 mouse model is useful using a lethal IN inoculation of the neuroadapted Ross strain of CHIKV [122]. The animals that were vaccinated with either 181/25 or CHIKV/IRESv1 produced similar PRNT<sub>80</sub> titers and were protected against an IN challenge. Obviously these

studies used unnatural routes of infection compared to mosquito transmission in nature. However, as an interesting bonus this study showed the possibility that CHIKV/IRESv1 could protect against a weaponized aerosol version of CHIKV. This is obviously conjecture, but it remains thought provoking.

The immunocompetent CD-1 mice were also used in this study to demonstrate safety. It was known that wt-CHIKV replicates in neonatal CD-1 mice quite efficiently; note the results of chapter 4 of this dissertation and the original model development work done by Ziegler *et al.* [73]. However, the CHIKV/IRES vaccine candidates do not replicate to measurable titers in these animals. Knowing this, we were interested to see whether the CHIKV/IRES vaccines could induce a measurable immune response in the form of a neutralizing antibody titer and whether a boosting vaccination was required. Note that these studies used PRNT<sub>50</sub> data, not PRNT<sub>80</sub> due to the lower neutralizing antibody titers seen in these young CD-1 mice compared to the adult A129. All the animals in the experiment did seroconvert with a single dose. Animals that received a boosting vaccination of the CHIKV/IRESv1 did not receive a large benefit from the second vaccination. However, animals that were primarily and secondarily vaccinated with CHIKV/IRESv2b did exhibit a notable increase in neutralizing titers. Though no small animal model correctly imitates all aspects of human infection with CHIKV, this is an interesting set of data that may warrant future studies on the benefits of using multiple doses. Recent NHP studies done at the Tulane National Primate Research Center have shown that not only do macaques generate relatively high levels of neutralizing antibodies, but the vaccines (CHIKV/IRESv1 and CHIKV/IRESv2b) protect against a challenge with wt-CHIKV (Chad Roy *et al.*, in revision).

Several experiments were completed using the highly sensitive safety and efficacy model of A129 mice. These experiments showed that CHIKV/IRESv1 (and in lesser detail CHIKV/IRESv2b) is protective to a high degree against lethal challenge. These animals were measured for multiple signs of disease manifestation post-challenge such as

survival, footpad swelling, temperature changes, and histopathological lesions in multiple tissues. Note that since these experiments were not necessarily reported here in the chronological order in which they were completed, we knew *a priori* to measure different aspects of virulence at different times. However, the point to be taken from these experiments is relatively straight forward. The CHIK/IRESv1 vaccine was found to cause slight swelling of the footpad site of vaccination. Yet, it protected against the severe swelling that accompanies the wt-CHIKV challenge. Vaccinated animals exhibited no temperature changes post-challenge, although they did suffer a slight weight loss approximately one week after challenge if they were vaccinated with the CHIKV/IRESv1 vaccine. There were no other outward appearances of illness in these mice. The animals that were sham-vaccinated and challenged suffered severe disruption of splenic architecture, which did not occur in animals that were vaccinated with the CHIKV/IRESv1 vaccine. A small side experiment was also completed using the CHIKV/IRESv2b vaccine strain, which also showed protection against a lethal challenge.

The next step was to measure the longitudinal effects of the CHIKV/IRES vaccine in the A129 model. It was decided that approximately 3 months was an appropriate timeframe to test whether CHIKV/IRESv1 could produce long lasting or only transient immunity and protection. Interestingly, neutralizing antibody titers in vaccinated mice increased with time. The CD-1 experiment showed this as well, suggesting that CHIKV/IRESv1 may cause some sort of persistent infection. This possibility was addressed with an experiment in A129 mice that will be described in chapter 6. These mice were found to produce  $\geq 640$  PRNT<sub>80</sub> titers after day 56 post-vaccination, and the mice were protected against lethal outcome, footpad swelling, and temperature change. Other work has been done in Dr. Weaver's laboratory by Dr. Seymour which has shown that CHIKV/IRES does not persist in the Rag1 KO mouse model that is deficient in mature B- or T-cells (Seymour *et al.* unpublished).

In summary, we believe that our data show conclusively that the CHIKV/IRESv1 vaccine candidate is a safe, stable and highly efficacious live-attenuated vaccine based on preclinical evaluations. We were interested in answering several questions that have come to light. First, does this vaccine replicate in vaccinated animals and, if it does, is it persistent? Are there other histopathological lesions missed by the single day of observation and tissue collection that we used? Also, can we demonstrate to a higher degree the stability of this live-attenuated virus to address the safety concerns faced by all vaccines that are under development, while expanding our academic knowledge of our vaccine and the CHIKV small animal model which has now become so commonly used? We will have to answer these questions in the next series of experiments.

## CHAPTER 6 EXTENDED SAFETY AND EFFICACY, TROPISM, AND STABILITY

### IN-VIVO

#### Rationale

In the previous chapters, evidence for the vaccine candidates' safety and efficacy has been shown. This chapter represents more recent work delving in greater detail into how the CHIKV/IRESv1, wt-CHIKV and the 181/25 vaccines behave *in vivo*. The work presented here was conducted to increase our knowledge of the safety and efficacy of the vaccine as well as to understand the course of CHIKV infection in the A129 model.

At the time these experiments were designed, knowledge of the course of infection in the A129 mice was limited to the initial studies that were done on the model [75]. Recently, Ryman *et al.* published a greater scope of work based on the A129 model [123]. However, for our studies we were very interested in the kinetics and tropism of wt-CHIKV. We were also interested in the tropism of our CHIKV/IRESv1 vaccine candidate. Previous work in CD-1 mice showed that CHIKV/IRESv1 did not produce a measurable viral load in the brain or knee tissue, and also caused no measurable viremia. However, due to the high PRNT<sub>80</sub> titers developed after vaccination it was thought that the virus must replicate in these animals.

Originally, tropism was going to be assessed by producing FfLuc-containing vaccine candidates and visualizing them via IVIS. A series of constructs for CHIKV/IRESv1, CHIKV/IRESv2b and wt-CHIKV was designed and constructed, but they ejected the FfLuc gene shortly after electroporation. Thus, to determine the tropism of these viruses it was decided that serial sacrifice experiments using transcardial perfusion would be undertaken. This technique had added benefits of more and better

quantifiable data. IVIS was utilized in some of the work described here, though not in the capacity in which we originally planned.

A large concern of any live-attenuated vaccine is its stability *in vivo* (i.e., if the vaccine spilled over into the normal transmission cycle, would it remain stable and safe or would it revert to virulence and cause disease). Also it is important that the vaccine remains stable inside of the vaccine. It is important to note that the IRES vaccine platform is designed to stop this by preventing replication in the vector, but we wanted to prove conclusively that even given the worst case scenario of accidental transmission it would remain safe.

The hypothesis pertaining to these experiments was simple; that the CHIKV/IRESv1 has a limited spread compared to wt-CHIKV and the 181/25 vaccine, and that CHIKV/IRESv1 would effectively limit the spread of replicating virus after a wt-CHIKV challenge. We also believed due to the severely attenuated phenotype and the failsafe construction of the CHIKV/IRESv1 vaccine candidate, it would remain attenuated after brain passaging in neonatal mice. It is believed the following studies address these concerns convincingly.

## **Results**

The first goal was to better our understanding of wt-CHIKV infection in the 10-week-old A129 mice and to compare that data against CHIKV/IRESv1 and the 181/25 vaccine. Two cohorts of 24 mice were infected with  $10^4$  pfu of either CHIKV/IRESv1, or 181/25 via the footpad. A 3<sup>rd</sup> cohort of 12 mice was given  $10^4$  pfu of the wt-CHIKV, and a 4<sup>th</sup> cohort of 8 mice was given PBS via the same route. Three animals were taken from each of the experimental cohorts at days 1-4, and the cohorts that received the vaccines were also harvested days 14, 21, and 28. The wt-CHIKV was not harvested at

this time due to animals generally succumbing to illness by day 4. Footpad swelling was also measured in all of these mice. The animals were then anesthetized and transcardially perfused as described in chapter 2. After the perfusion procedure, the animals' major organs were collected for titration and histopathology.

Interestingly, this is the first time we followed fp swelling for more than a single day after infection (previously it was just a day 2 observation). We did initially detect minor swelling in the PBS-inoculated animals, which we attributed to the trauma of a fp inoculation. wt-CHIKV caused severe fp swelling by day 2 and increased through day 4 (refer to figure 29). Both vaccines caused minor swelling early in the course of infection (days 1-4), which was expected because of the minor swelling seen previously at day 2 (figure 22). Interestingly, we saw prolonged minor swelling through the day 14 timepoint for both CHIKV/IRESv1 and 181/25 ( $p < .001$  via one-way ANOVA). The swelling did return to normal level by day 21.

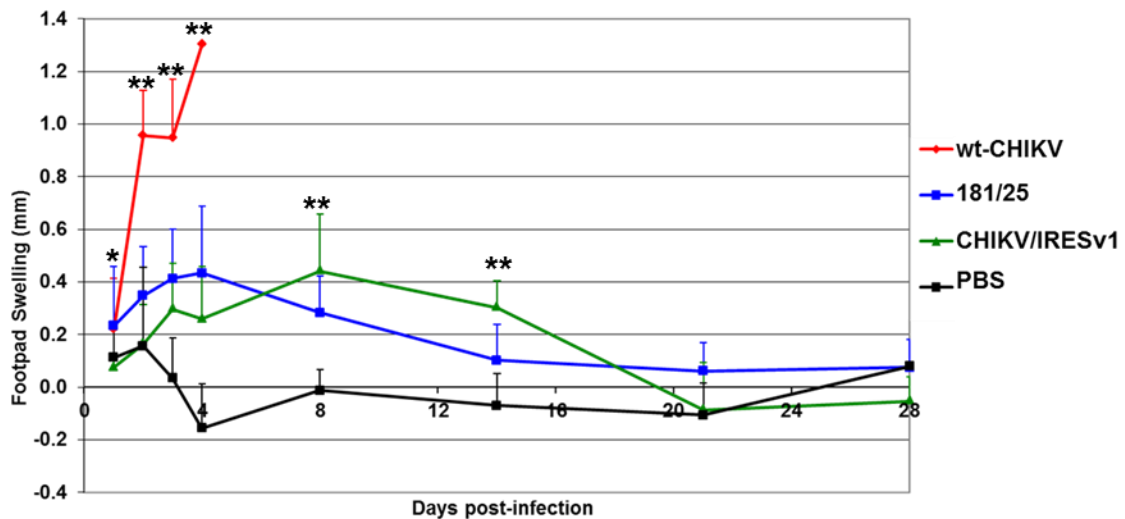


Figure 29: Footpad swelling in A129 mice

Footpad swelling in 10-week-old A129 mice. \* =  $p < 0.05$ . \*\* =  $p < 0.001$ . Statistical Analysis conducted by one-way ANOVA.

The major organs, sera and muscle extracted from the hind left leg (leg of inoculation) were collected for titration. These titers were taken for all cohorts at all

timepoints to define the kinetics of infection. wt-CHIKV virus produced systemic infection, with all tissues being positive by day one and the spleen and muscle having the highest viral load per gram. Viral loads increased through day 4 until the titers were between 6-8 log<sub>10</sub> pfu/g or pfu/ml in all tissues (figure 30).

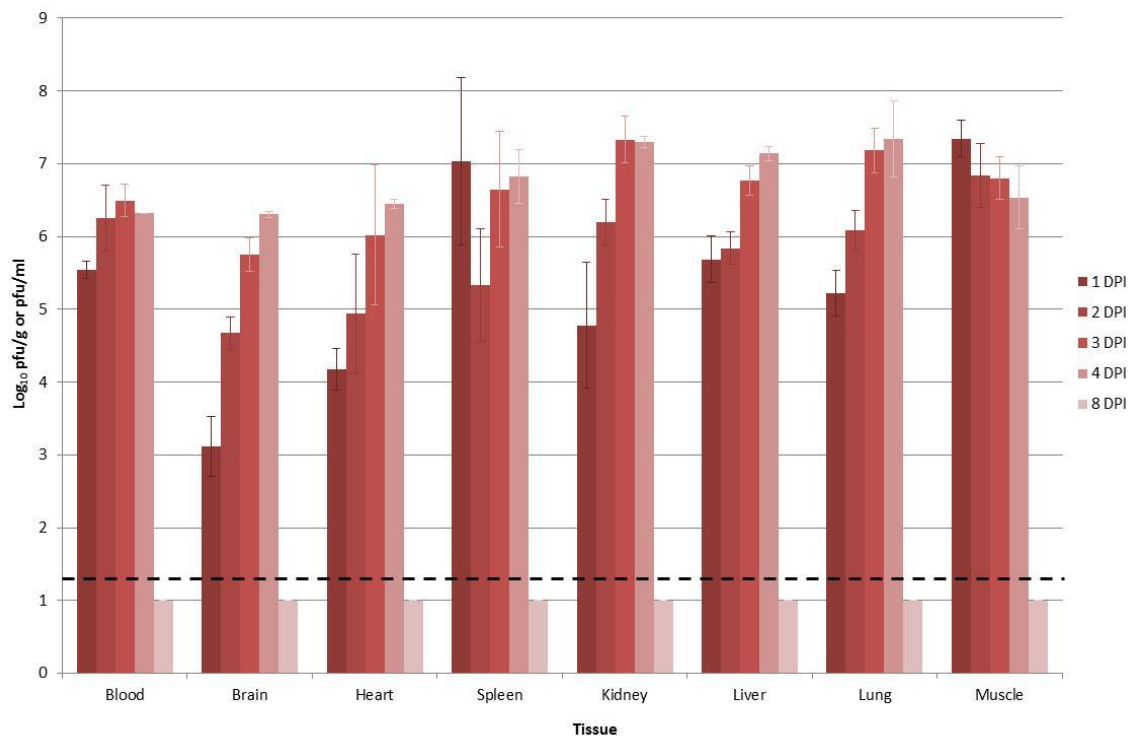


Figure 30: Tissue tropism of wt-CHIKV in A129 mice

Replication of wt-CHIKV in various tissues of A129 mice. Bars represent average titers, error bars represent standard deviations. Dashed line represents limit of detection.

The 181/25 vaccine also replicated relatively well in this animal model. On the first day, viral loads were only detectable in the spleen and muscle. However by day 2 the virus had spread to all tissues tested except the brain. By day 3 the animals were systemically infected, with the spleen and muscle having the highest viral load per gram. The day four samples had an increased viral load in all of the tissues tested except for a slight decrease in viremia. By day 8 the animals had cleared the virus (figure 31). The tissues remained negative at the 3 later timepoints.



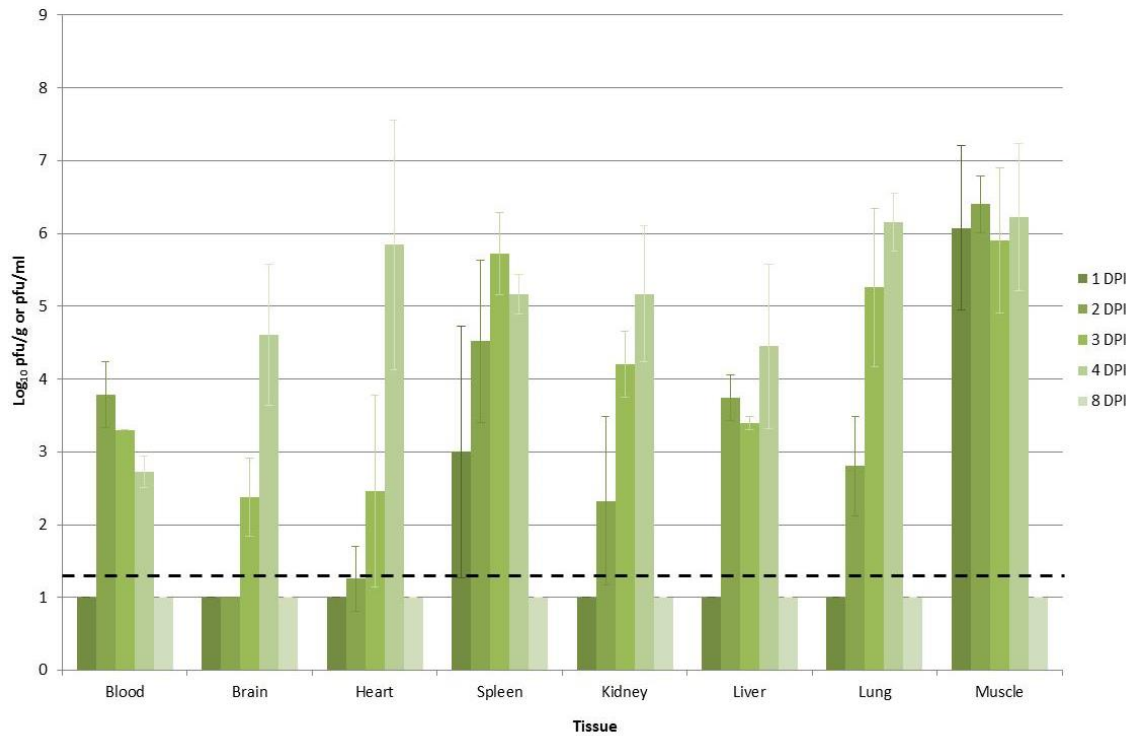


Figure 31: Tissue tropism of 181/25 in A129 mice

Replication of 181/25 in various tissues of A129 mice. Bars represent average titers, error bars represent standard deviations. Dashed line represents limit of detection.

CHIKV/IRESv1 was not detected in any of the tissues measured on day 1. On day 2, 2 of the 3 animals tested had very low-level viral loads in the muscle (just above our limit of detection). By day 3, there were still only 2 of 3 animals with measurable viral loads in the muscle, but the level has increased to  $\sim 3 \log_{10}$ . Day 4 samples revealed a slight spread with 2 of the 3 animals being positive in the spleen and leg muscle and 1 of 3 animals having a measurable viremia. No virus was found in the tissues by day 8, (figure 32). Later timepoints were also negative.

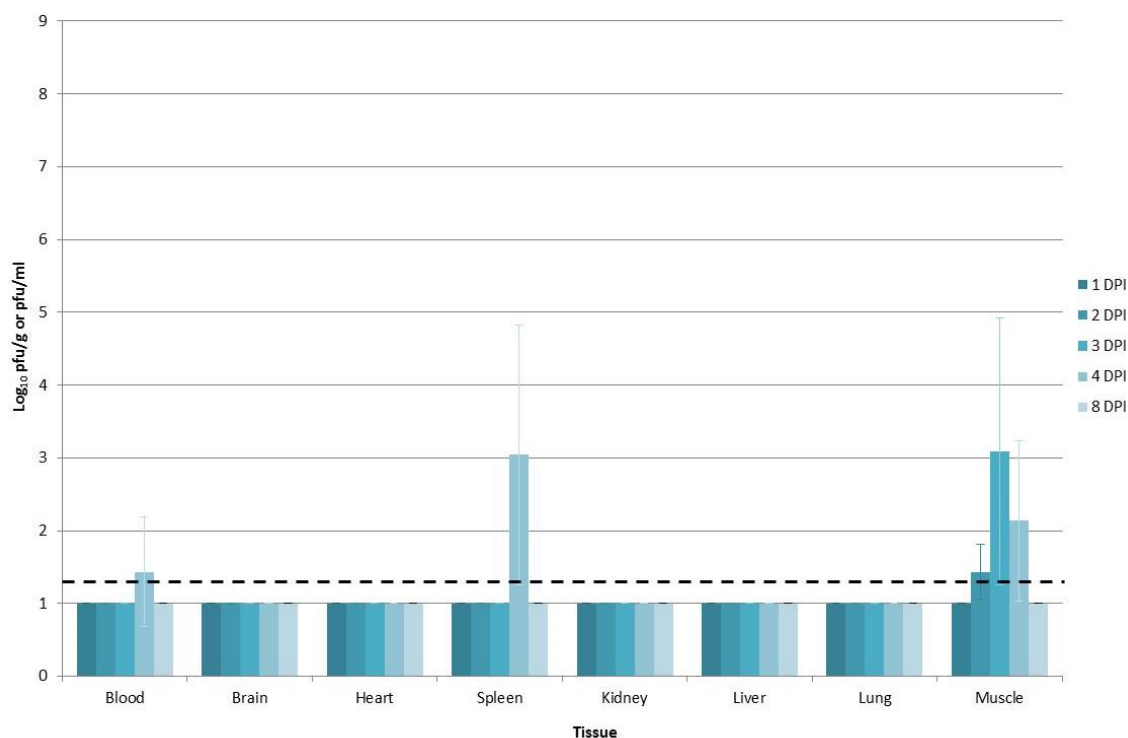


Figure 32: Tissue tropism of CHIKV/IRESv1 in A129 mice

Replication of CHIKV/IRESv1 in various tissues of A129 mice. Bars represent average titers, error bars represent standard deviations. Dashed line represents limit of detection.

A statistical comparison of tissue titers revealed significant variation by one-way ANOVA between the three virus groups for all organs at days one through four post-infection (Table 6). Bonferroni post-hoc analysis demonstrated that at one day post-infection, the two vaccine strains were essentially identical and were both different from wt-CHIKV. As time progressed, 181/25 came to resemble wt-CHIKV in multiple tissues especially the muscle and spleen. CHIKV/IRESv1, on the other hand, was significantly different from wt-CHIKV at all timepoints and for all organs tested. Note that post-hoc analysis was not possible for the blood samples at four days post-infection because there was only one wt-CHIKV sample available for the comparison.

Day	Organ	One-Way ANOVA	Bonferroni Post-Hoc Analysis		
			wt-CHIKV vs. 181/25	wt-CHIKV vs. CHIKV/IRESv1	181/25 vs. CHIKV/IRESv1
1	Blood	0.000	0.000	0.000	1.000
	Brain	0.000	0.000	0.000	1.000
	Heart	0.000	0.000	0.000	1.000
	Spleen	0.002	0.019	0.003	0.263
	Kidney	0.000	0.000	0.000	1.000
	Liver	0.000	0.000	0.000	1.000
	Lung	0.000	0.000	0.000	1.000
	Muscle	0.000	0.337	0.001	0.001
2	Blood	0.000	0.001	0.000	0.000
	Brain	0.000	0.000	0.000	1.000
	Heart	0.000	0.000	0.000	1.000
	Spleen	0.001	0.765	0.002	0.005
	Kidney	0.000	0.001	0.000	0.171
	Liver	0.000	0.000	0.000	0.000
	Lung	0.000	0.000	0.000	0.006
	Muscle	0.000	0.692	0.000	0.000
3	Blood	0.000	0.000	0.000	0.000
	Brain	0.000	0.000	0.000	0.007
	Heart	0.002	0.011	0.002	0.321
	Spleen	0.000	0.273	0.000	0.000
	Kidney	0.000	0.000	0.000	0.000
	Liver	0.000	0.000	0.000	0.000
	Lung	0.000	0.033	0.000	0.001
	Muscle	0.022	1.000	0.029	0.089
4	Blood	0.004	N/A	N/A	N/A
	Brain	0.000	0.089	0.001	0.002
	Heart	0.004	1.000	0.007	0.010
	Spleen	0.038	0.523	0.046	0.218
	Kidney	0.000	0.033	0.000	0.001
	Liver	0.001	0.028	0.001	0.006
	Lung	0.000	0.039	0.000	0.000
	Muscle	0.005	1.000	0.012	0.010

Table 6: Statistical Analysis of Tissue Titers in Perfused A129 Mice

Analysis of log<sub>10</sub> PFU/ml and PFU/g tissue titers from perfused A129 mice infected with wt-CHIKV, 181/25, or CHIKV/IRESv1. All virus groups were compared for a given tissue/timepoint combination by one-way ANOVA. Individual virus groups were compared for a given tissue/timepoint combination by Bonferroni post-hoc analysis. Red = not statistically significant, p≥0.05. Light green = statistically significant, p<0.05. Dark green statistically significant, p<0.001.

The only known histopathological lesions seen following infection with wt-CHIKV in this animal model were in the spleen at day 4. We were interested in looking at more timepoints to see if other lesions formed elsewhere at different times. We were also interested in looking at the fp of vaccinated animals later after inoculation. The organs previously listed and the whole hind left leg were analyzed as described in chapter 2. The splenic pathology was previously described (figure 24); lesions formed in the wt-CHIKV-infected animals as early as day 2. Animals receiving a CHIKV/IRESv1 or 181/25 vaccine or a PBS inoculation did not suffer splenic lesions, and a representative image is shown in figure 33. There were a small number of hepatic lesions in animals given wt-CHIKV by day 3, and to a lesser extent day 4. These lesions were not found in animals receiving PBS or either vaccine, refer to figure 34. The whole leg was observed days 1-4, and on day 4 there was a small level myositis seen in the wt-CHIKV infected animals, however this was very focal and rare. The day 4 leg histopathology can be seen in figure 35. Interestingly, though, by the later timepoints the 181/25 vaccine and the CHIKV/IRESv1 vaccine caused moderate myositis and cellulitis. This persisted until day 21, when it was healing, and then generally cleared by day 28 (refer to figure 36).

Initially, tropism studies were planned with using IVIS and FfLuc-containing constructs. However, as stated earlier these studies ran into many issues and were abandoned for the perfusion serial sacrifice study. However, we did obtain a stable capsid fusion wt-CHIKV FfLuc virus from Dr. Klimstra. Pilot studies showed that animals given this virus were able to be visualized via IVIS, though the images were found to be of limited use when it came to examination of tissue tropism (data not shown). Animals receiving the wt-CHIKV FfLuc construct succumbed to illness later compared to the standard wt-CHIKV, as shown in figure 37. Knowing the limitations of IVIS, we decided to use this tool in a different fashion. A study was designed to determine if animals that received our CHIKV/IRESv1 vaccine candidate could prevent



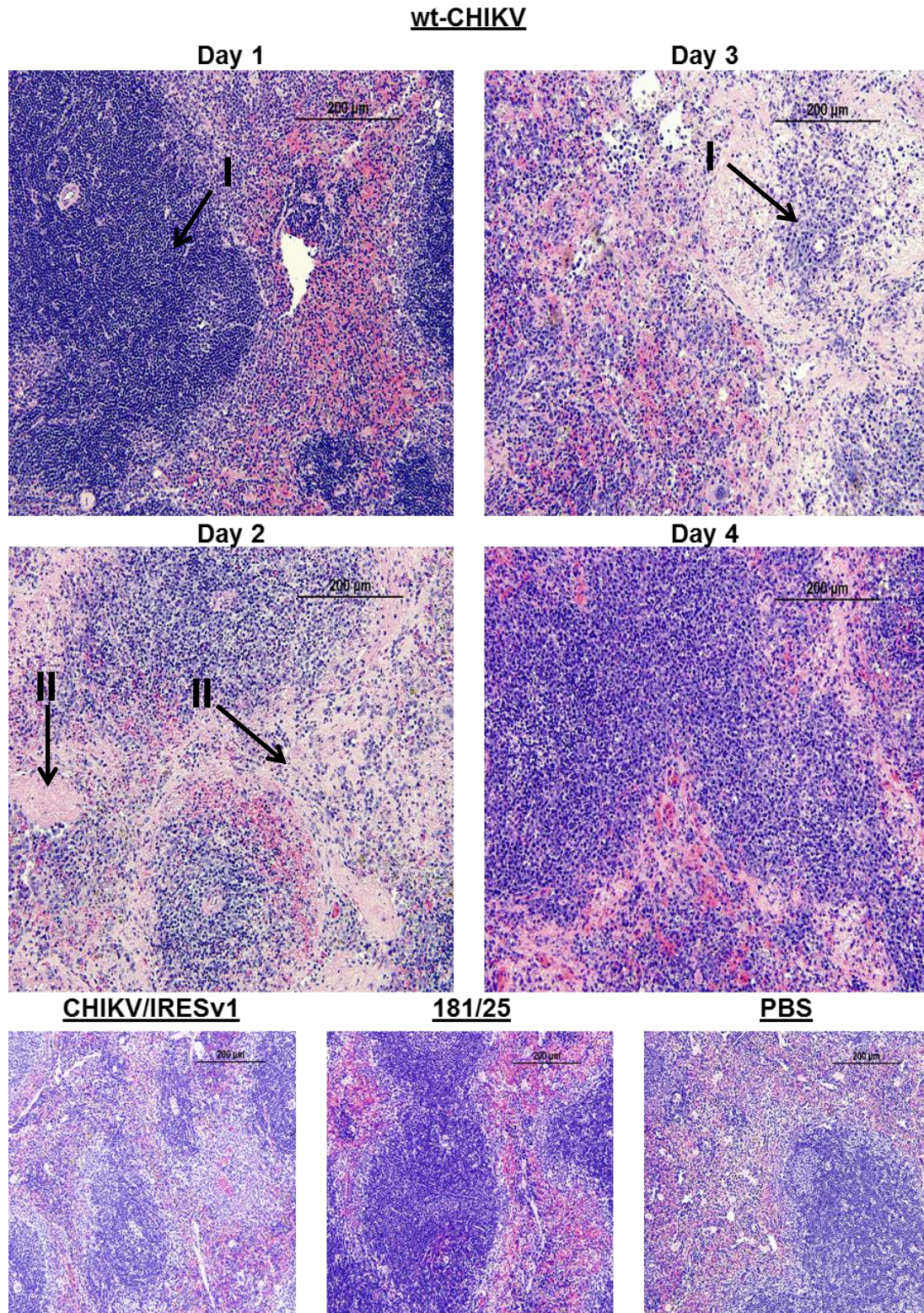


**Figure 33: Histopathology of the spleen in A129 mice**  
 Histopathology of spleen from A129 mice infected with either wt-CHIKV, CHIKV/IRESv1, 181/25, or PBS. The CHIKV/IRESv1, 181/25, and PBS images are from a representative day 3 sample. I = follicle. II = proteinaceous debris.



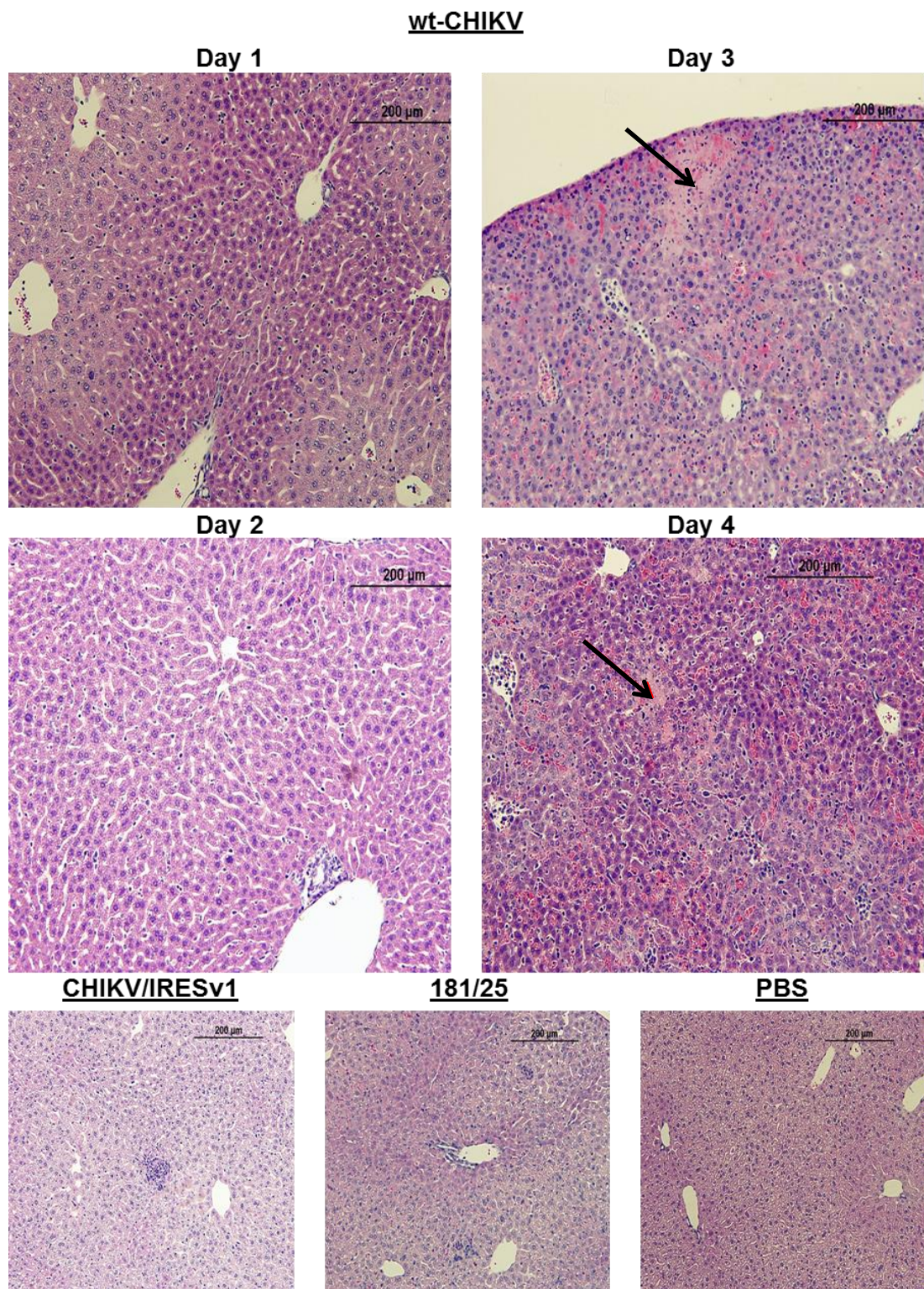


**Figure 34: Histopathology of the liver in A129 mice**

Histopathology of liver from A129 mice infected with either wt-CHIKV, CHIKV/IRESv1, 181/25, or PBS. The CHIKV/IRESv1, 181/25, and PBS images are from a representative day 3 sample. Arrows mark focal necrosis.



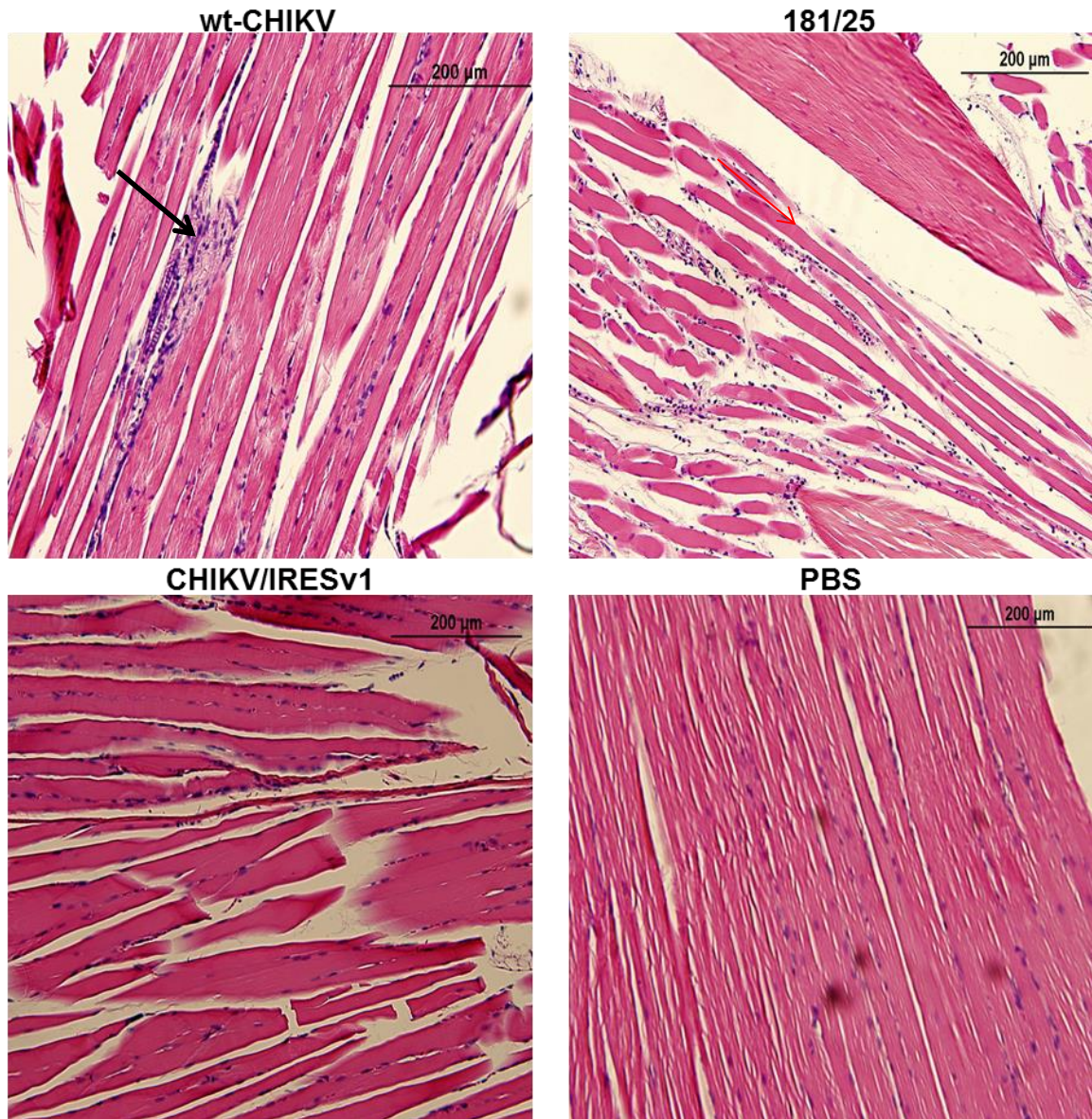


Figure 35: Histopathology of the leg in A129 mice

Histopathology of leg from A129 mice infected with either wt-CHIKV, CHIKV/IRESv1, 181/25, or PBS. Images are from representative day 3 and 4 samples. Arrow indicates focal myositis.



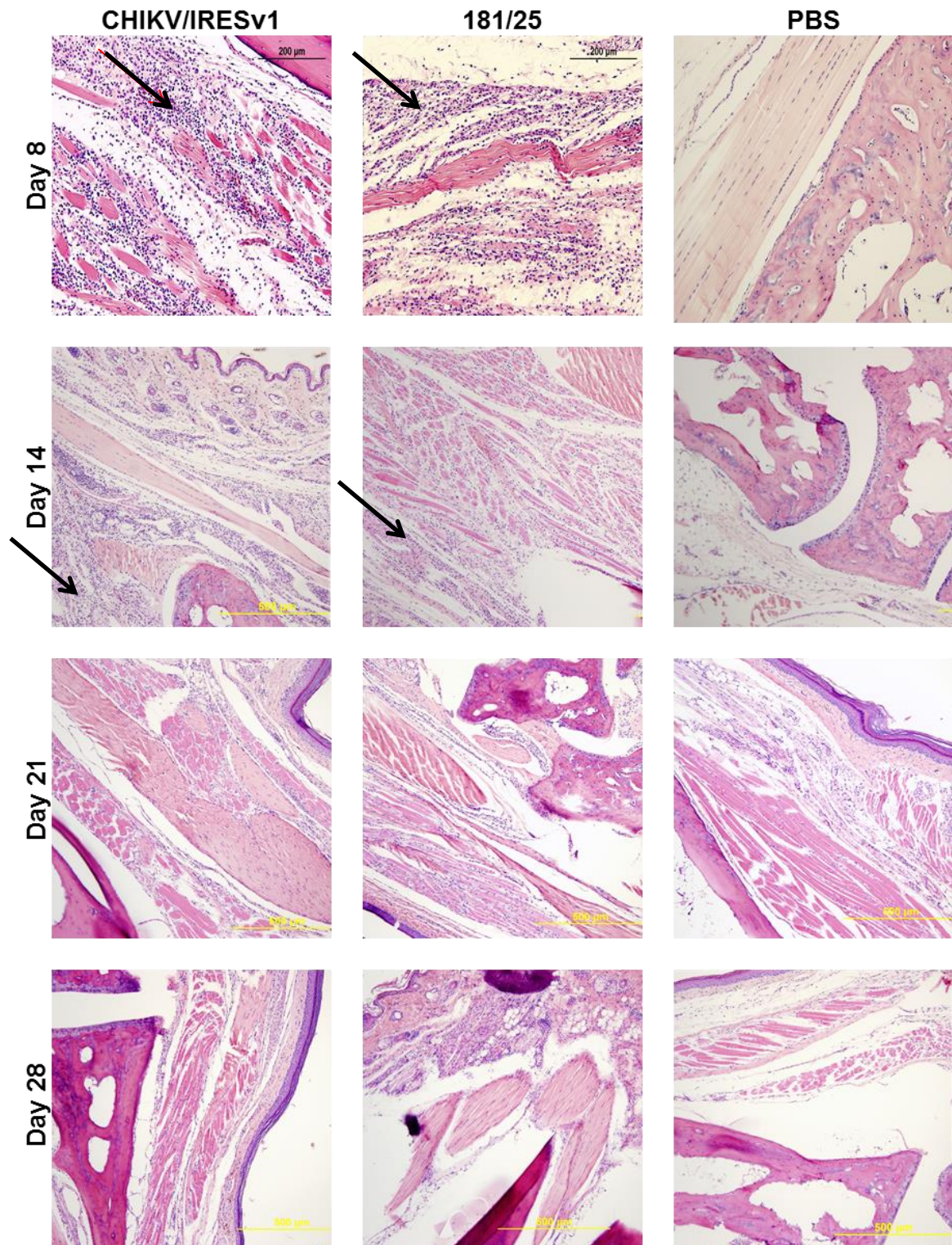


Figure 36: Histopathology of the footpad in A129 mice

Histopathology of footpad from A129 mice infected with either CHIKV/IRESv1, 181/25, or PBS. Arrows indicate sites of cellular infiltrate with myositis.



spread of the w-CHIKV FfLuc following a challenge 28 days post-vaccination. To this end, we inoculated 4 cohorts of animals with either  $10^4$  pfu of CHIKV/IRESv1 (1 cohort) or PBS (3 cohorts). Animals were challenged 1 month later. The cohort vaccinated with the CHIKV/IRESv1 was challenged with the wt-CHIKV FfLuc. One cohort each of the PBS inoculated was challenged with either wt-CHIKV, wt-CHIKV FfLuc, or PBS.

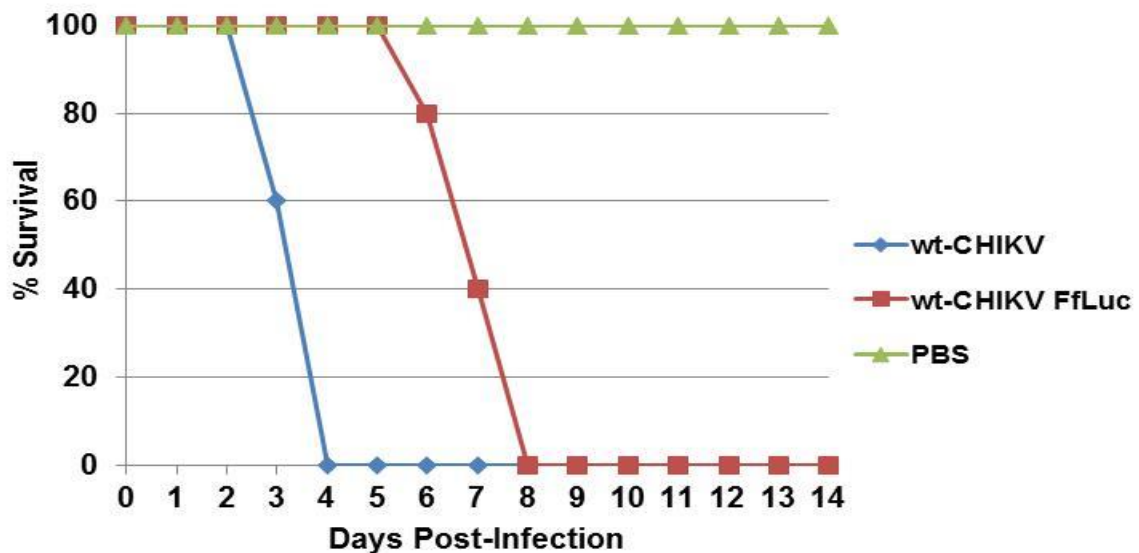


Figure 37: Impact of FfLuc on Lethality of wt-CHIKV in A129 mice

Survival of A129 mice infected with wt-CHIKV either with or without a FfLuc gene. P-value for Kaplan Meier log rank test of all three cohorts was 0.000. wt-CHIKV and wt-CHIKV FfLuc also differed significantly from each other ( $p=0.003$ ) and from PBS ( $p=0.003$  and  $0.003$ , respectively).

The animals were imaged via IVIS. An overview is found in figure 38, where the animals that were vaccinated with CHIKV/IRESv1 did not generate detectable luminescence after being challenged with the FfLuc-containing wt-CHIKV. Animals that received the standard wt-CHIKV or PBS, following PBS vaccination, also showed no luminescence, as expected. However, the animals that were PBS-vaccinated and challenged with FfLuc-containing wt-CHIKV did have strong luminescence seen in the inoculated fp. One limitation of the IVIS in this animal/viral model is the fact that the IVIS system has a limited dynamic range of signal acquisition. We looked closer at animals that were luminescent by blocking the strongest signals by covering the animals with black plastic. This allowed us to see that the animals vaccinated with PBS and

challenged with wt-CHIKV FfLuc were systemically infected, with the strongest image coming from the animals' musculature and spleen (refer to figure 39). At day 3, 2-3 animals were harvested from each cohort for tissue titers and histopathology. This part of the study was to help us define the differences of wt-CHIKV and wt-CHIKV FfLuc containing virus challenge following a PBS vaccination. On the whole, the tissue titers were lower in the wt-CHIKV FfLuc-infected animals compared to the wt-CHIKV-infected animals (refer to figure 40). The tissue lesions was also found to be different between the two challenge viruses in the spleen. Animals that received the wt-CHIKV challenge had moderate to severe splenic lesions, with the animals given wt-CHIKV FfLuc had a relatively normal spleen seen at day 3 (refer to figure 41).

The next series of experiments focused on the stability of the vaccine candidates after brain passaging. The brain was chosen due to its immune privileged nature possibly allowing for higher replication. Originally, an experiment focusing on passing the CHIKV/IRESv1 and 181/25 vaccines through neonatal CD-1 mice brains was attempted. An inoculation of  $10^4$  pfu was injected IC into 6-7-day-old CD-1 mice. The subjects' brains were harvested 48 hours post-infection and titrated as described previously. Only  $\frac{1}{3}$  of mice receiving CHIKV/IRESv1 developed a measurable viral load, and the process was repeated. By the second passage, CHIKV/IRESv1 could not be detected and 181/25 was detected at  $10^7$ - $10^9$  pfu/g, and the experiment was abandoned.

Knowing the inability of CHIKV/IRESv1 to replicate to measurable titers in immunocompetent mice, it was decided to modify this experiment by using the immunocompromised A129 model. To this end, our breeding colony was set up to produce pregnant mothers in a staggered fashion to allow for 5 serial brain passages in neonatal A129 mice. The A129 mice generally have litters of 2-4 surviving pups by day 6. The A129 mice litters have high attrition due to cannibalism. The experiment focused on the serially passing the CHIKV/IRESv1 and 181/25 vaccines in 2 separate parallel experiments. So for each passage 4 litters were required, 2 for each vaccine. These mice

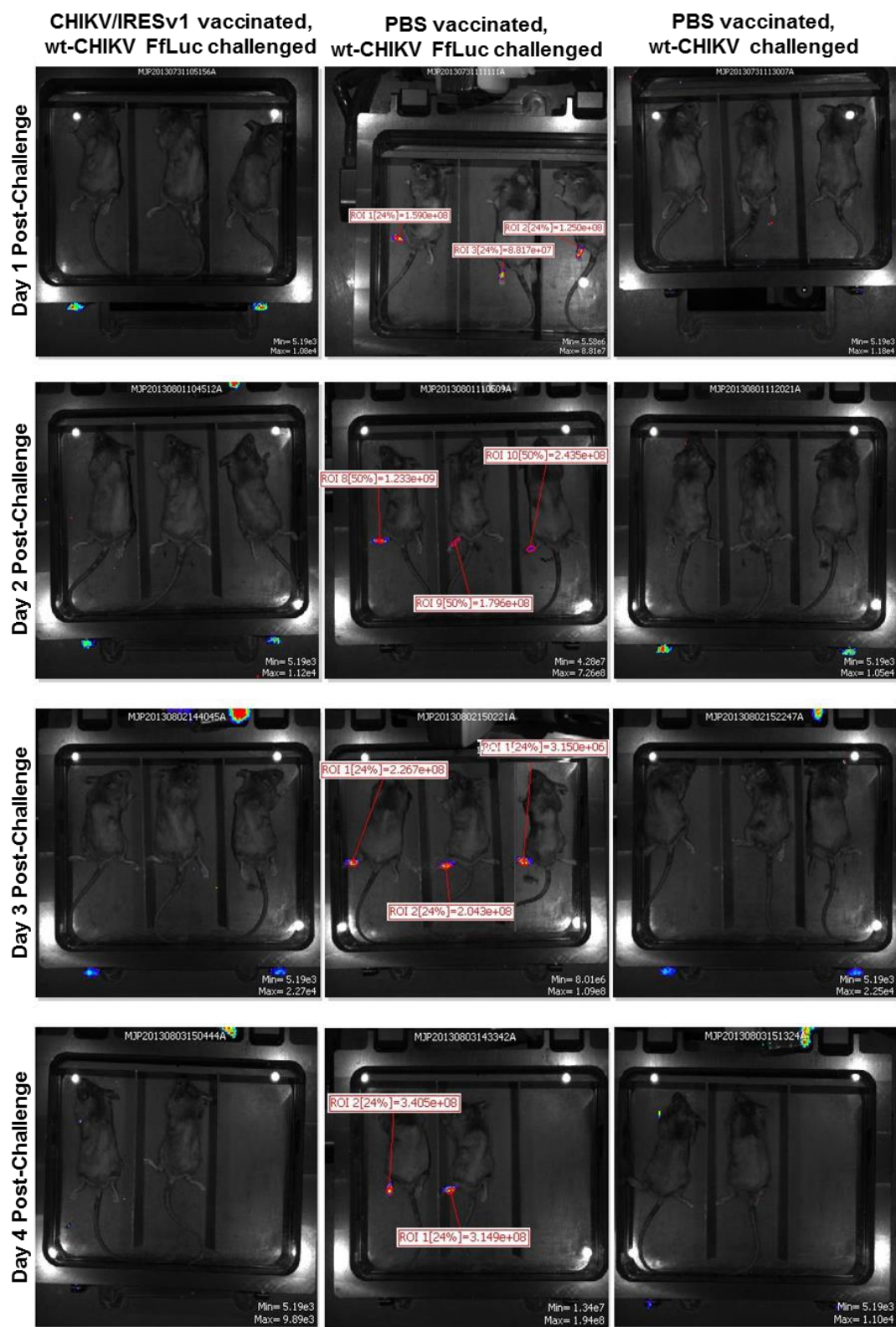


Figure 38: Overview of IVIS results

Image from viewing whole animals, highlighting the areas of strongest fluorescence.

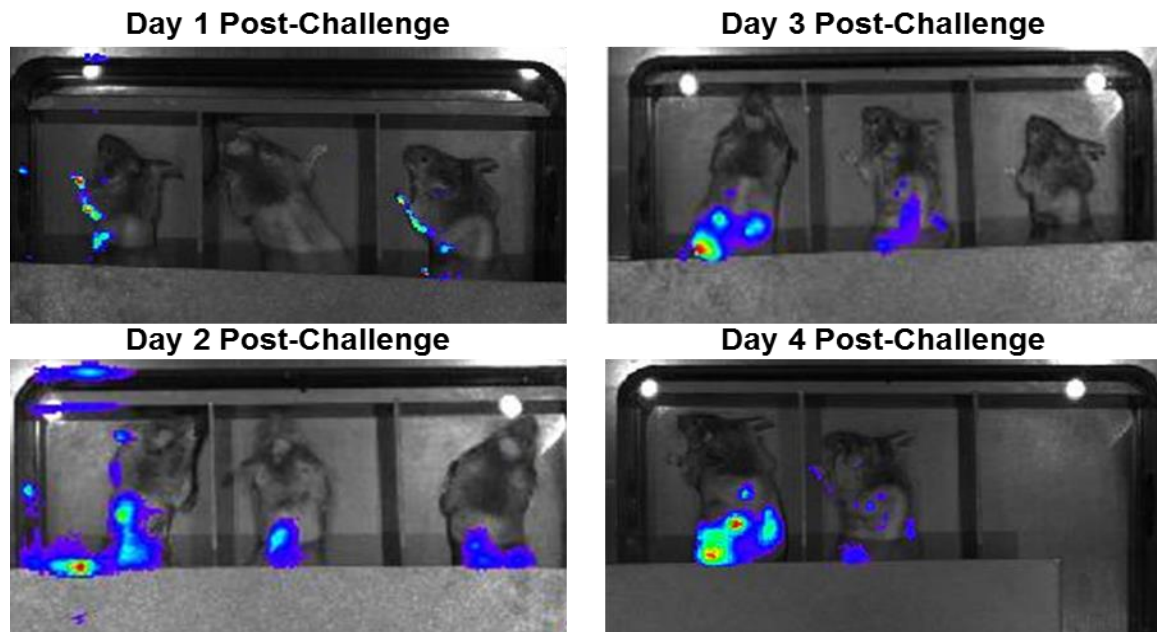


Figure 39: Foot-blocked IVIS images

Fluorescence in PBS-vaccinated, wt-CHIKV FfLuc-challenged A129 mice with the foot fluorescence physically blocked.

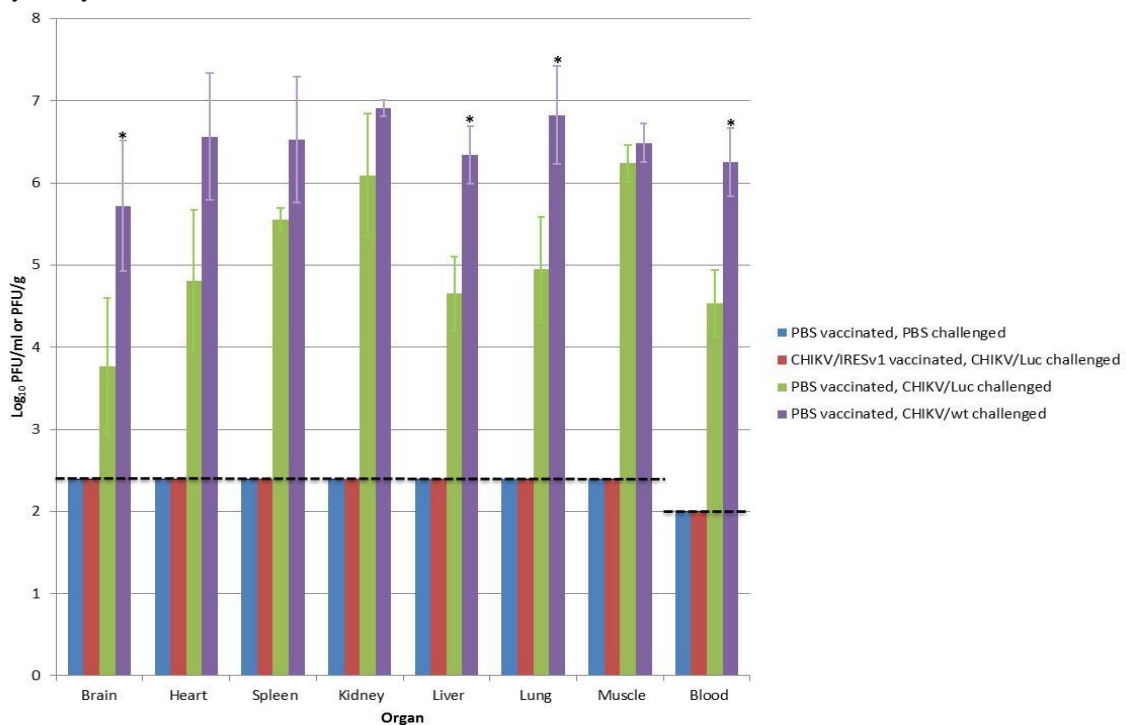


Figure 40: Tissue titers for wt-CHIKV- and wt-CHIKV FfLuc-challenged A129 mice

Tissue titers at day 3 post-challenge.  $\text{Log}_{10}$  PFU/ml and PFU/g values for PBS vaccinated, CHIKV/Luc challenged and PBS vaccinated, CHIKV/wt challenged cohorts were compared by unpaired, two-tailed Student's T-test. \* =  $p > 0.05$ . \*\* =  $p > 0.001$ . Dashed line represents limit of detection.



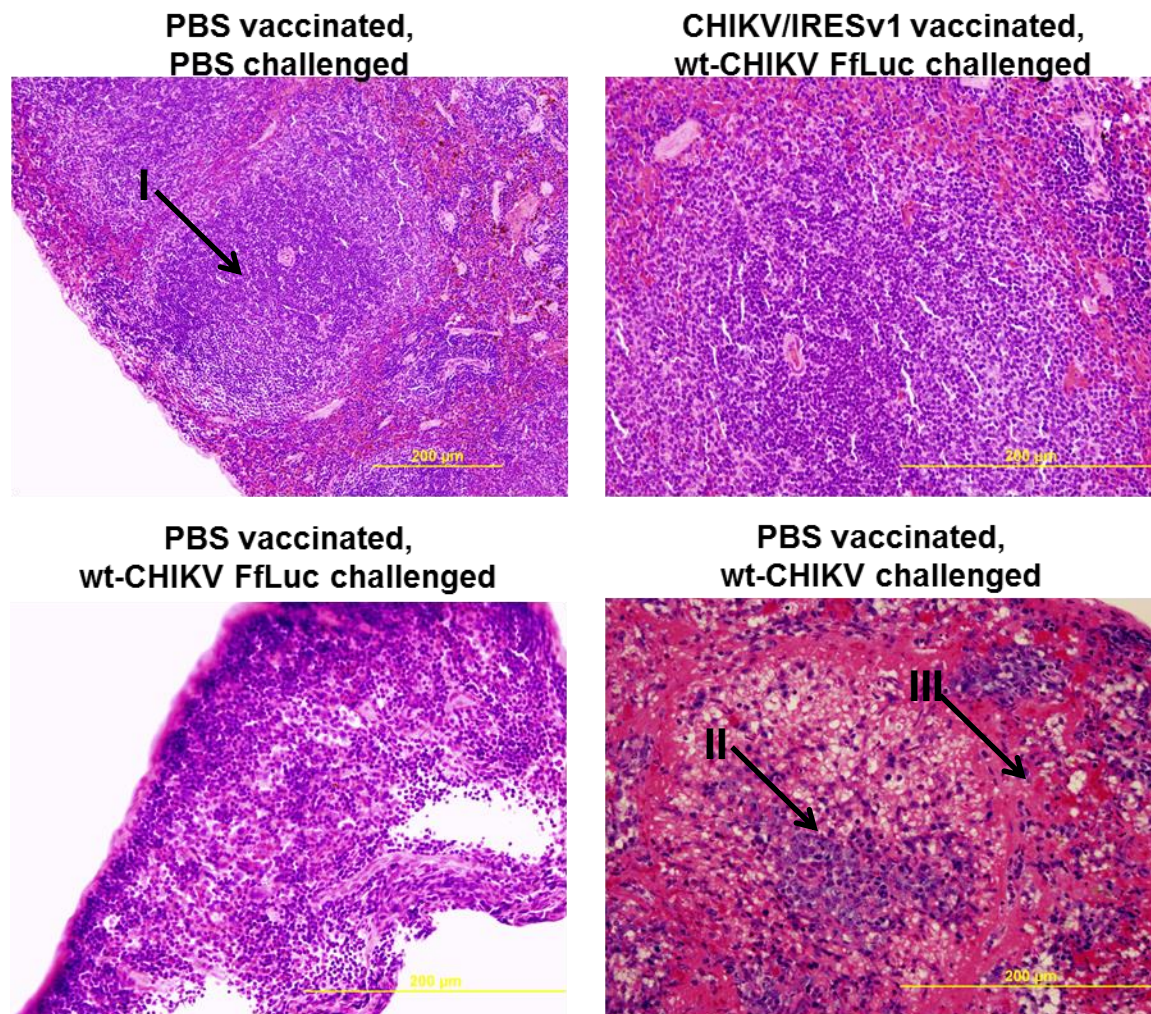


Figure 41: Histopathology of spleen in wt-CHIKV- and wt-CHIKV FfLuc-challenged A129 mice

Splenic architecture in A129 mice following challenge. I = intact follicle. II = Follicle with lymphocyte depletion. III = deposition of proteinaceous debris.

were injected IC with  $10^4$  pfu in a  $10\mu\text{l}$  volume and observed for 30-36 hours. This timing was due to morbidity seen in the animals inoculated with the 181/25 vaccine. The brain tissue was then homogenized and titrated. One of the brain homogenates, chosen by having the highest viral load was then used for the next passage. This was repeated for 5 serial passages and the samples were stored at  $-80^{\circ}\text{C}$ . The titers in between these passages can be found in figure 42. There was no significant change from the beginning through the end of the passages for either vaccine or between the parallel passages. There was a difference in titers in between the 181/25 and CHIKV/IRESv1 vaccine of

approximately 1.5 log<sub>10</sub>. However, there was a difference in plaque morphology of the 181/25 vaccine over the course of the experiments. Large plaques did appear and signified some change in the viruses. These changed plaques were found in both lines, defined as line 1 and line 2, of the passaged 181/25 vaccine and is represented in figure 42. The CHIKV/IRESv1 passaged vaccine plaques ranged from 0.5-1 mm at 2.5 days post-infection with the 181/25 passaged virus ranging from 0.5-2.5.

The next part of the experiment was designed to test any change of virulence in these passaged vaccine strains. It was decided that a 6-7-week-old A129 mouse model would be used to determine any change of virulence. The experiment used 8 cohorts of 4-5 mice to determine the difference between 181/25 passage 5 lines 1 and 2, CHIKV/IRESv1 passage 5 lines 1 and 2, the original parent vaccines, wt-CHIKV, and PBS. The mice were observed for changes in weight, fp swelling, and mortality for a period of 14 days.

The animals that received the CHIKV/IRESv1 vaccine parent or passages experienced no reduction in weight. These animals did experience moderate levels of fp swelling. The passaged viruses produced significantly more fp swelling than the parent strain on day 6, determined by a 1-way ANOVA  $p < 0.05$  (figure 43). During the duration of the experiment the animals did not develop other signs of illness such as ruffled fur or hunched posture. The animals survived the duration of the study, refer to figure 44.

Animals receiving the 181/25 parent or passages strains, however, showed some interesting data. The passage-infected animals experienced a large weight decline at day 6. The parent strain produced a similar trend of starting to lose weight by day 6, as seen previously in our original experiments (figure 17). However, instead of their weights plateauing and recovering, the animals that received either passage virus experienced a more severe weight loss (refer to figure 45). The passage-infected animals also experienced a similar level of fp swelling compared to wt-CHIKV. All animals that received the passaged 181/25 viruses succumbed to illness (refer to figure 42). The

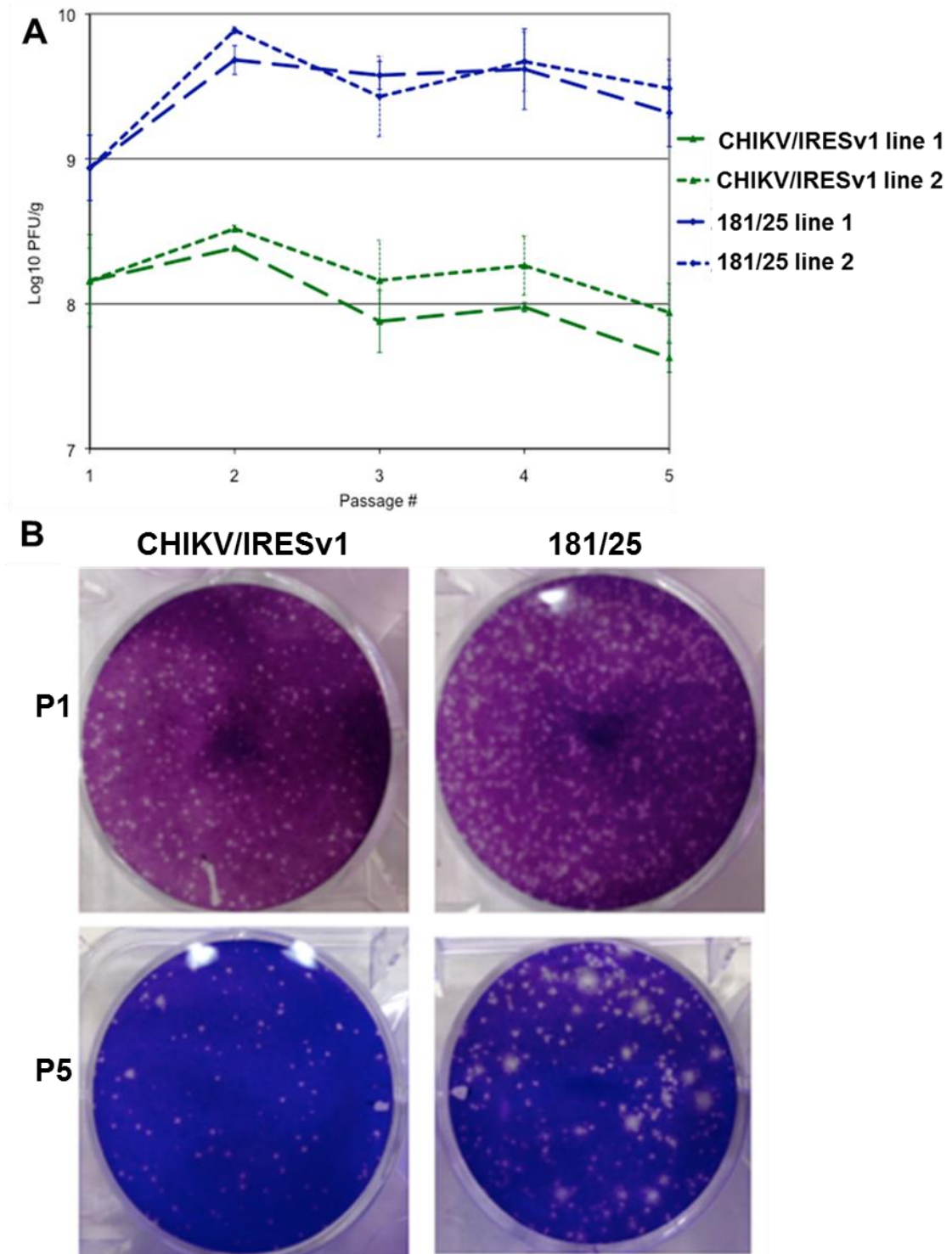


Figure 42: Titers and plaque morphologies during brain passaging

(A) Titers of brains collected 36 hours post-IC inoculation. (B) Representative plaque morphologies of the passages. P1 plaques range from pinpoint to 1mm for both CHIKV/IRESv1 and 181/25. P5 CHIKV/IRESv1 plaques were unchanged from P1. P5 181/25 plaques ranged from pinpoint to 2.5mm. Plates were fixed 2.5 days post-infection.

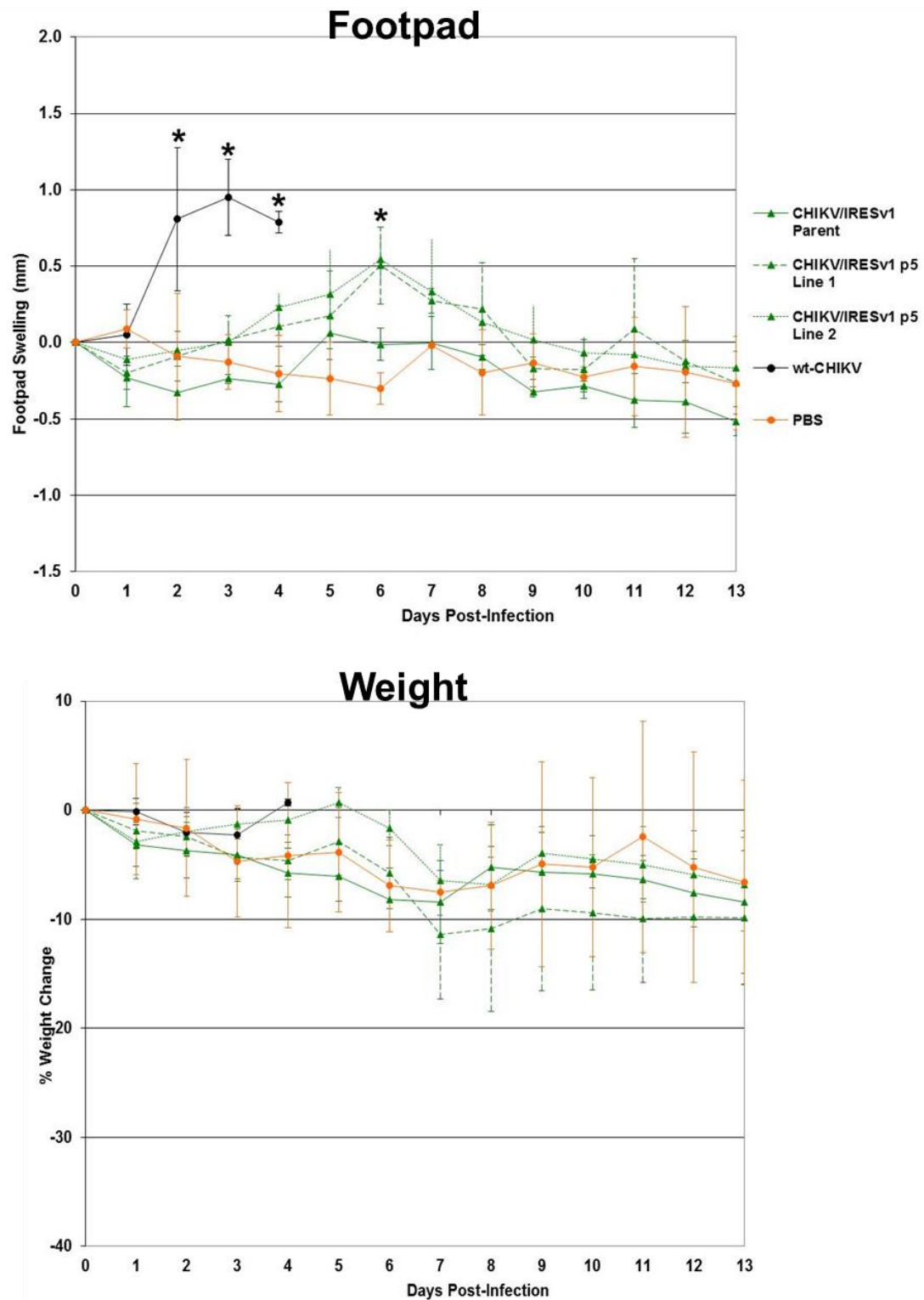


Figure 43: Weight change and footpad swelling induced by passaged CHIKV/IRESv1

Observations following infection with either parent, passage 5 line 1, or passage 5 line 2 CHIKV/IRESv1, or wt-CHIKV or PBS. \* =  $p < 0.05$ . \*\* =  $p < 0.001$ . Statistical Analysis conducted by one-way ANOVA.



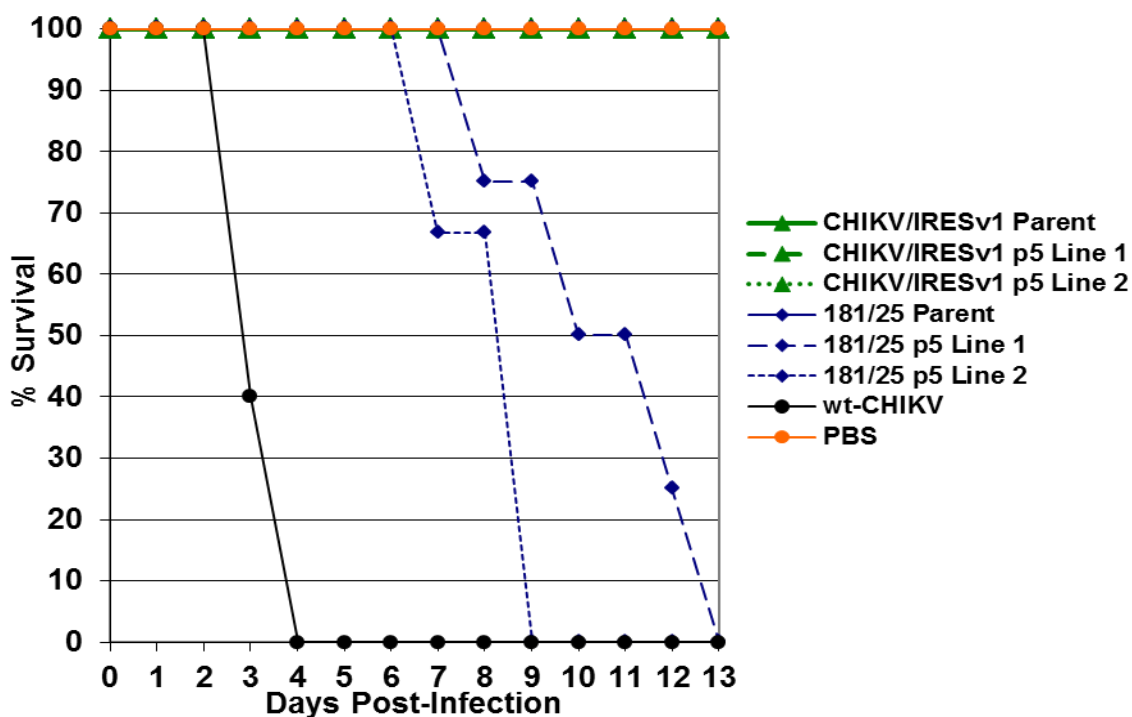


Figure 44: Survival of A129 mice challenged with CHIKV/IRESv1 and 181/25 parent and passage viruses

Survival of A129 mice following challenge with parent and passage strains of CHIKV/IRESv1 and 181/25. Statistical analysis of all 8 cohorts via Kaplan Meier log-rank test  $p=0.000$ .

animals infected with 181/25 line 1 succumbed to illness by day 13 whereas the animals that were infected with the line 2 passage were euthanized or found dead by day 9, and the Kaplan Meier log-rank analysis yielded a significance of  $p=0.11$  for these two groups. Although this is not significant, an experiment with larger cohorts would likely yield statistically significant results.

A second study was designed using the day 3 timepoint for tissue collection following infections as described above. The tissues were assessed for histopathological lesions and viral titrations to increase our knowledge of virulence. The 8 cohorts were limited to 3 mice each since we only measured a single timepoint. The tissue titrations of the CHIKV/IRESv1 passage viruses generally followed the same trend of the parent vaccine with animals being positive for virus in the spleen, muscle and serum. The passaged virus generally had higher titers in the spleen and the muscle tissue (refer to figure 46).

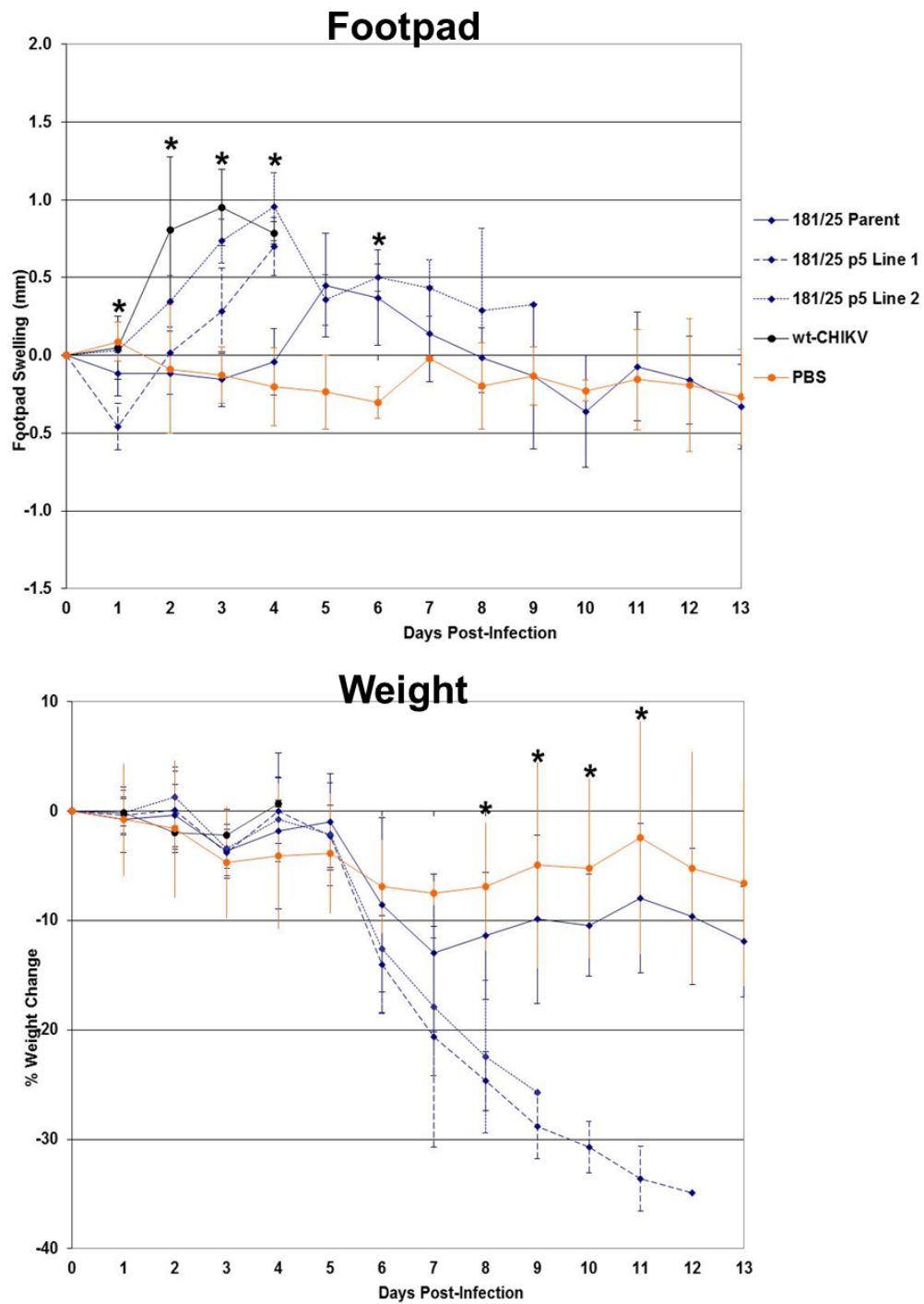


Figure 45: Weight change and footpad swelling induced by passaged 181/25

Observations following infection with either parent, passage 5 line 1, or passage 5 line 2 181/25, or wt-CHIKV or PBS. \* =  $p < 0.05$ . \*\* =  $p < 0.001$ . Statistical Analysis conducted by one-way ANOVA.

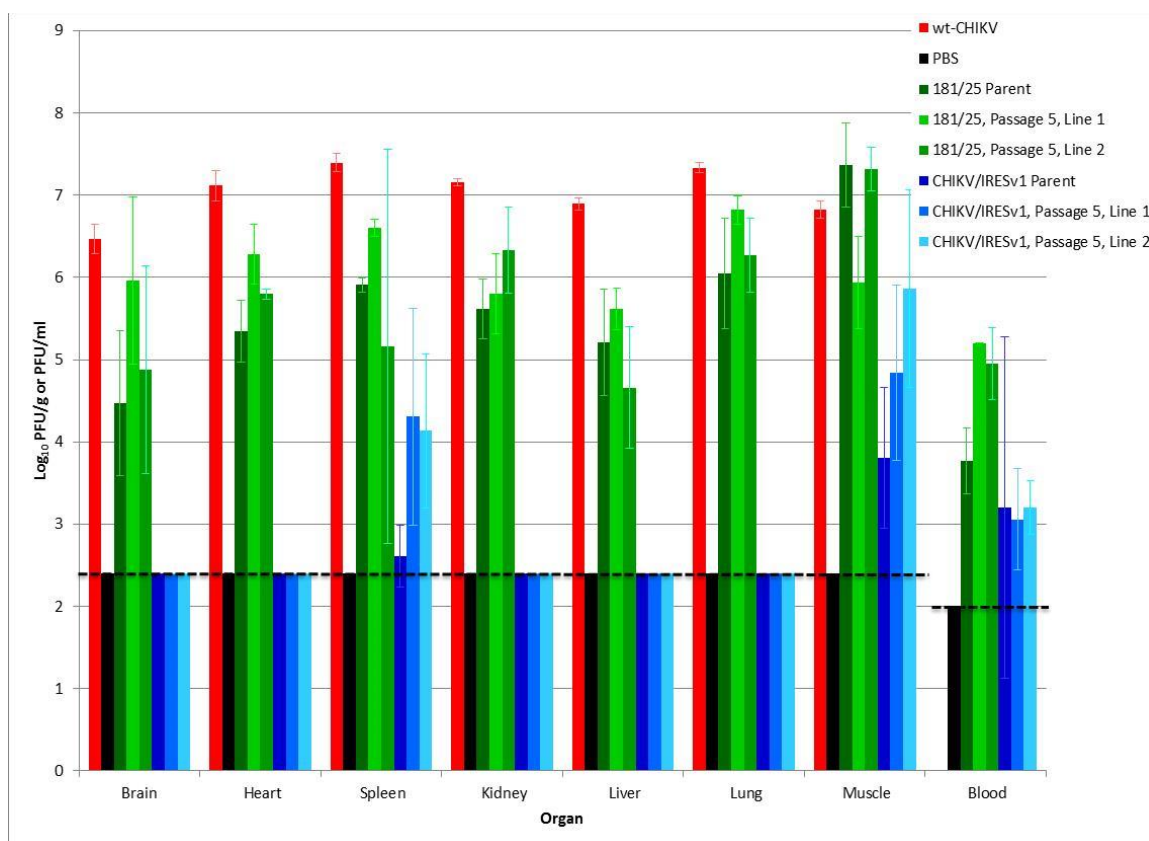


Figure 46: Tissue titers of passaged CHIKV/IRESv1 and 181/25

Tissue titers of 6-7-week-old A129 mice infected with either parent or passaged CHIKV/IRESv1 or 181/25.

Statistical analysis of the tissue titers for the passaged virus resulted in significant variation between the titers of all virus-infected cohorts for all tested organs, although the blood titer values were at the border of significance ( $p=0.048$ ) (table 7). When Bonferroni post-hoc analysis was performed to compare individual cohorts for each organ, it was noticed that all three CHIKV/IRESv1 strains differed significantly from both wt-CHIKV and all three 181/25 strains in the heart, kidney, liver, and lung, but differed only from wt-CHIKV and 181/25 p5 Line 2 in the brain and had less prevalent significant differences in the muscle. The 181/25 strains, on the other hand, only rarely differed significantly from wt-CHIKV. There were no widespread significant differences in the blood or spleen.

Organ	ANOVA p-Value	Bonferroni p<0.05	Bonferroni p<0.001
Brain	0.000	181/25 p5 Line 2 vs. CHIKV/IRESv1 Parent 181/25 p5 Line 2 vs. CHIKV/IRESv1 p5 Line 1 181/25 p5 Line 2 vs. CHIKV/IRESv1 p5 Line 2	wt-CHIKV vs. CHIKV/IRESv1 Parent wt-CHIKV vs. CHIKV/IRESv1 p5 Line 1 wt-CHIKV vs. CHIKV/IRESv1 p5 Line 2
Heart	0.000	181/25 Parent vs. 181/25 p5 Line 1	wt-CHIKV vs. 181/25 Parent wt-CHIKV vs. 181/25 p5 Line 1 wt-CHIKV vs. 181/25 p5 Line 2 wt-CHIKV vs. CHIKV/IRESv1 Parent wt-CHIKV vs. CHIKV/IRESv1 p5 Line 1 wt-CHIKV vs. CHIKV/IRESv1 p5 Line 2 181/25 Parent vs. CHIKV/IRESv1 Parent 181/25 Parent vs. CHIKV/IRESv1 p5 Line 1 181/25 Parent vs. CHIKV/IRESv1 p5 Line 2 181/25 p5 Line 1 vs. CHIKV/IRESv1 Parent 181/25 p5 Line 1 vs. CHIKV/IRESv1 p5 Line 1 181/25 p5 Line 1 vs. CHIKV/IRESv1 p5 Line 2 181/25 p5 Line 2 vs. CHIKV/IRESv1 Parent 181/25 p5 Line 2 vs. CHIKV/IRESv1 p5 Line 1 181/25 p5 Line 2 vs. CHIKV/IRESv1 p5 Line 2
Spleen	0.002	wt-CHIKV vs. CHIKV/IRESv1 Parent 181/25 p5 Line 1 vs. CHIKV/IRESv1 Parent	
Kidney	0.000		wt-CHIKV vs. 181/25 Parent wt-CHIKV vs. CHIKV/IRESv1 Parent wt-CHIKV vs. CHIKV/IRESv1 p5 Line 1 wt-CHIKV vs. CHIKV/IRESv1 p5 Line 2 181/25 Parent vs. CHIKV/IRESv1 Parent 181/25 Parent vs. CHIKV/IRESv1 p5 Line 1 181/25 Parent vs. CHIKV/IRESv1 p5 Line 2 181/25 p5 Line 1 vs. CHIKV/IRESv1 Parent 181/25 p5 Line 1 vs. CHIKV/IRESv1 p5 Line 1 181/25 p5 Line 1 vs. CHIKV/IRESv1 p5 Line 2 181/25 p5 Line 2 vs. CHIKV/IRESv1 Parent 181/25 p5 Line 2 vs. CHIKV/IRESv1 p5 Line 1 181/25 p5 Line 2 vs. CHIKV/IRESv1 p5 Line 2
Liver	0.000	wt-CHIKV vs. 181/25 Parent wt-CHIKV vs. 181/25 p5 Line 1	wt-CHIKV vs. 181/25 p5 Line 2 wt-CHIKV vs. CHIKV/IRESv1 Parent wt-CHIKV vs. CHIKV/IRESv1 p5 Line 1 wt-CHIKV vs. CHIKV/IRESv1 p5 Line 2 181/25 Parent vs. CHIKV/IRESv1 Parent 181/25 Parent vs. CHIKV/IRESv1 p5 Line 1 181/25 Parent vs. CHIKV/IRESv1 p5 Line 2 181/25 p5 Line 1 vs. CHIKV/IRESv1 Parent 181/25 p5 Line 1 vs. CHIKV/IRESv1 p5 Line 1 181/25 p5 Line 1 vs. CHIKV/IRESv1 p5 Line 2 181/25 p5 Line 2 vs. CHIKV/IRESv1 Parent 181/25 p5 Line 2 vs. CHIKV/IRESv1 p5 Line 1 181/25 p5 Line 2 vs. CHIKV/IRESv1 p5 Line 2
Lung	0.000	wt-CHIKV vs. 181/25 Parent wt-CHIKV vs. 181/25 p5 Line 1 wt-CHIKV vs. 181/25 p5 Line 2	wt-CHIKV vs. CHIKV/IRESv1 Parent wt-CHIKV vs. CHIKV/IRESv1 p5 Line 1 wt-CHIKV vs. CHIKV/IRESv1 p5 Line 2 181/25 Parent vs. CHIKV/IRESv1 Parent 181/25 Parent vs. CHIKV/IRESv1 p5 Line 1 181/25 Parent vs. CHIKV/IRESv1 p5 Line 2 181/25 p5 Line 1 vs. CHIKV/IRESv1 Parent 181/25 p5 Line 1 vs. CHIKV/IRESv1 p5 Line 1 181/25 p5 Line 1 vs. CHIKV/IRESv1 p5 Line 2 181/25 p5 Line 2 vs. CHIKV/IRESv1 Parent 181/25 p5 Line 2 vs. CHIKV/IRESv1 p5 Line 1 181/25 p5 Line 2 vs. CHIKV/IRESv1 p5 Line 2

			181/25 p5 Line 2 vs. CHIKV/IRESv1 p5 Line 2
Muscle	0.000	wt-CHIKV vs. CHIKV/IRESv1 Parent 181/25 Parent vs. CHIKV/IRESv1 Parent 181/25 Parent vs. CHIKV/IRESv1 p5 Line 1 181/25 p5 Line 1 vs. CHIKV/IRESv1 Parent 181/25 p5 Line 1 vs. CHIKV/IRESv1 p5 Line 1 181/25 p5 Line 2 vs. CHIKV/IRESv1 Parent 181/25 p5 Line 2 vs. CHIKV/IRESv1 p5 Line 1	
Blood	0.048		

**Table 7: Statistical Analysis of Tissue Titers in A129 Mice Infected with Parent and Passaged CHIKV**

Results of one-way ANOVA analysis of log<sub>10</sub> PFU/ml and PFU/g titers from mice infected with parent or passaged CHIKV strains. Individual strain combinations with significant differences for each organ are noted. Strain combinations not specified had  $p \geq 0.05$  in Bonferroni post-hoc analysis. Crossed-out cells indicate that no strain combinations reached the specified level of significance.

The animals that received the 181/25 passages or parent virus showed systemic infection of all tissues measured, with relatively similar viral loads in comparison to the original parent vaccine strain. The animals that received the passaged virus did have a significant difference in viremia titers. These tissue viral loads were, on the whole, lower than those following wt-CHIKV infection.

The histopathologic findings produced from this study were relatively unremarkable. The CHIKV/IRESv1 passaged viruses had only a small differences in the level of edema seen in the fp (figure 47). The rest of the tissues were similar to those of the PBS-infected mice. Animals that received the 181/25 passages also had an increase of edema in the fp compared to its parent virus. The spleen did show mild disruption as well, as can be seen in figure 48.

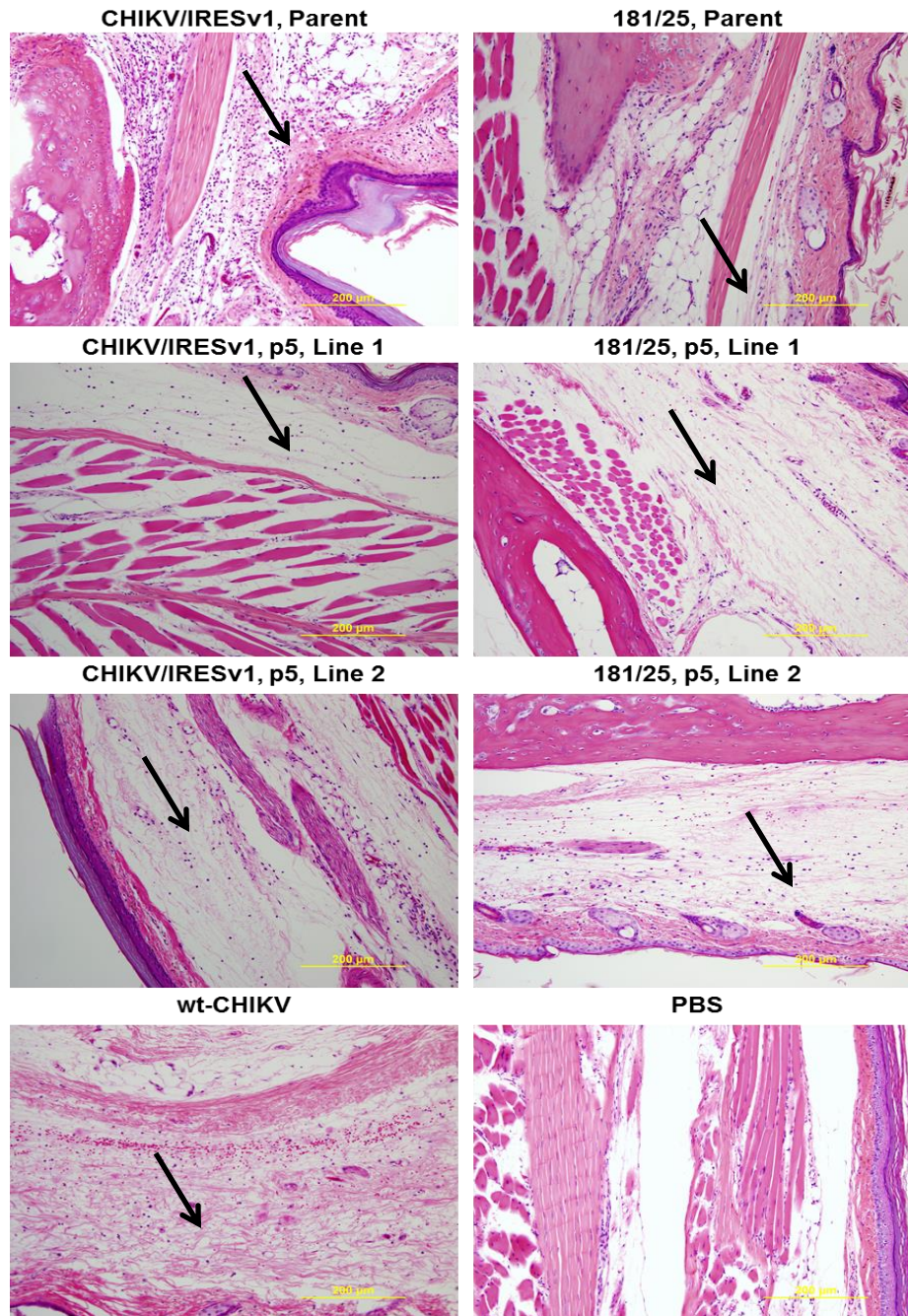


Figure 47: Footpad histopathology of A129 mice infected with parent or passaged CHIKV/IRESv1 or 181/25

Day 3 footpad observations for A129 infected with parent or passaged CHIKV. Arrows indicate areas with slight to moderate edema.



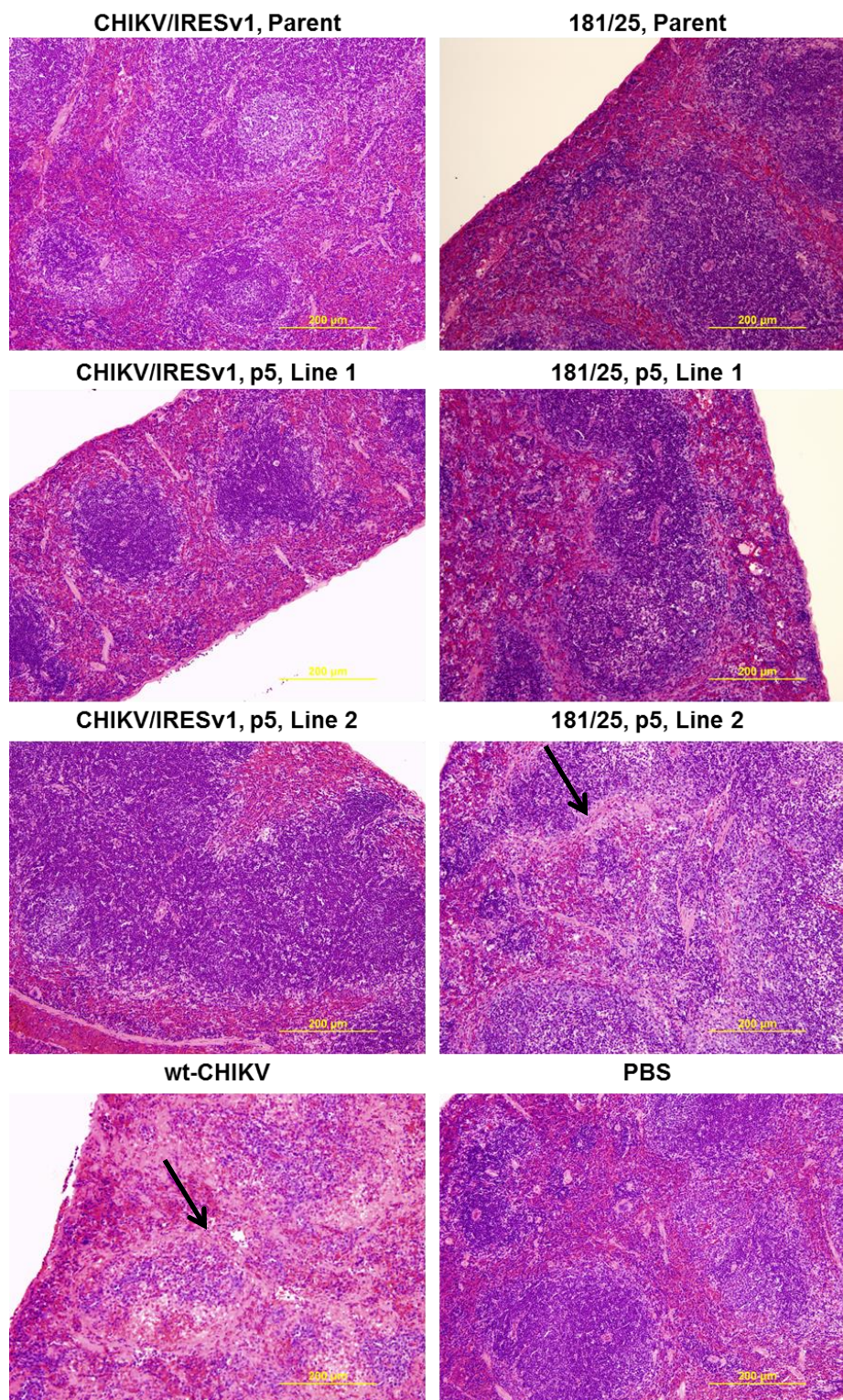


Figure 48: Spleen histopathology of A129 mice infected with parent or passaged CHIKV/IRESv1 or 181/25

Day 3 spleen observations for A129 infected with parent or passaged CHIKV. Arrows indicate deposition of proteinaceous debris and slight disruption of splenic architecture.

The passaged viruses were then consensus sequenced for the ORFs, primers can be found in table 1. Briefly, the harvested RNA was then put into several PCR reactions and produced 6 overlapping fragments that covered the genome. These fragments were then sequenced. The CHIKV/IRESv1 passaged viruses had no consensus sequence changes. The 181/25 passaged viruses, on the other hand, did have some consensus mutations as listed in table 8. We were interested in the E2 mutations of these viruses in particular due to the previous studies on 181/25 attenuated mutations done by Gorchakov *et al.* [86]. This study showed that 2 of the mutations found in the E2 protein were responsible for the attenuating phenotype. To this end, we harvested large and small plaques for the 181/25 passaged viruses, and multiple plaques of the CHIKV/IRESv1 passaged viruses. As with the consensus sequencing results, the plaque-purified CHIKV/IRESv1 passages did not have any consensus sequence changes. The plaque-purified 181/25 passaged viruses did have mutations. The line 1 passage large plaque harvest had a (+) charge loss substitution at aa 80 of the E2 protein. Line 2 had two substitutions in E2 at aa 57 and 82. Both of these mutations resulted in loss of (+) charge and can be seen in table 9.

NT Position	NT Substitution	Mixed Population?	AA Position	AA Substitution
978	T→C	Yes	nsP1 301	Ile→Thr
1016	A→T	Yes	nsP1 314	Met→Leu
3706	G→A	No	nsP2 675	Non-coding
6043	T→C	Yes	nsP4 126	Non-coding

Table 8: Consensus substitutions acquired by 181/25 subsequent to passage in mouse brains

Consensus amino acid mutations acquired by 181/25 during passage in mouse brains. Mutations were found in both line 1 and line 2.



<b>Virus</b>	<b>Plaque Size</b>	<b>NT Position</b>	<b>NT Substitution</b>	<b>AA Position</b>	<b>AA Substitution</b>	<b>Charge Change?</b>
181/25 p5 line 1	Big	8780	G→C	E2 80	Arg→Thr	Yes (+→Polar)
	Small	8280	A→G	C 238	Non-coding	N/A
181/25 p5 line 2	Big	8712	G→T	E2 57	Lys→Asn	Yes (+→Polar)
		8785	A→G	E2 82	Arg→Gly	Yes (+→0)
	Small	8564	T→C	E2 8	Val→Ala	No

Table 9: Substitutions acquired by plaque purified 181/25 subsequent to passage in mouse brains

Amino acid substitutions acquired by plaque purified 181/25 brain-passaged virus.

## Summary/Conclusions

In this chapter I wanted to expand knowledge of CHIKV/IRESv1 vaccine candidate as well as a wt-CHIKV infection in the now common CHIKV small animal model, A129 mice. These studies were generally more in-depth due to our expanded knowledge of the capabilities and limitations of the models used. Going into these experiments I knew that CHIKV/IRESv1 can provide protection against a lethal challenge and against multiple measures of virulence such as fp swelling and splenic pathology.

Another aspect of these studies was to examine the difference between the 181/25 vaccine and CHIKV/IRESv1. Though I believed I had shown a strong difference between these viruses virulence, I wanted to expand those data. In the tropism study shown in figures 30-32, we saw that the spread of infection for wt-CHIKV in these mice is rapid. A systemic infection seemed to appear 24-hours post infection, including the brain, with the highest viral loads being found in the spleen and the muscle. It is important to remember that the animals were perfused to eliminate viremic blood. Throughout the course of infection, leading to the animals' death by days 3 and 4, with increasing viral loads in the tissues measured.

The 181/25 vaccine followed a similar course of infection though with a slight time delay. By day one only the spleen and muscle tissue were positive for virus. At day 2, the virus was found in all other tissues in these infected animals except the brain. The systemic infection then appears by day 3, with increasing tissue titers through day 4. The virus was cleared at the later timepoints. CHIKV/IRESv1 was limited in its spread. The virus could not be detected until day 2, at which point it was detected at very low levels in the musculature. On day 3 the infection remained limited to the musculature in the 10-week-old animals, but the titers were increased. On day 4 these animals had virus in the spleen, and one animal was viremic. The virus was cleared from the animals by day 8 and remained undetectable at the later timepoints. These data also answered a previously posed question of persistence; at least to the sensitivity limits of viral titrations, neither our CHIKV/IRESv1 vaccine candidate nor the 181/25 vaccine persist in the A129 mouse model.

The IVIS experiment was originally designed to assess tropism and spread. However, as previously stated, my constructs ejected the FfLuc gene after electroporation. We then received a construct using the OPY-1 viral backbone with FfLuc as a capsid fusion; this was provided kindly by Dr. William Klimstra. In the initial pilot studies it became obvious that, due to the systemic nature of wt-CHIKV in the A129 model, we could not track the spread of virus in great detail. We did decide to attempt an experiment that uses the IVIS technology for another reason. wt-CHIKV FfLuc was used in conjunction with IVIS as a challenge virus to determine the efficacy of possible CHIKV vaccine candidates. This allowed us to use a small number of animals, not requiring large cohort sizes typically needed for standard serial sacrifice experiments. It also allowed us to get measurements on the same animals day after day. To this end the IVIS experiments proved successful. The animals that received the CHIKV/IRESv1 vaccine did not show the systemic spread of luminescence, which indicates the spread of virus that releases the enzyme that reacts with the substrate luciferin. The IVIS also has

the capability of generating a 3D image which could possibly help in tropism studies. An example can be seen in figure 49, where we highlight a strong signal coming from the spleen of a day 4 animal infected with wt-CHIKV containing FfLuc. Though this technology isn't the most accurate or useful using CHIKV in A129 mice due to the systemic nature of infection, it is my belief that this could be a powerful tool in other viral infections in an animal model which has a more limited tropism.

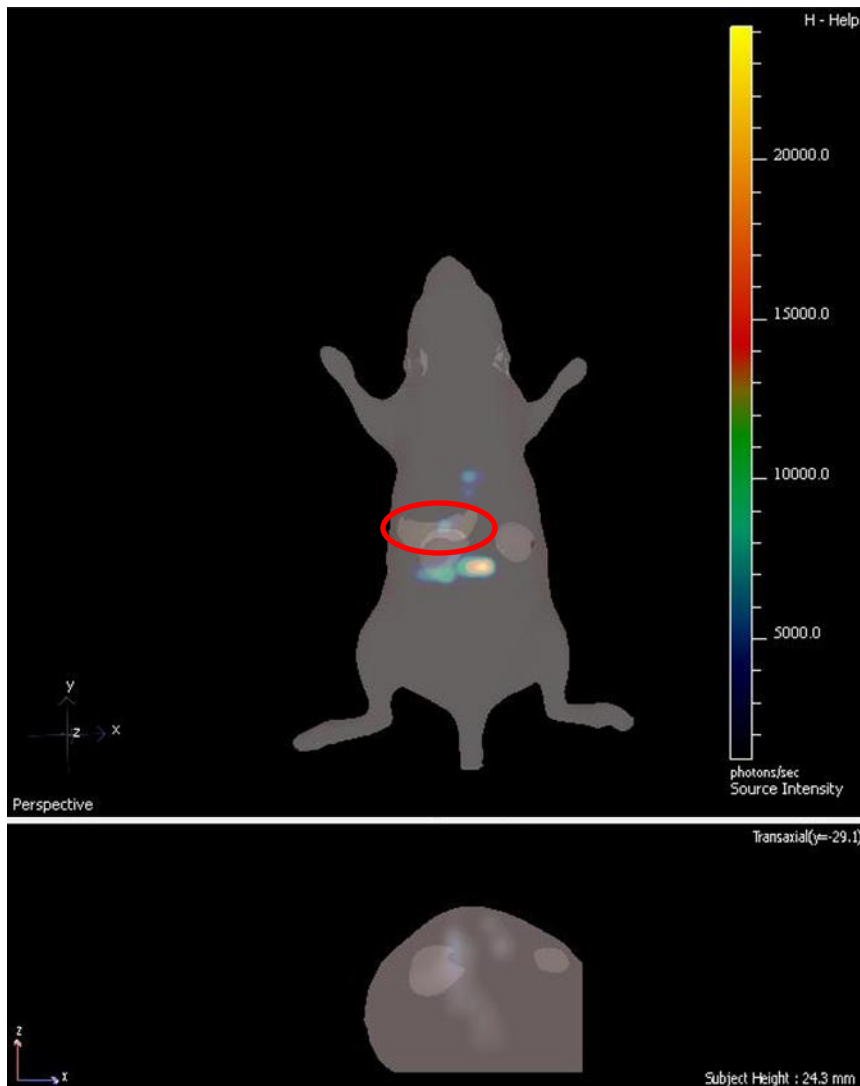


Figure 49: Three-dimensional IVIS image

Three-dimensional image of a PBS-vaccinated A129 mouse, 4 days post-wt-CHIKV FfLuc challenge. Red circle indicates suspected region of spleen.

I also wanted to test the stability of CHIKV/IRESv1 and 181/25 *in vivo* using what I believe is the most stringent test, a serial brain passage. CHIKV/IRESv1 was actually unable to maintain high enough titers in neonatal CD-1 mice to accommodate a serial passage experiment. This result by itself increased our confidence in the highly attenuated nature of our vaccine. We decided to increase the sensitivity by the use of neonatal type I IFN receptor KO mice. During the passages of these vaccine viruses there was no significant change in the titers from the first to last passage. However, the plaque morphologies did change for the 181/25 vaccine passages. This hinted that there were some changes to the 181/25 vaccine, but to be sure we ran multiple virulence studies. We decided to test virulence in the 6-7-week-old animal model. The rationale behind this was that we knew that the A129 model had increased sensitivity to CHIKV infection the younger the subject. We saw previously that a 3-week-old animal will succumb to infection with the parent 181/25 vaccine (figure 18). We wanted to make sure that the model we were using could differentiate between small changes in virulence, yet not be too sensitive. The model proved successful, with wt-CHIKV succumbing by day 3-4 and our parent vaccines not experiencing extensive morbidity.

The CHIKV/IRESv1 passages did have a few differences compared to the parent. The animals did suffer moderate fp swelling on day 6, which was significantly different from the parent. The tissue tropism by day 3 did remain similar to that of the parent, though the viral loads were generally higher. However, statistically there was no difference between the parent and the passage viruses regarding tissue titers. The histopathology also showed no remarkable change. When these viruses were sequenced there were no changes in the consensus sequence. Subsequent plaque purifications also revealed no substitutions. Obviously, there was at least a small difference in virulence between the passages and parent strains. Though we did not see any consensus mutations, it is possible that minority populations of virus do contain mutations that could slightly increase virulence.

The 181/25 passages did differ greatly from their parent strain. The A129 model universally experiences weight loss post-inoculation with 181/25 at day 6, but then recovers. The passaged 181/25 viruses, though, started to lose weight by day 6 and continued to do so until the animals succumbed to illness. The animals suffered a wt-CHIKV-like fp swelling phenotype early in the infection. The swelling then dissipated and the measurements actually fell below the day 0 measurement. We also saw this to a slight degree with the CHIKV/IRESv1 parent and passage viruses. We attribute this to muscle atrophy. The 181/25 passaged day 3 tissue viral loads were also similar to those of the parent virus. We did not see any extensive histopathological lesions. We did notice small changes in the spleen and fp. We believe that the reason why we didn't see the same splenic lesions that we saw in wt-CHIKV-infected animals is the delayed time to death being between 8-13 days.

We did see mutations in these 181/25 passaged viruses. In the initial testing it seemed that the passaged viruses were different in their virulence. Animals that received the line two passage of 181/25 died 4 days earlier than line 1. The sequence analysis possibly explains the difference. The work done by Gorchakov *et al.* showed that the predominant mutations that are responsible for the attenuated phenotype of vaccine strain 181/25 are at amino acid position 82 and 12 of the E2 protein [86]. The strongest attenuating mutation was at aa 82 in E2, which in the 181/25 is an arginine. The line 1 passage had a loss-of-charge mutation at aa position 80, adjacent to the critical aa 82. The line two substitutions were at aa 57 and 82. Both of these mutations involved losing large (+) charge amino acids. When these residues were visualized in PyMol on an E2 trimer representation (figure 50), we saw that these mutations are surface exposed, hinting that these mutations are probably loss of function for binding heparin sulfate. This would explain the increase in virulence. Note, this figure also highlighted the mutation responsible for the attenuation of CHIKV/IRESv2b. This mutation was actually introduced into the wt-CHIKV cDNA backbone. We designed a small experiment also

using the 6-7-week-old A129 mice alongside the previous experiments. We were interested in this mutation's ability to attenuate the wt-CHIKV virus on its own. We saw that the virus, 7139, did have a similar effect on the fp swelling in these animals compared to the wt-CHIKV. However the mutation was able to ablate the lethal phenotype (refer to figure 51). The mutation is located outside of the transmembrane domain, but as you can see in figure 50, it is not freely accessible on the surface of the protein.

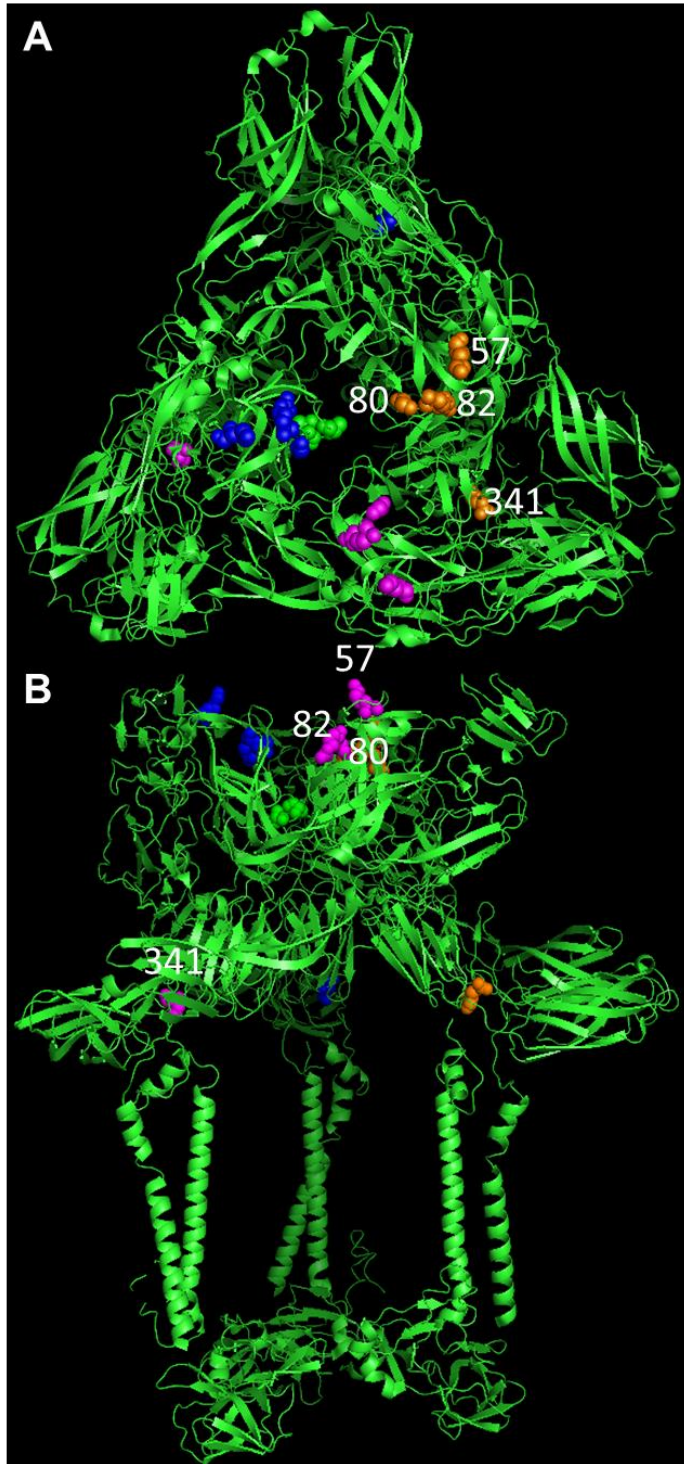


Figure 50: Location of important mutations in CHIKV E2

AA 80 is the residue suspected to confer reversion to virulence in 181/25 p5 line 1. AAs 82 and 57 are suspected to confer reversion to virulence in 181/25 p5 line 2. AA341 is the attenuating mutation of CHIKV/IRESv2 acquired during cell passage and incorporated into CHIKV/IRESv2b. Image generated using the PyMol Graphics System, Version 1.3, Schrödinger, LLC with PDB ID 3J2W.

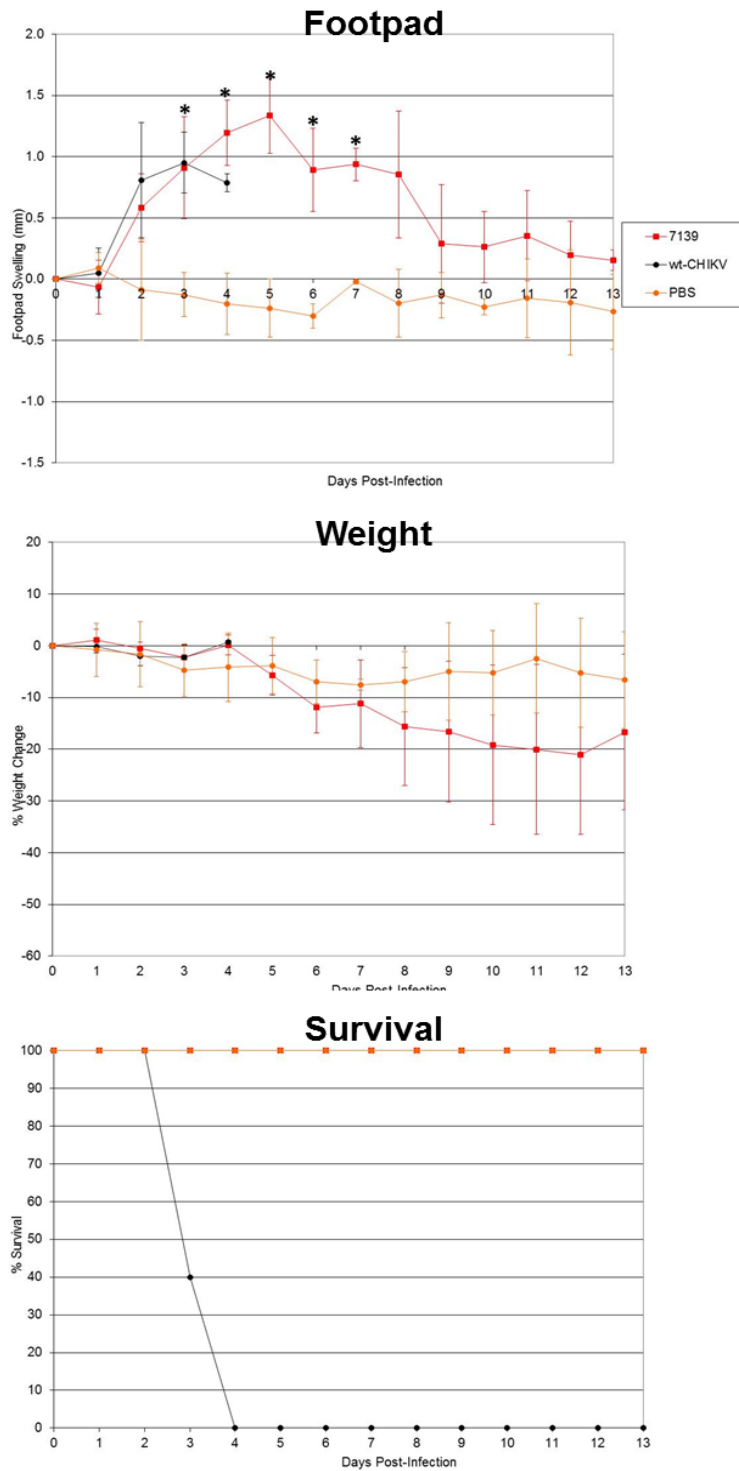


Figure 51: Impact of 7139 infection on A129 mice

Footpad swelling, weight change, and lethality induced by 7139 (with mutated E2 amino acid 341) compared to wt-CHIKV in A129 mice. \* =  $p < 0.05$ . \*\* =  $p < 0.001$ . Statistical Analysis conducted by one-way ANOVA.



## CHAPTER 7 OVERALL SUMMARY, FUTURE DIRECTIONS, AND STATE OF CHIKUNGUNYA VACCINE CANDIDATES

### Overall Summary

The goal of the studies presented here was to adapt a vaccine platform to CHIKV which was efficacious, safe, and stable. Through the experiments presented here, we believe that we accomplished this goal. The benchmark for our vaccine was 181/25 vaccine. This vaccine was efficacious and safe in small animal models and NHPs. In a phase I clinical trial it was also shown to be safe [84]. The phase II clinical trials demonstrated strong immunogenicity over a period of 1 year. However, the vaccine was found to be slightly virulent, with a small number of vaccinees complaining of a slight, transient arthralgia. It was the goal of this dissertation to produce a vaccine utilizing the IRES vaccine strategy that would retain the strong immunogenicity of a live-attenuated vaccine, remain stable *in vitro* and *in vivo*, and be sufficiently attenuated.

The initial cloning of the vaccine candidates was relatively straightforward. Multiple strains of a vaccine were produced following the approach developed in previous studies with a TC-83 IRES vaccine (figure 1). These previous studies showed that the version 1 strategy may produce an overly attenuated vaccine [67]. Later studies showed that the version 2 vaccine was less attenuated and more capable of producing neutralizing antibodies *in vivo* [68]. We decided that the use of a wt-CHIKV backbone, OPY-1, representing a recent outbreak strain may address the problem of over-attenuation. Version 2 was also produced utilizing a strategy developed also for TC-83. Two other versions were also designed and produced, yet were abandoned due to the results surrounding the first versions.

After the vaccines were produced, the first series of tests were to determine the stability of these vaccines *in vitro*. The primary vaccine candidate, CHIKV/IRESv1, did not accrue any consensus, nonsynonymous mutations in the ORFs after 10 serial passages in Vero cells. CHIKV/IRESv2 accumulated three consensus mutations, one of which was used to produce our adapted CHIKV/IRESv2b. The stability of the CHIKV/IRESv1 was one of the main reasons it was decided early to focus the bulk of our studies on it.

The IRES platform was designed to eliminate viral replication in mosquitoes. To this end we tested CHIKV/IRESv1 in mosquitoes and in C6/36 cell cultures. The virus was unable to replicate during a C6/36 cell passage. The virus was also undetectable after an IT inoculation of *Aedes albopictus*. These experiments allowed us to be confident that the live-attenuated vaccine would be unlikely to be accidentally transmitted, also limiting its chances to revert to wt-CHIKV phenotype. In the version one strain we eliminated the sg-promoter and thereby eliminated the transcription of sg-RNA. To translate the structural proteins it was necessary for internal initiation of the ribosome on the genomic RNA. The version 2 vaccines still produced a sg-RNA but placed the capsid gene under the translational control of the IRES at the 3' end of the sg-RNA. We tested the RNA species produced by our vaccines to also demonstrate that the strategy was working as expected, refer to figure 12. Knowing that the correct RNA species were produced and the version 1 vaccine was incapable of replicating in mosquitoes, we were confident to take our vaccines into small animal models.

As stated before, during the start of our studies there were very limited CHIKV infection mouse models. Our first goal was to measure virulence, and to do so we tested the vaccines in neonatal CD-1 mice. CHIKV/IRESv1 was unable to be detected via plaque titration in this model, whereas the wt-CHIKV and 181/25 viruses replicated well. In a smaller study we also tested CHIKV/IRESv2 in this model and found it incapable of producing detectable viremia. Knowing this was not a highly permissive model, another study was conducted with a STAT1 KO mouse model. In this study, we found that the

mice infected CHIKV/IRESv1 suffered no signs of illness, but CHIKV/IRESv2 proved lethal. This study removed the CHIKV/IRESv2 from our future experiments, due to our goal to emphasize safety and produce a vaccine that was more attenuated than 181/25. With predominant focus being put on the CHIKV/IRESv1 we decided to continue our virulence studies with the use of the A129 mouse model. We used multiple aged mice for these studies. Animals at 3 and 9-10-weeks-old were used. These experiments showed that animals showed no obvious signs of illness after infection with CHIKV/IRESv1. The 181/25 vaccine was lethal when given to 3-week-old animals and caused weight loss in the older mice.

With one of the last experiments, we decided to look at tissue titers and histopathology in the older A129 model. The older model, 9-10-week-old, was the model we also used for challenge experiments. To this end, we wanted to run a study to increase our knowledge of wt-CHIKV infection in the A129, while also allowing us to measure differences in viral replication of the different vaccine candidates. Our acceptable outcome was a vaccine that did not replicate systemically and was well tolerated in the immunocompromised A129 mouse model. Interestingly we saw that the wt-CHIKV and the vaccines, 181/25 and CHIKV/IRESv1, all utilize the musculature and the spleen as predominant sites of replication. The differences between the viruses were in the overall tropism, kinetics of the infection, and severity. wt-CHIKV caused a systemic infection by day 1, and 181/25 also spread to all tissues tested, but only by day 3 post-infection. CHIKV/IRESv1 was found only in the sera, spleen, and musculature by day 4 post-infection.

The study also allowed us to measure any persistence in the A129 model, which was negative for both vaccines tested. Interestingly we did not find much in the way of histopathological lesions in the mice receiving the wt-CHIKV. Our predominant finding was the disruption of the splenic architecture. CHIKV/IRESv1 did not produce this sign of illness after infection. Interestingly, the animals' fp were found to have fluid in the

sites of swelling only up to four days post-infection. The animals that received the vaccines, however, did develop a strong cellular infiltrate and moderate myositis at 8 days post-infection. This pathology did clear completely by day 28.

With the first part of our goal demonstrated, we needed to test the efficacy of the vaccines. The first challenge experiment done was done utilizing the IN challenge of C57Bl/6 mice with a neuroadapted CHIKV strain, Ross. 181/25 vaccine and CHIKV/IRESv1 were able to protect against a lethal challenge, and both vaccines produced similar levels of neutralizing antibodies. The bulk of our work focused on the use of the A129 animal model due to its permissive nature regarding CHIKV/IRES infection. We showed in multiple experiments that animals vaccinated with either CHIKV/IRESv1 or CHIKV/IRESv2b were protected against a lethal challenge with wt-CHIKV. We also showed that animals were protected against multiple other forms of virulence seen after a wt-CHIKV challenge such as fp swelling, histopathological lesions, and viral replication. We did measure a small loss of weight when animals vaccinated with CHIKV/IRESv1 were challenged with a wt-CHIKV. These animals did survive the infection though, and showed no other signs of illness (figure 22). We were also able to measure tropism after challenge with a wt-CHIKV FfLuc strain via IVIS, which showed that no measurable viral spread occurred after challenge, and 3 days after challenge there was no measurable viral load in the tissues. Though the IVIS experiments are a less sensitive means of measuring viral spread after challenge, they allowed us a different model for testing vaccine candidates.

Our vaccine candidate CHIKV/IRESv1 was also tested for genetic stability and was stable in cell culture passages as well as serial brain passages. On the other hand, the 181/25 vaccine reverted to a lethal phenotype quite readily in 6-7-week old A129 mice following serial passaging. This trait was exacerbated by the fact that this reversion only required 5 passages and that two independent revertant mutations were observed. Gorchakov *et al.* found that only two mutations are responsible for attenuation of vaccine

strain 181/25v[86]. We found that a mutation, AA 80, that was a loss a (+) charge mutation two AA away from the known attenuating mutation of AA 82 was sufficient to render this virus lethal in A129 mice. In the more virulent passage, line 2, we saw that reversion of the 82 mutation in conjunction with the loss-of-charge mutation on the surface exposed AA 57 resulted in a virulent virus as well.

In summary, we adapted a vaccine platform to CHIKV with great success. We tested its characteristics in cell culture, arthropods, and animal models. We found it to be highly attenuating yet capable of producing long lived immunity in the form of neutralizing antibodies and capable of protecting against a lethal challenge. Collaborators at the Tulane National Primate Research Center have also tested the vaccine in NHPs and have obtained similar results.

### **Future Directions**

The benchmarks of a “good” vaccine, testing efficacy, safety, and stability, have been utilized in other projects with differing levels of success. However the main focus of this dissertation was to develop and test a safe and efficacious live-attenuated vaccine. To this end I believe I was successful. However, the interaction between the vaccine and the vaccinee has not been completely elucidated. We focused on the humoral response for our studies, yet others in our laboratory such as Dr. Seymour believe that the T-cell response is probably also important to alphavirus protection. To this end, he works with various KO mice to elucidate the importance of the various T-cell populations and effectors.

Other studies could be developed to determine the safety and efficacy of this vaccine in newer CHIKV mouse models such as the expanded C57Bl/6 mouse model presented by Morrison *et al.* [124]. I bring this up due to the weaknesses of the immunocompromised mouse model and the disease signs exhibited by the animals. The

A129 model proved useful to us in our studies due to its highly sensitive nature. The issue is that the IFN receptor KO is not represented in any known human population, and the course of infection is not like what is seen in humans. We did see in our tests trying to answer these questions that a smaller immune response was seen in vaccinated animals with intact immune systems then we saw in the A129. We believe this is due to the increased levels of replication seen in the compromised model. These disease signs seen in the C57Bl/6 model do resemble symptoms experienced in human cases. Though less sensitive to the safety aspects of our measurement, it would give a greater understanding of the efficacy afforded by CHIKV/IRES vaccines.

A great deal of work could be done to increase our knowledge not only on the attenuation mechanism afforded by the IRES platform, but also on the mutations of interest discovered in these studies. I observed that a live-attenuated vaccine candidate that was approved for phase II clinical trials was easily reverted to a virulent phenotype during serial passages. I hypothesize that this was due to the loss of heparin sulfate binding mutations, and in the future studies could be done to demonstrate these mutations were actually heparin binding mutations. We also are interested in the mutation at aa341 in E2. The mutation of Gln→Arg follows a similar pattern of heparin sulfate binding, through a large positive charge change located in the E2 protein. It is located just above the envelope, refer to figure 50, but is not as surface exposed as the other 3 mutations listed in the figure. If this mutation could be shown to have heparin binding affinity it would be the first mutation located this close to the envelope to do so.

Other studies could be done on the brain-passaged vaccines. The CHIKV/IRESv1 passages did have a slight virulence difference compared to the parent strain. However, no sequence data could be ascertained to explain the difference. An experiment to focus on the deep sequencing of these viruses could show the impact of minority populations of this vaccine. Deep sequencing could open any live-attenuated vaccine to increased scrutiny. Academically several interesting questions could be answered about the impact

of minority populations in a virus pool. Running deep sequencing on tissue homogenates was very difficult due to the large amount of host genetic material in the samples. It is also possible that small quasi-species may be present that have no discernable impact on the course of infection.

### **State of Chikungunya Vaccines**

We have shown here that we could produce and test a vaccine in an academic setting, while providing enough data to help future clinical development. Yet the question we pose here is two-fold: is this vaccine realistically suitable for further development, and what challenges would any CHIKV vaccine encounter? As stated in the introduction, CHIKV is currently circulating in Africa, India, and Southeast Asia. The virus has a low case fatality rate, estimated to be approximately 0.1%. Though this would place CHIKV on a low priority compared to the encephalitic alphaviruses, there are other reasons why a CHIKV vaccine could be beneficial. First, the debilitating nature of CHIKF has obvious economic impact due to the prolonged symptoms experienced by some infected persons. Another large market for a CHIKV vaccine would be for the United States military, which operates in endemic regions for this virus.

Another key rationale for developing a CHIKV vaccine also involves tourism. There may be a market for a traveler vaccine of people entering endemic regions. Introduction of this virus to a region where CHIKV is not currently active, yet supports the mosquito vectors could start another explosive outbreak. The New World is currently capable of propagating a large-scale outbreak, and it is possible that it could sustain sylvatic maintenance cycle. Due to the susceptibility of so many highly populated regions that are completely naïve to CHIKV, a need for a CHIKV vaccine could always be argued.

With all these factors pointing towards the importance of a CHIKV vaccine, several other factors point in a different direction. The first and most obvious is that, although the outbreaks of 2006 were large and explosive, the more recent outbreaks are small and isolated. Many contributing factors may influence these recent characteristics of outbreaks. Some include mosquito control, better public health, and diagnostic testing. The most important in my opinion is the development of herd immunity. The outbreaks have been large and rapid, yet due to the seasonality of arbovirus infections and exacerbated by the lack of an enzootic cycle in India, it seems to have become less common for a susceptible person to come into contact with a transmitting mosquito. Generally, current outbreaks involve as 20-200 people being found positive in small remote townships in Southeast Asia or India. It is highly unlikely that an outbreak the size of that seen in La Reunion will occur in the regions currently afflicted until herd immunity is lost. However with the long lived immunity of people that have been infected, it could be a long period of time until this disease is explosive again in these regions.

We now have to ask the question of how a vaccine could be produced, brought successfully through clinical trials, and enter licensure and production? The first obstacle is that of taking a vaccine candidate from an academic setting to an industrial one. Thankfully, during the initial stages of this experiment CHIKV became a high priority pathogen due to the 2006 outbreaks. The next obstacle would be the academic proof-of-concept of a vaccine, which in this specific case, it was our pleasure to undertake. The vaccine then needs to be successfully tested for safety, efficacy, and neurovirulence in a NHP model. The next step would be to complete a series of experiments under good laboratory practices (GLP) to focus on safety and efficacy. These studies then can be used to get an investigational new drug (IND) status from the FDA. With all of these previous steps, a CHIKV vaccine should encounter nothing insurmountable.



The next step would be to enter the phases of the clinical trials. The first clinical trial should not prove exceedingly difficult. A study using a small number of people (10-50) with the focus on safety could be completed at any well-equipped hospital with personnel that have clinical trial expertise. The focus of these studies would be close observation for adverse events following a vaccination with either the candidate or placebo. If the results of this phase I clinical trial showed exceedingly high levels of safety (i.e., no increase in adverse events compared to a placebo control group), a phase II clinical could begin. It is my opinion that this would also be feasible. The n-value would be larger (50-500 likely), but in these experiments a large portion of the focus would be on efficacy. The efficacy, however, could be measured through correlates of protection such as neutralizing antibody titers. The biggest hurdle to development would most likely be encountered during a phase III clinical trial. During phase III a large cohort of people, generally numbering in the thousands, are vaccinated with either the vaccine candidate or placebo. Safety would be a concern, with participants being closely monitored by medical personnel. Yet efficacy would be measured generally by disease incidence in the different cohorts, alongside measurements such as neutralizing antibodies or other correlates of protection. This aspect is what could prove difficult for a CHIKV vaccine to succeed. This aspect means that the phase III clinical trials have to be held in an area where there is a large naïve population and disease is actively occurring, meaning that the study would likely have to be held in India or Southeast Asia. Yet, this is where problems would be encountered. A detailed serological survey is not currently available. Also, due to the recent sporadic nature of CHIKV outbreaks, it is very possible that a study could be held and have insufficient power due to a low incidence of disease, even in the control groups. Vaccines have used correlates of immunity to prove efficacy such as influenza, though disease incidence is the preferred mark of protection [125].

There is a way to circumnavigate this problem with the use of the animal rule. The animal rule stipulates that, if human data is impractical or impossible to collect,

animal studies may be used as a substitute to demonstrate safety and efficacy. It is strongly encouraged that multiple animal models be utilized when attempting to gain approval using the animal rule. Obviously the largest drawback of this is the fact it has never been used successfully to license an arbovirus vaccine. Also, with the lack of good animal models that resemble human infection, it is highly unlikely that this could be used. The FDA uses a strict guideline for that appropriateness of rule CFR 601.90 for anything containing bioproducts, which can be found in detail at the following website, <http://www.fda.gov/downloads/Drugs/GuidanceComplianceRegulatoryInformation/Guidances/ucm078923.pdf>.

A phase III trial could be run, but due to the issues presented here it could prove difficult to generate conclusive data. Some things could be done to make a clinical trial more likely to produce positive data. If studies were done to increase surveillance of CHIKV in active transmission locations, it is likely that a trial could be run because pockets of naïve populations could be found. However, estimating where an outbreak will occur in advance would prove difficult and could never be done with certainty. If a large population of naïve people could be located in an area where mosquitoes are actively feeding and the virus is capable of entering the outbreak cycle, it is possible that a study could prove successful in this area. However a more realistic response to these issues would be the use of far ranging sites. All other factors being equal (presence of mosquito vector, frequent exposure of humans to mosquitoes, etc.), a naïve population would be more conducive of an outbreak than a population where a significant portion of humans were previously infected and therefore immune. People in multiple locations that were naïve for CHIKV antibodies could be used in the study. The varied locations would increase the likely hood that at least one area would encounter the infection and produce useful data. This would involve the use of multiple facilities, locations, and personnel. However this type of trial would add complexity, financial, and logistical issues which

could prove difficult in a country with low socioeconomic status and infrastructure such as India.

Overall, we decided that a live-attenuated vaccine would be the best option considering the current characteristics of CHIKV infection and epidemiology. The virus is found in generally poor areas where a live-attenuated vaccine's low cost would be almost required. The highly immunogenic nature of the live-attenuated vaccine could possibly allow for a single dose eliciting a life-long immunity, which is preferred in an area with poor healthcare and logistical capabilities. I believe that the data presented here show a safe and efficacious vaccine that could be produced in relatively high amounts in a stable fashion.

In this dissertation, I have shown evidence that CHIKV/IRESv1 is a safe and efficacious live-attenuated vaccine which may be used to combat the spread and impact of CHIKV. In different sections, I have given my opinion on possible limitations of this vaccine. However, the data and design of the experiments have consistently demonstrated the positive attributes of this vaccine. Although I do not believe the current environment is conducive to the production of a CHIKV vaccine, I do believe that if a vaccine ever were required this platform could be used very effectively in endemic regions. While results in small animal models do not always correlate well with results in humans, I have consistently used the 181/25 vaccine as an experimental control. Because human data is available for 181/25, I hypothesize that the combined animal model results of 181/25 and CHIKV/IRESv1 presented here indicates that CHIKV/IRESv1 should be well tolerated in humans and should be efficacious. In conclusion, I believe that CHIKV/IRESv1 could be effective in controlling disease caused by CHIKV, and should be pursued in clinical trials.

## REFERENCES

1. Kuhn RJ (2007) Togaviridae: The viruses and their replication. In: Knipe DM, Howley PM, editors. *Fields' Virology*, Fifth Edition. New York, NY: Lippincott, Williams and Wilkins. pp. 1001-1022.
2. Higashi N, Matsumoto A, Tabata K, Nagatomo Y (1967) Electron microscope study of development of Chikungunya virus in green monkey kidney stable (VERO) cells. *Virology* 33: 55-69.
3. Klimstra WB, Nangle EM, Smith MS, Yurochko AD, Ryman KD (2003) DC-SIGN and L-SIGN can act as attachment receptors for alphaviruses and distinguish between mosquito cell- and mammalian cell-derived viruses. *J Virol* 77: 12022-12032.
4. Wang K-S, Kuhn RJ, Strauss EG, Ou S, Strauss JH (1992) High-affinity laminin receptor is a receptor for Sindbis virus in mammalian cells. *J Virol* 66: 4992-5001.
5. Byrnes AP, Griffin DE (1998) Binding of Sindbis virus to cell surface heparan sulfate. *J Virol* 72: 7349-7356.
6. Klimstra WB, Ryman KD, Johnston RE (1998) Adaptation of Sindbis virus to BHK cells selects for use of heparan sulfate as an attachment receptor. *J Virol* 72: 7357-7366.
7. Phalen T, Kielian M (1991) Cholesterol is required for infection by Semliki Forest virus. *J Cell Biol* 112: 615-623.
8. Marquardt MT, Kielian M (1996) Cholesterol-depleted cells that are relatively permissive for Semliki Forest virus infection. *Virology* 224: 198-205.
9. Waarts BL, Bittman R, Wilschut J (2002) Sphingolipid and cholesterol dependence of alphavirus membrane fusion. Lack of correlation with lipid raft formation in target liposomes. *J Biol Chem* 277: 38141-38147.
10. Kononchik JP, Hernandez R, Brown DT (2011) An alternative pathway for alphavirus entry. *Virol J* 8: 304.
11. De Tulleo L, Kirchhausen T (1998) The clathrin endocytic pathway in viral infection. *Embo Journal* 17: 4585-4593.
12. Vaananen P, Kaariainen L (1980) Fusion and Hemolysis of Erythrocytes Caused by 3 Togaviruses - Semliki-Forest, Sindbis and Rubella. *Journal of General Virology* 46: 467-475.
13. Smit JM, Bittman R, Wilschut J (1999) Low-pH-dependent fusion of sindbis virus with receptor-free cholesterol- and sphingolipid-containing liposomes. *Journal of Virology* 73: 8476-8484.
14. Wahlberg JM, Bron R, Wilschut J, Garoff H (1992) Membrane-Fusion of Semliki Forest Virus Involves Homotrimers of the Fusion Protein. *Journal of Virology* 66: 7309-7318.
15. Wahlberg JM, Garoff H (1992) Membrane-Fusion Process of Semliki Forest Virus .1. Low Ph-Induced Rearrangement in Spike Protein Quaternary Structure Precedes Virus Penetration into Cells. *Journal of Cell Biology* 116: 339-348.

16. Wengler G, Warkner D, Wengler G (1992) Identification of a Sequence Element in the Alphavirus Core Protein Which Mediates Interaction of Cores with Ribosomes and the Disassembly of Cores. *Virology* 191: 880-888.
17. Geigenmullergnirke U, Nitschko H, Schlesinger S (1993) Deletion Analysis of the Capsid Protein of Sindbis Virus - Identification of the Rna-Binding Region. *Journal of Virology* 67: 1620-1626.
18. Owen KE, Kuhn RJ (1996) Identification of a region in the sindbis virus nucleocapsid protein that is involved in specificity of RNA encapsidation. *Journal of Virology* 70: 2757-2763.
19. Vancini R, Wang GB, Ferreira D, Hernandez R, Brown DT (2013) Alphavirus Genome Delivery Occurs Directly at the Plasma Membrane in a Time- and Temperature-Dependent Process. *Journal of Virology* 87: 4352-4359.
20. Dalrymple JM, Schlesinger S, Russell PK (1976) Antigenic characterization of two sindbis envelope glycoproteins separated by isoelectric focusing. *Virology* 69: 93-103.
21. Dalgarno L, Rice CM, Strauss JH (1983) Ross River virus 26 s RNA: complete nucleotide sequence and deduced sequence of the encoded structural proteins. *Virology* 129: 170-187.
22. Hayes CG, Wallis RC (1977) Ecology of Western equine encephalomyelitis in the eastern United States. *Adv Virus Res* 21: 37-83.
23. Chanas AC, Gould EA, Clegg JCS, Varma MGR (1982) Monoclonal-Antibodies to Sindbis Virus Glycoprotein-E1 Can Neutralize, Enhance Infectivity, and Independently Inhibit Hemagglutination or Hemolysis. *Journal of General Virology* 58: 37-46.
24. Kim DY, Atasheva S, Frolova EI, Frolov I (2013) Venezuelan Equine Encephalitis Virus nsP2 Protein Regulates Packaging of the Viral Genome into Infectious Virions. *Journal of Virology* 87: 4202-4213.
25. Frolova E, Frolov I, Schlesinger S (1997) Packaging signals in alphaviruses. *Journal of Virology* 71: 248-258.
26. Weiss B, Geigenmullergnirke U, Schlesinger S (1994) Interactions between Sindbis Virus Rnas and a 68 Amino-Acid Derivative of the Viral Capsid Protein Further Defines the Capsid Binding-Site. *Nucleic Acids Research* 22: 780-786.
27. Weiss B, Nitschko H, Ghattas I, Wright R, Schlesinger S (1989) Evidence for Specificity in the Encapsidation of Sindbis Virus Rnas. *Journal of Virology* 63: 5310-5318.
28. Cadd TL, Skoging U, Liljestrom P (1997) Budding of enveloped viruses from the plasma membrane. *Bioessays* 19: 993-1000.
29. Garoff H, Hewson R, Opstelten DJ (1998) Virus maturation by budding. *Microbiol Mol Biol Rev* 62: 1171-1190.
30. Aguilar PV, Weaver SC, Basler CF (2007) Capsid protein of eastern equine encephalitis virus inhibits host cell gene expression. *J Virol* 81: 3866-3876.
31. Garmashova N, Atasheva S, Kang W, Weaver SC, Frolova E, et al. (2007) Analysis of Venezuelan equine encephalitis virus capsid protein function in the inhibition of cellular transcription. *J Virol* 81: 13552-13565.

32. Atasheva S, Garmashova N, Frolov I, Frolova E (2008) Venezuelan equine encephalitis virus capsid protein inhibits nuclear import in Mammalian but not in mosquito cells. *J Virol* 82: 4028-4041.
33. Atasheva S, Fish A, Fornerod M, Frolova EI (2010) Venezuelan equine Encephalitis virus capsid protein forms a tetrameric complex with CRM1 and importin alpha/beta that obstructs nuclear pore complex function. *J Virol* 84: 4158-4171.
34. Atasheva S, Krendelchtchikova V, Liopo A, Frolova E, Frolov I (2010) Interplay of acute and persistent infections caused by Venezuelan equine encephalitis virus encoding mutated capsid protein. *J Virol* 84: 10004-10015.
35. Fazakerley JK, Boyd A, Mikkola ML, Kaariainen L (2002) A single amino acid change in the nuclear localization sequence of the nsP2 protein affects the neurovirulence of Semliki Forest virus. *J Virol* 76: 392-396.
36. Frolova EI, Fayzulin RZ, Cook SH, Griffin DE, Rice CM, et al. (2002) Roles of nonstructural protein nsP2 and Alpha/Beta interferons in determining the outcome of Sindbis virus infection. *J Virol* 76: 11254-11264.
37. Frolov I, Garmashova N, Atasheva S, Frolova EI (2009) Random insertion mutagenesis of sindbis virus nonstructural protein 2 and selection of variants incapable of downregulating cellular transcription. *J Virol* 83: 9031-9044.
38. Garmashova N, Gorchakov R, Frolova E, Frolov I (2006) Sindbis virus nonstructural protein nsP2 is cytotoxic and inhibits cellular transcription. *J Virol* 80: 5686-5696.
39. Robinson MC (1955) An epidemic of virus disease in Southern Province, Tanganyika Territory, in 1952-53. *Trans Royal Soc Trop Med Hyg* 49: 28.
40. Lumsden WH (1955) An epidemic of virus disease in Southern Province, Tanganyika Territory, in 1952-53. II. General description and epidemiology. *Trans R Soc Trop Med Hyg* 49: 33-57.
41. Ross RW (1956) The Newala epidemic. III. The virus: isolation, pathogenic properties and relationship to the epidemic. *J Hyg (Lond)* 54: 177-191.
42. Casals J, Whitman L (1957) Mayaro virus: a new human disease agent. I. Relationship to other arbor viruses. *Am J Trop Med Hyg* 6: 1004-1011.
43. Queyriaux B, Simon F, Grandadam M, Michel R, Tolou H, et al. (2008) Clinical burden of chikungunya virus infection. *Lancet Infect Dis* 8: 2-3.
44. Lemant J, Boisson V, Winer A, Thibault L, Andre H, et al. (2008) Serious acute chikungunya virus infection requiring intensive care during the Reunion Island outbreak in 2005-2006. *Crit Care Med* 36: 2536-2541.
45. Borgherini G, Poubeau P, Staikowsky F, Lory M, Le Moullec N, et al. (2007) Outbreak of chikungunya on Reunion Island: early clinical and laboratory features in 157 adult patients. *Clin Infect Dis* 44: 1401-1407.
46. Sissoko D, Malvy D, Ezzedine K, Renault P, Moscetti F, et al. (2009) Post-epidemic Chikungunya disease on Reunion Island: course of rheumatic manifestations and associated factors over a 15-month period. *PLoS Negl Trop Dis* 3: e389.
47. Panning M, Charrel RN, Donoso Mantke O, Landt O, Niedrig M, et al. (2009) Coordinated implementation of chikungunya virus reverse transcription-PCR. *Emerg Infect Dis* 15: 469-471.

48. Parola P, de Lamballerie X, Jourdan J, Rovey C, Vaillant V, et al. (2006) Novel chikungunya virus variant in travelers returning from Indian Ocean islands. *Emerg Infect Dis* 12: 1493-1499.
49. Lakshmi V, Neeraja M, Subbalaxmi MV, Parida MM, Dash PK, et al. (2008) Clinical features and molecular diagnosis of Chikungunya fever from South India. *Clin Infect Dis* 46: 1436-1442.
50. Litzba N, Schuffenecker I, Zeller H, Drosten C, Emmerich P, et al. (2008) Evaluation of the first commercial chikungunya virus indirect immunofluorescence test. *J Virol Methods* 149: 175-179.
51. Lanciotti RS, Kosoy OL, Laven JJ, Panella AJ, Velez JO, et al. (2007) Chikungunya virus in US travelers returning from India, 2006. *Emerg Infect Dis* 13: 764-767.
52. Jackson RJ, Hellen CU, Pestova TV (2010) The mechanism of eukaryotic translation initiation and principles of its regulation. *Nat Rev Mol Cell Biol* 11: 113-127.
53. Jang SK, Krausslich HG, Nicklin MJ, Duke GM, Palmenberg AC, et al. (1988) A segment of the 5' nontranslated region of encephalomyocarditis virus RNA directs internal entry of ribosomes during in vitro translation. *J Virol* 62: 2636-2643.
54. Pelletier J, Sonenberg N (1988) Internal initiation of translation of eukaryotic mRNA directed by a sequence derived from poliovirus RNA. *Nature* 334: 320-325.
55. Chen CY, Sarnow P (1995) Initiation of protein synthesis by the eukaryotic translational apparatus on circular RNAs. *Science* 268: 415-417.
56. Baird SD, Turcotte M, Korneluk RG, Holcik M (2006) Searching for IRES. *RNA* 12: 1755-1785.
57. Thompson SR (2012) So you want to know if your message has an IRES? *Wiley Interdisciplinary Reviews-Rna* 3: 697-705.
58. Pestova TV, Hellen CUT, Shatsky IN (1996) Canonical eukaryotic initiation factors determine initiation of translation by internal ribosomal entry. *Molecular and Cellular Biology* 16: 6859-6869.
59. Pestova TV, Shatsky IN, Hellen CUT (1996) Functional dissection of eukaryotic initiation factor 4F: The 4A subunit and the central domain of the 4G subunit are sufficient to mediate internal entry of 43S preinitiation complexes. *Molecular and Cellular Biology* 16: 6870-6878.
60. Skabkin MA, Skabkina OV, Dhote V, Komar AA, Hellen CUT, et al. (2010) Activities of Ligatin and MCT-1/DENR in eukaryotic translation initiation and ribosomal recycling. *Genes & Development* 24: 1787-1801.
61. Kim JH, Park SM, Park JH, Keum SJ, Jang SK (2011) eIF2A mediates translation of hepatitis C viral mRNA under stress conditions. *Embo Journal* 30: 2454-2464.
62. Brown EA, Day SP, Jansen RW, Lemon SM (1991) The 5' Nontranslated Region of Hepatitis-a Virus-Rna - Secondary Structure and Elements Required for Translation In vitro. *Journal of Virology* 65: 5828-5838.
63. Finkelstein Y, Faktor O, Elroy-Stein O, Levi BZ (1999) The use of bi-cistronic transfer vectors for the baculovirus expression system. *Journal of Biotechnology* 75: 33-44.
64. Berge TO, Banks IS, Tigertt WD (1961) Attenuation of Venezuelan equine encephalomyelitis virus by *in vitro* cultivation in guinea pig heart cells. *Am J Hyg* 73: 209-218.

65. Alevizatos AC, McKinney RW, Feigin RD (1967) Live, attenuated Venezuelan equine encephalomyelitis virus vaccine. I. Clinical effects in man. *Am J Trop Med Hyg* 16: 762-768.
66. Pedersen CE, Jr., Robinson DM, Cole FE, Jr. (1972) Isolation of the vaccine strain of Venezuelan equine encephalomyelitis virus from mosquitoes in Louisiana. *Am J Epidemiol* 95: 490-496.
67. Volkova E, Frolova E, Darwin JR, Forrester NL, Weaver SC, et al. (2008) IRES-dependent replication of Venezuelan equine encephalitis virus makes it highly attenuated and incapable of replicating in mosquito cells. *Virology* 377: 160-169.
68. Guerbois M, Volkova E, Forrester NL, Rossi SL, Frolov I, et al. (2013) IRES-driven expression of the capsid protein of the Venezuelan equine encephalitis virus TC-83 vaccine strain increases its attenuation and safety. *PLoS Negl Trop Dis* 7: e2197.
69. Plante K, Wang E, Partidos CD, Weger J, Gorchakov R, et al. (2011) Novel chikungunya vaccine candidate with an IRES-based attenuation and host range alteration mechanism. *PLoS Pathog* 7: e1002142.
70. Wang E, Kim DY, Weaver SC, Frolov I (2011) Chimeric Chikungunya viruses are nonpathogenic in highly sensitive mouse models but efficiently induce a protective immune response. *J Virol* 85: 9249-9252.
71. Pandya J, Gorchakov R, Wang E, Leal G, Weaver SC (2012) A vaccine candidate for eastern equine encephalitis virus based on IRES-mediated attenuation. *Vaccine* 30: 1276-1282.
72. Rossi SL, Guerbois M, Gorchakov R, Plante KS, Forrester NL, et al. (2013) IRES-based Venezuelan equine encephalitis vaccine candidate elicits protective immunity in mice. *Virology* 437: 81-88.
73. Ziegler SA, Lu L, da Rosa AP, Xiao SY, Tesh RB (2008) An animal model for studying the pathogenesis of chikungunya virus infection. *Am J Trop Med Hyg* 79: 133-139.
74. Gardner J, Anraku I, Le TT, Larcher T, Major L, et al. (2010) Chikungunya virus arthritis in adult wild-type mice. *J Virol* 84: 8021-8032.
75. Couderc T, Chretien F, Schilte C, Disson O, Brigitte M, et al. (2008) A mouse model for Chikungunya: young age and inefficient type-I interferon signaling are risk factors for severe disease. *PLoS Pathog* 4: e29.
76. Grieder FB, Vogel SN (1999) Role of interferon and interferon regulatory factors in early protection against Venezuelan equine encephalitis virus infection. *Virology* 257: 106-118.
77. Ryman KD, Klimstra WB, Nguyen KB, Biron CA, Johnston RE (2000) Alpha/beta interferon protects adult mice from fatal Sindbis virus infection and is an important determinant of cell and tissue tropism. *J Virol* 74: 3366-3378.
78. Barbosa LH, London WT, Hamilton R, Buckler C (1974) Interferon response of the fetal Rhesus monkey after viral infection. *Proc Soc Exp Biol Med* 146: 398-400.
79. Labadie K, Larcher T, Joubert C, Mannioui A, Delache B, et al. (2010) Chikungunya disease in nonhuman primates involves long-term viral persistence in macrophages. *J Clin Invest* 120: 894-906.



80. White A, Berman S, Lowenthal JP (1972) Comparative immunogenicities of Chikungunya vaccines propagated in monkey kidney monolayers and chick embryo suspension cultures. *Appl Microbiol* 23: 951-952.
81. Levitt NH, Ramsburg HH, Hasty SE, Repik PM, Cole FE, et al. (1986) Development of an attenuated strain of chikungunya virus for use in vaccine production. *Vaccine* 4: 157-162.
82. Harrison VR, Eckels KH, Bartelloni PJ, Hampton C (1971) Production and evaluation of a formalin-killed Chikungunya vaccine. *J Immunol* 107: 643-647.
83. Turell MJ, Malinoski FJ (1992) Limited potential for mosquito transmission of a live, attenuated chikungunya virus vaccine. *Am J Trop Med Hyg* 47: 98-103.
84. McClain DJ, Pittman PR, Ramsburg HH, Nelson GO, Rossi CA, et al. (1998) Immunologic interference from sequential administration of live attenuated alphavirus vaccines. *J Infect Dis* 177: 634-641.
85. Edelman R, Tacket CO, Wasserman SS, Bodison SA, Perry JG, et al. (2000) Phase II safety and immunogenicity study of live chikungunya virus vaccine TSI-GSD-218. *Am J Trop Med Hyg* 62: 681-685.
86. Gorchakov R, Wang E, Leal G, Forrester NL, Plante K, et al. (2012) Attenuation of Chikungunya virus vaccine strain 181/clone 25 is determined by two amino acid substitutions in the E2 envelope glycoprotein. *J Virol* 86: 6084-6096.
87. Wang E, Volkova E, Adams AP, Forrester N, Xiao SY, et al. (2008) Chimeric alphavirus vaccine candidates for chikungunya. *Vaccine* 26: 5030-5039.
88. Muthumani K, Lankaraman KM, Laddy DJ, Sundaram SG, Chung CW, et al. (2008) Immunogenicity of novel consensus-based DNA vaccines against Chikungunya virus. *Vaccine* 26: 5128-5134.
89. Mallilankaraman K, Shedlock DJ, Bao H, Kawalekar OU, Fagone P, et al. (2011) A DNA vaccine against chikungunya virus is protective in mice and induces neutralizing antibodies in mice and nonhuman primates. *PLoS Negl Trop Dis* 5: e928.
90. Akahata W, Yang ZY, Andersen H, Sun S, Holdaway HA, et al. (2010) A virus-like particle vaccine for epidemic Chikungunya virus protects nonhuman primates against infection. *Nat Med* 16: 334-338.
91. Metz SW, Geertsema C, Martina BE, Andrade P, Heldens JG, et al. (2011) Functional processing and secretion of Chikungunya virus E1 and E2 glycoproteins in insect cells. *Virol J* 8: 353.
92. Shah KV, Gilotra SK, Gibbs CJ, Jr., Rozeboom LE (1964) Laboratory Studies of Transmission of Chikungunya Virus by Mosquitoes: A Preliminary Report. *Indian J Med Res* 52: 703-709.
93. Pavri KM (1964) Presence of Chikungunya Antibodies in Human Sera Collected from Calcutta and Jamshedpur before 1963. *Indian J Med Res* 52: 698-702.
94. Rao TR (1964) Vectors of Dengue and Chikungunya Viruses: A Brief Review. *Indian J Med Res* 52: 719-726.
95. Schuffenecker I, Itman I, Michault A, Murri S, Frangeul L, et al. (2006) Genome microevolution of chikungunya viruses causing the Indian Ocean outbreak. *PLoS Med* 3: e263.

96. Tsetsarkin KA, Vanlandingham DL, McGee CE, Higgs S (2007) A single mutation in chikungunya virus affects vector specificity and epidemic potential. *PLoS Pathog* 3: e201.
97. Vazeille M, Moutailler S, Coudrier D, Rousseaux C, Khun H, et al. (2007) Two Chikungunya isolates from the outbreak of La Reunion (Indian Ocean) exhibit different patterns of infection in the mosquito, *Aedes albopictus*. *PLoS ONE* 2: e1168.
98. Diallo M, Thonnon J, Traore-Lamizana M, Fontenille D (1999) Vectors of Chikungunya virus in Senegal: Current data and transmission cycles. *American Journal of Tropical Medicine and Hygiene* 60: 281-286.
99. Jupp PG, McIntosh BM (1990) *Aedes-Furcifer* and Other Mosquitos as Vectors of Chikungunya Virus at Mica, Northeastern Transvaal, South-Africa. *Journal of the American Mosquito Control Association* 6: 415-420.
100. Paul SD, Singh KR (1968) Experimental infection of *Macaca radiata* with Chikungunya virus and transmission of virus by mosquitoes. *Indian Journal of Medical Research* 56: 802-811.
101. Diallo M, Thonnon J, Traore-Lamizana M, Fontenille D (1999) Vectors of chikungunya virus in Senegal: current data and transmission cycles. *Am J Trop Med Hyg* 60: 281-286.
102. Carey DE (1971) Chikungunya and dengue: a case of mistaken identity? *J Hist Med Allied Sci* 26: 243-262.
103. Powers AM, Logue CH (2007) Changing patterns of chikungunya virus: re-emergence of a zoonotic arbovirus. *J Gen Virol* 88: 2363-2377.
104. Thaung U, Ming CK, Swe T, Thein S (1975) Epidemiological features of dengue and chikungunya infections in Burma. *Southeast Asian J Trop Med Public Health* 6: 276-283.
105. Thein S, La Linn M, Aaskov J, Aung MM, Aye M, et al. (1992) Development of a simple indirect enzyme-linked immunosorbent assay for the detection of immunoglobulin M antibody in serum from patients following an outbreak of chikungunya virus infection in Yangon, Myanmar. *Trans R Soc Trop Med Hyg* 86: 438-442.
106. Nimmannitya S, Halstead SB, Cohen SN, Margiotta MR (1969) Dengue and chikungunya virus infection in man in Thailand, 1962-1964. I. Observations on hospitalized patients with hemorrhagic fever. *Am J Trop Med Hyg* 18: 954-971.
107. Carey DE, Myers RM, DeRanitz CM, Jadhav M, Reuben R (1969) The 1964 chikungunya epidemic at Vellore, South India, including observations on concurrent dengue. *Trans R Soc Trop Med Hyg* 63: 434-445.
108. Jadhav M, Namboodripad M, Carman RH, Carey DE, Myers RM (1965) Chikungunya disease in infants and children in Vellore: a report of clinical and haematological features of virologically proved cases. *Indian Journal of Medical Research* 53: 764-776.
109. Thaikruea L, Charearnsook O, Reanphumkarnkit S, Dissomboon P, Phonjan R, et al. (1997) Chikungunya in Thailand: a re-emerging disease? *Southeast Asian J Trop Med Public Health* 28: 359-364.

110. Chretien JP, Anyamba A, Bedno SA, Breiman RF, Sang R, et al. (2007) Drought-associated chikungunya emergence along coastal East Africa. *Am J Trop Med Hyg* 76: 405-407.
111. Gerardin P, Guernier V, Perrau J, Fianu A, Le Roux K, et al. (2008) Estimating Chikungunya prevalence in La Reunion Island outbreak by serosurveys: two methods for two critical times of the epidemic. *BMC Infect Dis* 8: 99.
112. Arankalle VA, Shrivastava S, Cherian S, Gunjekar RS, Walimbe AM, et al. (2007) Genetic divergence of Chikungunya viruses in India (1963-2006) with special reference to the 2005-2006 explosive epidemic. *J Gen Virol* 88: 1967-1976.
113. Ng LC, Tan LK, Tan CH, Tan SS, Hapuarachchi HC, et al. (2009) Entomologic and virologic investigation of Chikungunya, Singapore. *Emerg Infect Dis* 15: 1243-1249.
114. Grandadam M, Caro V, Plumet S, Thiberge JM, Souares Y, et al. (2011) Chikungunya virus, southeastern France. *Emerg Infect Dis* 17: 910-913.
115. Rezza G, Nicoletti L, Angelini R, Romi R, Finarelli AC, et al. (2007) Infection with chikungunya virus in Italy: an outbreak in a temperate region. *Lancet* 370: 1840-1846.
116. Powers AM, Brault AC, Tesh RB, Weaver SC (2000) Re-emergence of Chikungunya and O'nyong-nyong viruses: evidence for distinct geographical lineages and distant evolutionary relationships. *J Gen Virol* 81: 471-479.
117. Volk SM, Chen R, Tsetsarkin KA, Adams AP, Garcia TI, et al. (2010) Genome-scale phylogenetic analyses of chikungunya virus reveal independent emergences of recent epidemics and various evolutionary rates. *J Virol* 84: 6497-6504.
118. Tsetsarkin K, Higgs S, McGee CE, De Lamballerie X, Charrel RN, et al. (2006) Infectious clones of Chikungunya virus (La Reunion isolate) for vector competence studies. *Vector Borne Zoonotic Dis* 6: 325-337.
119. Heil ML, Albee A, Strauss JH, Kuhn RJ (2001) An amino acid substitution in the coding region of the E2 glycoprotein adapts Ross River virus to utilize heparan sulfate as an attachment moiety. *J Virol* 75: 6303-6309.
120. Bernard KA, Klimstra WB, Johnston RE (2000) Mutations in the E2 glycoprotein of Venezuelan equine encephalitis virus confer heparan sulfate interaction, low morbidity, and rapid clearance from blood of mice. *Virology* 276: 93-103.
121. Finkelstein Y, Faktor O, Elroy-Stein O, Levi BZ (1999) The use of bi-cistronic transfer vectors for the baculovirus expression system. *J Biotechnol* 75: 33-44.
122. Wang E, Volkova E, Adams AP, Forrester N, Xiao SY, et al. (2008) Chimeric alphavirus vaccine candidates for chikungunya. *Vaccine* 26: 5030-5039.
123. Gardner CL, Burke CW, Higgs ST, Klimstra WB, Ryman KD (2012) Interferon-alpha/beta deficiency greatly exacerbates arthritogenic disease in mice infected with wild-type chikungunya virus but not with the cell culture-adapted live-attenuated 181/25 vaccine candidate. *Virology* 425: 103-112.
124. Morrison TE, Oko L, Montgomery SA, Whitmore AC, Lotstein AR, et al. (2011) A mouse model of chikungunya virus-induced musculoskeletal inflammatory disease: evidence of arthritis, tenosynovitis, myositis, and persistence. *Am J Pathol* 178: 32-40.

125. Dowdle WR, Coleman MT, Mostow SR, Kaye HS, Schoenbaum SC (1973)  
Inactivated influenza vaccines. 2. Laboratory indices of protection. Postgrad Med  
J 49: 159-163.

## Vita

### NAME

Kenneth Steven Plante  
13 Manor Way, Galveston, Texas. 77550  
(978) 726-1697

### PRESENT POSITION AND ADDRESS

Graduate Student  
University of Texas Medical Branch  
Route 0609  
301 University Boulevard  
Galveston, TX 77555

### BIOGRAPHICAL

Birthdate: February 25, 1985  
Birthplace: Billerica, MA  
Citizenship: USA

### EDUCATION

DATES	INSTITUTION	DEGREE	MAJOR
09/2003 – 05/2007	University of Massachusetts at Lowell	B.S.	Biotechnology
08/2007 – present	University of Texas Medical Branch	Ph.D.	Experimental Pathology

### PROFESSIONAL WORK HISTORY AND TEACHING EXPERIENCE

#### WORK HISTORY

2005 – 2007 Undergraduate Research Associate, Department of Biotechnology,  
University of Massachusetts at Lowell

#### RESEARCH MENTORSHIP

01/2010 – 03/2010 Lynn Felts, GSBS research rotation  
01/2010 – Present Animal Trainer ABSL2/ABSL3. Tiffany Kautz, Rose  
Langsjoen, Nick Bergren, Albert Auguste.

### RESEARCH ACTIVITIES

#### AREAS OF RESEARCH

My research focuses on the development of a live-attenuated vaccine for chikungunya, a re-emerging arbovirus. The main attenuation strategy for my work is the incorporation of an encephalomyocarditis virus internal ribosome entry site, which is poorly translated in insect cells and will prevent accidental transmission of the vaccine by the mosquito vector. Multiple vaccine candidates have been produced and tested for safety and efficacy in mice and non-human primates. Additionally, the tissue tropism of the vaccines and wt-virus have been

determined using IVIS technology and traditional experiments. The vaccine has also been tested for stability in small animal models, cell culture and arthropods.

#### GRANT SUPPORT

09/2009 – 09/2011 Sealy Center for Vaccine Development Pre-Doctoral Fellow  
09/2011 – 09/2013 T32 Emerging and Tropical Infectious Diseases Trainee

#### HONORS

2005 – 2007 (UMASS)	Charles J. Hoff Scholarship for Scientific Excellence
2007	Award for Undergraduate Research Excellence (UMASS)
2007	Magna Cum Laude Graduate (UMASS)
2009 – 2011	Sealy Center for Vaccine Development Pre-Doctoral Fellow
2009	Sealy Center for Vaccine Development Poster Award
2010	Edward S. Reynolds Experimental Pathology Poster Award
2010 Austria	Edward Jenner Poster Award, Vaccine Congress, Vienna,
2011	Sealy Center for Vaccine Development Scholarship Award
2011	Betty Williams Award
2011 – present	T32 Emerging and Tropical Infectious Diseases Trainee
2012	McLaughlin Poster Award.
2012	Edward S. Reynolds Experimental Pathology Poster Award.
2012	Zhou Sisters Award Graduate Student Award
2012	Stephen C. Silverthorne Memorial Award.

#### PUBLICATIONS

Atasheva S, Wang E, Adams AP, **Plante KS**, Ni S, Taylor K, Miller ME, Frolov I, Weaver SC. Chimeric alphavirus vaccine candidates protect mice from intranasal challenge with western equine encephalitis virus. *Vaccine*. Volume 27, Issue 32. July 2009. 4309-4319.

**Plante KS**, Wang E, Partidos CD, Weger J, Gorchakov R, Tsetsarkin K, Borland EM, Powers AM, Seymour R, Stinchcomb DT, Osorio JE, Frolov I, Weaver SC. Novel chikungunya vaccine candidate with an IRES-based attenuation and host range alteration mechanism. *PLoS Pathogens*. Volume 7, Issue 7. July 2011.

McGee CE, Tsetsarin K, Guy B, Lang J, **Plante KS**, Vanlandingham DL, Higgs S. Stability of yellow fever virus under recombinatory pressure as compared with chikungunya virus. *PLoS One*. Volume 6, Issue 8. August 2011.

Gorchakov R, Wang E, Leal G, Forrester NL, **Plante K**, Rossi SL, Partidos CD, Adams AP, Seymour R, Weger J, Borland EM, Sherman MB, Powers AM, Osorio JE, Weaver SC. attenuation of chikungunya vaccine strain 181/clone 25 is determined by 2 amino acid substitutions in the E2 envelope glycoprotein. *J Virol*. 2012 Mar 28

Rossi SL, Guerbois M, Gorchakov R, **Plante KS**, Forrester NL, Weaver SC. IRES-based Venezuelan equine encephalitis vaccine candidate elicits protective immunity in mice. *Virology*. 2013 Mar 15;437(2):81-8.

Seymour RL, Rossi SL, Bergren NA, **Plante KS**, Weaver SC. The Role of Innate versus Adaptive Immune Responses in a Mouse Model of O'Nyong-Nyong Virus Infection. *Am J Trop Med Hyg*. 2013 Apr 8.

Permanent address: 13 Manor Way, Galveston, TX 77550

This dissertation was typed by Kenneth Steven Plante.